

University of Alberta

Novel roles for zebrafish Sfrp1a and Sfrp5 in neural retina patterning

by

Vanessa Leigh Holly

A thesis submitted to the Faculty of Graduate Studies and Research
in partial fulfillment of the requirements for the degree of

Master of Science

in

Molecular Biology and Genetics

Department of Biological Sciences

©Vanessa Leigh Holly

Fall 2012

Edmonton, Alberta

Permission is hereby granted to the University of Alberta Libraries to reproduce single copies of this thesis and to lend or sell such copies for private, scholarly or scientific research purposes only. Where the thesis is converted to, or otherwise made available in digital form, the University of Alberta will advise potential users of the thesis of these terms.

The author reserves all other publication and other rights in association with the copyright in the thesis and, except as herein before provided, neither the thesis nor any substantial portion thereof may be printed or otherwise reproduced in any material form whatsoever without the author's prior written permission.

Abstract

Sensory systems are complex structures that receive stimuli from the surrounding environment and convert them into interpretable information. In the visual system, light hitting the eye is transmitted to the brain in a way that preserves the spatial conformation of the pictures we see. Retinal ganglion cells are given directional cues of where to innervate the brain, based on the unique cohort of genes activated during retinal development. If there are alterations in gene expression, it can result in aberrant axon projection to the brain and improper choroid fissure closure (ocular coloboma). Using zebrafish as a model system, I demonstrate that Sfrp1a (Secreted frizzled-related protein) and Sfrp5 work cooperatively to establish dorsal retinal identity by facilitating signaling from two well known dorsal retina specification pathways, bone morphogenic protein (BMP) and Wnt. Previous experiments identify Sfrps as BMP inhibitors, revealing a novel, positive interaction between Sfrps and BMPs.

Acknowledgements

Thank you to all the members (past and present) of my lab family. I doubt the Biological Sciences Building has ever experienced so much laughter.

Table of Contents

Chapter 1: Introduction	1
<i>1.1 Development of the neural system and specification of the eye field ..</i>	<i>2</i>
<i>1.2 Zebrafish eye development and structure</i>	<i>4</i>
<i>1.3 Retinal patterning and retinotectal mapping</i>	<i>5</i>
<i>1.4 Dorsal-ventral axis formation</i>	<i>7</i>
<i>1.5 Choroid fissure closure and ocular coloboma</i>	<i>8</i>
<i>1.6 Wnt signaling</i>	<i>9</i>
<i>1.7 Wnt signaling and eye development</i>	<i>11</i>
<i>1.8 Bone morphogenic proteins (BMP) signaling.....</i>	<i>12</i>
<i>1.9 BMP signaling and eye development.....</i>	<i>15</i>
<i>1.10 Secreted frizzled-related proteins</i>	<i>17</i>
<i>1.11 Zebrafish secreted frizzled-related proteins</i>	<i>18</i>
<i>1.12 Sfrp protein structure and function</i>	<i>19</i>
<i>1.13 Sfrp interaction with other pathways</i>	<i>20</i>
<i>1.14 Sfrps and eye development</i>	<i>22</i>
<i>1.15 Purpose of research and working hypothesis</i>	<i>23</i>

<i>1.16 Figures</i>	24
<i>1.17 Literature cited</i>	28
Chapter 2: Materials and Methods	42
<i>2.1 Zebrafish lines & animal care</i>	43
<i>2.2 Morpholino preparation/injection and embryo treatment</i>	43
<i>2.3 Phusion high fidelity PCR and TOPO cloning</i>	44
<i>2.4 In vitro mRNA transcription</i>	47
<i>2.5 Total RNA extraction</i>	48
<i>2.6 RT-PCR reactions</i>	50
<i>2.7 cDNA synthesis and quantitative real-time PCR (qRT-PCR)</i>	50
<i>2.8 mRNA in situ hybridization (ISH)</i>	52
<i>2.8.1 Riboprobe synthesis (Plasmid and PCR-based approach)</i> ...	52
<i>2.8.2 mRNA ISH protocol</i>	53
<i>2.9 Whole mount immunohistochemistry (Laminin staining)</i>	56
<i>2.10 mRNA and DNA construct (rx3:gdf6a) injection</i>	57
<i>2.11 Live imaging</i>	57
<i>2.12 Tables</i>	59

2.13 Literature cited	65
Chapter 3: Results and Discussion	67
3.1 Zebrafish <i>sfrp1a</i> and <i>sfrp5</i> are expressed during early eye development	68
3.2 Zebrafish <i>sfrp1a</i> & <i>sfrp5</i> have potential alternative transcripts	70
3.3 Confirmation of morpholino specificity	71
3.4 Survey of phenotypes caused by <i>sfrp1a</i> & <i>sfrp5</i> morpholino knockdown	73
3.5 <i>sfrp1a</i> & <i>sfrp5</i> act synergistically during eye development	75
3.6 Knockdown of <i>sfrp1a/sfrp5</i> does not cause changes in nasal/temporal gene expression	76
3.7 <i>sfrp</i> -depleted embryos have mild defects in ventral retina markers (<i>ephB2</i> , <i>ephB3</i> , <i>zic2a</i>) at 28hpf	77
3.8 Ventral retina markers <i>aldh1a3</i> and <i>vax2</i> are expanded in <i>sfrp1a/sfrp5</i> double morphants at 2dpf	78
3.9 <i>sfrp</i> -depleted embryos have reduction in multiple dorsal retina markers (<i>aldh1a2</i> , <i>bambi</i> , <i>tbx5</i>)	79
3.10 <i>sfrp</i> -depleted embryos have increased BMP gene expression but reduced BMP signaling	80

<i>3.11 sfrp1a/sfrp5 double morphants have increased wnt gene expression but decreased Wnt signaling</i>	82
<i>3.12 Altered Wnt signaling does not account for Sfrp-dependent changes in BMP expression</i>	85
<i>3.13 Figures</i>	86
<i>3.14 Tables</i>	105
<i>3.14 Literature cited</i>	106

Chapter 4: Conclusions and Future Directions111

<i>4.1 Summary of findings</i>	112
<i>4.2 Unanswered questions and future directions</i>	115
<i>4.2.1 Sfrps as BMP signaling facilitators</i>	115
<i>4.2.2. BMP and Wnt negative feedback loops</i>	117
<i>4.2.3 Sfrp expression in the ventral retina</i>	117
<i>4.2.4 Discrepancies with previously published data on Sfrp1 and Sfrp5</i>	118
<i>4.2.5 Other future experiments</i>	119
<i>4.3 Final conclusions</i>	120
<i>4.4 Figures</i>	121

4.5 Literature cited122

Appendix A: Hedgehog acyltransferases and retinal patterning ..124

A.1 Introduction125

A.2 Results126

A.2.1 Expression profile of zebrafish *hhatlb*126

A.2.2 *hhatlb* morphant phenotypes128

A.2.3 Loss of *hhatlb* does not phenocopy loss of *Shh* signaling ..129

A.3 Conclusions129

A.4 Figures131

A.5 Literature cited136

Appendix B: *hmx4* regulates retinoic acid-mediated *Shh* signaling during forebrain patterning138

B.1 Introduction139

B.2 Results139

B.2.1 Loss of *hmx4* causes defects in *Shh* signaling139

B.2.2 Defects in *Shh* signaling can be rescued by addition of RA140

B.3 Conclusions140

B.4 Figures141

B.5 Literature cited143

List of Tables

Table 2.1: Morpholino oligonucleotide sequences	59
Table 2.2: mRNA overexpression primer sequences	60
Table 2.3: RT-PCR primer sequences for morpholino controls	61
Table 2.4: Quantitative real time PCR (qRT-PCR) primer sequences	62
Table 2.5: PCR-based probe primer sequences	63
Table 2.6: mRNA in situ hybridization probe plasmids	64
Table 3.1: mRNA in situ hybridization quantification and statistics	105

List of Figures

Figure 1.1: Dorsal-ventral retinotectal mapping in zebrafish	24
Figure 1.2: Overview of the canonical Wnt pathway	25
Figure 1.3: Overview of canonical bone morphogenic protein (BMP) signaling	26
Figure 3.1: mRNA in situ hybridization expression of <i>sfrp1a</i> , <i>sfrp2</i> , and <i>sfrp5</i> in the developing zebrafish embryo	87
Figure 3.2: <i>sfrp1a</i> , <i>sfrp2</i> , and <i>sfrp5</i> expression in the zebrafish eye	89
Figure 3.3: Comparison of <i>sfrp1a</i> and <i>sfrp5</i> alternative transcripts	90
Figure 3.4: Morpholino design and specificity controls	91
Figure 3.5: Phenotypic survey of <i>sfrp1a/sfrp5</i> -depletion	92
Figure 3.6: Phenocopy of morphological defects caused by multiple <i>sfrp1a</i> and <i>sfrp5</i> morpholino cocktails	93
Figure 3.7: Survey of eye formation in <i>sfrp1a/sfrp5</i> morphants	94
Figure 3.8: Sfrp1a and Sfrp5 share functional redundancy during ocular development	95
Figure 3.9: Depletion of <i>sfrp1a</i> and <i>sfrp5</i> does not cause changes in nasal or temporal retinal gene markers	96

Figure 3.10: <i>sfrp1a/sfrp5</i> morphants show changes in ventral gene expression consistent with ventralization of the retina	97
Figure 3.11: Depletion of <i>sfrp1a</i> and <i>sfrp5</i> causes decrease in dorsal markers at multiple stages (28hpf, 2dpf) consistent with ventralization of the retina	99
Figure 3.12: Embryos injected with <i>sfrp1a/sfrp5</i> morpholinos have defects in BMP signaling but an increase in <i>BMP</i> gene expression	100
Figure 3.13: Reduction of <i>sfrp1a</i> and <i>sfrp5</i> results in a decrease in Wnt signaling but an increase in <i>wnt</i> gene expression	102
Figure 3.14: Changes in Wnt signaling cannot account for all of the changes seen in <i>sfrp1a/sfrp5</i> morphants	103
Figure 4.1: Proposed model of Sfrp function during eye patterning	121
Figure A1: Proposed model of Hhat-mediated Shh palmitoylation	131
Figure A2: Expression of <i>hhatlb</i> during zebrafish development	132
Figure A3: <i>hhatlb</i> is not expressed in the notochord but is maternally provided during early embryonic development	133
Figure A4: <i>hhatlb</i> -depleted embryos have coloboma and changes in ventral eye markers	134
Figure A5: <i>hhatlb</i> eye phenotypes do not phenocopy loss of Shh signaling	135
Figure B1: <i>hmx4</i> morphants have alterations in Shh signaling	141

Figure B2: Defects in Shh signaling can be rescued by RA treatment142

List of Abbreviations

ADAM – a disintegrin and metalloprotease domain-containing protein

Aldh – aldehyde dehydrogenase

APC – adenomatous polyposis coli

Bambi – BMP and activin membrane bound inhibitor

BCIP – bromo-chloro indoyl phosphate

BMP – bone morphogenic protein

BMPR – BMP receptor

bp – base pair

BRE – BMP responsive element

CaMK – calcium-responsive calcium calmodulin dependent kinase

cDNA – complementary DNA

CK - casein kinase

CRD – cysteine rich domain

depC - diethylpyrocarbonate

EDTA - ethylenediaminetetraacetic acid

GPB – GSK3 binding protein

Daam - dishevelled associated activator of morphogenesis

DAG – diacylglycerol

DEAB – diethylaminobenzaldehyde

DIG – digoxigenin

Dkk – dickkopf

DMSO – dimethyl sulfoxide

dpf – days post fertilization

Dpp – decapentaplegic

DSH – dishevelled

ECM – extracellular matrix

Eph – Eph receptor tyrosine kinase

EM – embryo media

Emx – empty spiracles homeobox

EST – expressed sequence tag

Fz – Frizzled

Gdf – Growth and differentiation factor

GFP – green fluorescent protein

Gli - GLI-Kruppel family member

GSK – glycogen synthase kinase

HEPES – hydroxyethyl piperazineethanesulfonic acid

Hhat – hedgehog acyltransferase

hpf – hours post fertilization

IHC – immunohistochemistry

INL – inner nuclear layer

IP3 – inositol triphosphate

IPL – inner plexiform layer

ISH – *in situ* hybridization

Lef – lymphoid enhancer factor

Lhx – lim homeobox

LRP - low density lipoprotein receptor-related protein

MO – morpholino

NBT – nitroblue tetrazolium

NICD – intracellular domain of notch

Nkx – NK2 transcription factor related

NTR – netrin

ONL – outer nuclear layer

OPL – outer plexiform layer

Otx – orthodenticle homeobox

Pax – paired box gene

PBS – phosphate buffered saline

PBSDTT – phosphate buffered saline, 0.1% Tween-20, 1% DMSO, 0.1% Triton-X 100

PCP – planar cell polarity

PCR – polymerase chain reaction

PFA – paraformaldehyde

PKC – protein kinase C

Ptc – patched

PTU – 1-phenyl 2-thiourea

qRT-PCR – quantitative real time polymerase chain reaction

RA - retinoic acid

Rac – ras-related C3 botulinum toxin substrate

RAR – retinoic acid receptor

RGC – retinal ganglion cell

Rho – ras homolog family member

RGCL – retinal ganglion cell layer

RPE - retinal pigmented epithelium

Rx - retinal homeobox

RXR – retinoid x receptor

SDS – sodium dodecyl sulfate

Sfrp – secreted frizzled-related protein

Shh – sonic hedgehog

Six - SIX homeobox

snRNP – small nuclear riboproteins

SMAD – Mothers against decapentaplegic homolog family members

Smo – smoothened

So – sine oculis

ss – somite stage

Tbx – T-box

Tcf – T-cell factor

TGF – transforming growth factor

Tll1 – Tolloid-like protein 1

Vax - ventral anterior homeobox

Wnt – Wingless-type MMTV integration site family member

Zic – zic family member (odd-paired homolog)

Chapter 1

Introduction

1.1 Development of the Neural System & Specification of the Eye Field

Organogenesis is a complex process that requires coordination and specification of diverse cell types during embryonic development. A subsection of vertebrate neural ectoderm, the presumptive eye field, forms from the specification of retinal precursor cells in the anterior neural plate. This retinal anlage is specified early on in development, with eye field markers detectable during late gastrulation (Carl et al., 2002; Loosli et al., 1999; Oliver et al., 1995; Seo et al., 1998). If the eye field is not specified properly, it can lead to eye deformation or, in the most extreme cases, prevent the eye from forming entirely.

There are four transcription factors that are regionally expressed in the vertebrate anterior neural tissue and regulate eye field specification: *SIX homeobox 3 (six3)*, *paired box gene 6 (pax6)*, *orthodenticle homoeobox 2 (otx2)*, and *retinal homoeobox (rx)* (reviewed in (Bailey et al., 2004)). All four genes are essential to eye development, as loss of any one gene can inhibit eye formation. The first gene, *six3*, functions as a regulator of anterior brain development. Mutations in human and mouse *six3* cause severe forebrain defects, including loss of anterior forebrain or holoprosencephaly (Pasquier et al., 2000; Wallis et al., 1999), a condition where the cerebral hemispheres fail to separate. (Lagutin et al., 2003). More strikingly, *six3* mRNA overexpression in Medaka fish results in ectopic eye formation whereas *six3* knockdown prohibits eye formation, demonstrating that *six3* is essential for eye morphogenesis (Carl et al., 2002; Loosli et al., 1999). Medaka *six3* expression is also maintained in later eye development, a process dependent on continued *rx* expression, in order to aid in retinal neuron cell division and differentiation (Del Bene et al., 2004). Mutations in the *Drosophila six3* orthologue, *sine oculis (so)*, also cause an array of defects including small, malformed eyes (microphthalmia) or absent eyes (anophthalmia), thought to be coupled to changes in apoptosis (Cheyette et al., 1994; Heitzler et al., 1993).

In addition to Six3, the Paired Homeodomain Pax6 transcription factor is critical for specifying retinal identity. Mutation of *Pax6* prevents the formation of

eyes in homozygous mutant humans, mice, and *Drosophila* ((Quiring et al., 1994); reviewed in (Hanson and Van Heyningen, 1995)). Similar to *six3*, overexpression of *pax6* (*eyeless*) in *Drosophila* and *Xenopus* is sufficient to induce the formation of ectopic eyes (Chow et al., 1999; Halder et al., 1995). In humans, heterozygous mutations in *pax6* allow patients to form eyes, however, affected individuals display microphthalmia (small eyes), aniridia (failure to form an iris) and development of cataracts (Glaser et al., 1992; Jordan et al., 1992; Ton et al., 1991). Later in development, *pax6* expression is maintained by the *rx* genes, similar to *six3*. Continued *pax6* expression helps specify the retinal ganglion cells, neurons that send visual information via their axon projections to processing centres in the brain (Del Bene et al., 2004). In addition, both *pax6* and *six3* positively regulate each other's expression (Chow et al., 1999; Loosli et al., 1999; Wargelius et al., 2003). Further investigation of the relationship between these two genes revealed that single *six3* or *pax6* mutants have comparable phenotypes to double mutants, suggesting that the two genes function in the same pathway during eye development (Wargelius et al., 2003).

The orthodenticle homoeobox gene *otx2* also plays a critical role during eye specification. Unlike *six3* and *pax6*, whose expression is maintained by *rx* expression, *rx* is an inhibitor of *otx2*. The Otx2 transcription factor is initially excluded from the eye field, presumably due to Rx expression in that tissue, but remains functionally important for specification of the anterior neural tissue (Martinez-Morales et al., 2003); *otx2*^{-/-} mutant mice fail to form forebrain or midbrain (Acampora et al., 1995). As eye morphogenesis continues, *otx* is expressed throughout the optic vesicle, the earliest stage of the budding eye, and later becomes restricted to the developing retinal pigmented epithelium (RPE). Loss of mouse *otx* (*otx1*^{-/-}/*otx2*^{+/-}) results in defects in RPE specification, leading to expansion of other ocular tissues such as the neural retina (Martinez-Morales et al., 2001). Expression of mouse *otx2* also becomes restricted to specific retinal cell types in later eye development and regulates photoreceptor terminal differentiation (Nishida et al., 2003). Additionally, heterozygous mutations in human *otx2* result in microphthalmia or anophthalmia (Wyatt et al., 2008).

The retinal homeobox gene, *rx*, functions in a different facet of eye development than the other three transcription factors. Specification of the eye field in Medaka *rx* loss-of-function models occurs normally, as *pax6* and *six3* expression is unchanged. In addition, over-expression of *six3* is unable to rescue *rx*-depletion eye defects, indicating that *rx* is downstream of *six3*-induced eye field specification (Loosli et al., 2001). Instead, *rx* loss-of-function prevents the eye field from forming bilateral optic vesicles. Supporting this hypothesis, misexpression of *rx* causes an increase in optic vesicle size (Loosli et al., 2001). mRNA overexpression of *rx* genes such as zebrafish *rx1/rx2* or *Xenopus Xrx1* also induces expansion of retinal tissue (Andreazzoli et al., 1999; Chuang and Raymond, 2001). Furthermore, known vertebrate orthologs of *rx* are all expressed in the early eye and homozygous mutations in murine *Mrx*, zebrafish *rx3*, *xenopus Xrx1*, or human *RX* all prevent eye formation (Andreazzoli et al., 1999; Andreazzoli et al., 2003; Furukawa et al., 1997; Loosli et al., 2003; Mathers et al., 1997; Voronina et al., 2004).

1.2 Zebrafish Eye Development and Structure

Although precursors of the zebrafish visual system are specified as early as tailbud stage (10 hpf) (Loosli et al., 2003), physical eye development begins at 12 hpf (6-7ss) when the lateral edges of the diencephalon evaginate to form the optic vesicles (Schmitt and Dowling, 1994). Optic vesicle evagination is a result of anterior, medial migration of single diencephalic retinal precursor cells, as well as anterior movement of the underlying neural keel. These two events force the retinal precursor cells laterally, forming bilateral optic projections (Rembold et al., 2006). These projections of tissue expand outwards until they approach the overlying non-neural ectoderm. Complex signaling cues expressed from the optic vesicles specify the overlying non-neural ectoderm to thicken and form the lens placode (reviewed in (Donner et al., 2006)). Invagination of the lens placode produces the lens vesicle, which pinches off by 24 hpf to form the lens (Greiling and Clark, 2009). The movement of lens tissue inwards is also concurrent with the invagination of the underlying optic vesicles to form two bilateral, double-layered

optic cups. Eventually, the outer layer of the cup gives rise to the retinal pigmented epithelium (RPE), which is important for photoreceptor maintenance (Gu et al., 1997) and lamination of the eye (Jensen and Westerfield, 2004), and the inner layer of the optic cup forms the neural retina, which will differentiate into distinct layers of cell types.

The neural retina is composed of three nuclear layers (the outer nuclear layer (ONL), inner nuclear layer (INL), and retinal ganglion cell layer (RGCL)) and two plexiform layers (the inner plexiform layer (IPL) and outer plexiform layer (OPL)). Within these layers are six different cell types: rod and cone photoreceptors, bipolar cells, horizontal cells, amacrine cells, and retinal ganglion cells (RGCs). In the most direct route, photoreceptors in the ONL, following a light stimulus, will transmit signals to bipolar cells contained within the INL. Bipolar cells then transfer information to the RGCs, which send their axon projections to visual processing centres of the brain. In zebrafish, the visual processing centre is composed of two lobes, jointly called the optic tectum; in humans and other mammals, the analogous region of the brain is the superior colliculus. Horizontal and amacrine cells are interneurons present in the outer and inner plexiform layers, respectively, and are responsible for modulating visual stimuli during lateral information transfer. Retinal cell differentiation begins at 32hpf, with the RGCs forming the first, post-mitotic cell type following a wave of *sonic hedgehog* (*shh*) expression (Neumann and Nüsslein-Volhard, 2000; Schmitt and Dowling, 1994). By 72hpf, the system is functional and can elicit visual responses in larval zebrafish (Branchek and Bremiller, 1984).

1.3 Retinal Patterning and Retinotectal Mapping

In order for an organism to properly interpret visual information, correct connections need to be made between the eye and brain. During eye development, expression patterns of retinal marker genes are spatially restricted to quadrants of the eye that correspond to the dorsal, ventral, nasal, and temporal axes. Initiation of axis markers is functionally important because it sets the boundaries for expression of subsequent genes; these boundaries then provide vital cues for

mapping retinal projections to correct regions of the brain (reviewed in (Lemke and Reber, 2005)). These cues come from the expression of the guidance cue molecules, Eph and Ephrin. Eph receptors are a family of receptor tyrosine kinases that bind Ephrin ligands to mediate changes in the cytoskeleton of RGC growth cones during axon guidance (Scicolone et al., 2009). Interactions between the Eph receptor and Ephrin ligand can elicit either attractive or repulsive forces, depending on the subtype. There are two classifications of Eph/Ephrin interactions that define the eye axes: EphA receptors bind EphrinA ligands to specify nasal/temporal axon projection and Eph B receptors bind Ephrin B ligands to specify dorsal/ventral axon projection.

Both Ephs and Ephrins are expressed in opposing gradients within the retina and tectum in order to guide the axons to their appropriate destination. This process of preserving spatial arrangement between RGCs in the retina and innervation of the tectum is called retinotectal mapping. During nasal/temporal retinotectal mapping, RGC axons from the nasal retina project to the posterior tectum, whereas temporal RGC axons project to the anterior tectum. This is mediated by a repulsive interaction between the EphA receptor and EphrinA ligand (Roskies and O'Leary, 1994). For example, the RGCs from the nasal retina express high levels of *ephrinA*, making them more suited to project to an area of the tectum where there are lower levels of *ephA* expression. Because the receptor *ephA* is expressed at higher levels in the anterior tectum (Rashid et al., 2005), RGC axons from the nasal retina project further into the posterior tectum. Conversely, temporal RGCs instead express higher levels of *ephA* receptors, making their axon projections more attracted to the anterior tectum, where there are lower levels of *ephrinA* (Cheng et al., 1995). In fact, if the temporal retina is ablated, the anterior tectum no longer becomes innervated (Sperry, 1963)

The dorsal-ventral RGCs are postulated to project to the tectum in a similar fashion, but using attractive EphB/EphrinB interactions (Hindges et al., 2002). Although the boundaries are not as distinct at the nasal/temporally-expressed *ephAs/ephrinAs*, ventral RGCs express higher levels of *ephB* (Holash and

Pasquale, 1995). Attractive forces then guide axons from the ventral retina to the medial tectum, where there are high levels of *ephrinB* ligand present (Hindges et al., 2002). Dorsal RGCs instead express high levels of *ephrinB* ligand and project to the lateral tectum, which has increased levels of the *ephrB* receptor (Hindges et al., 2002). As a result, neurons that begin in the dorsal retina typically send their axon projections to ventro-lateral portion of the contralateral tectum, and ventral retinal neurons send their axon projections to the dorso-medial portion of the contralateral tectum (Trowe et al., 1996) (Figure 1.16.1).

1.4 Dorsal-Ventral Axis Formation

Although dorsal-ventral axes are established in the eye early on, the retina requires continued gene expression for proper RGC axon guidance. In this sense, eye development can be studied with respect to two phases of dorso-ventral axis patterning. The first is the initiation phase, where asymmetric dorsal and ventral gene expression is established in the presumptive eye. The second is the maintenance phase, where axial marker expression must continue to ensure the eye forms proper connections to the brain. At this stage, dorsal and ventral markers mutually inhibit each other to ensure neither tissue encompasses the entire retina. Therefore, the maintenance phase is sensitive to changes in retinal gene expression boundaries. For example, ectopic expression of ventral genes can expand ventral identity at the expense of dorsal retina; *ventral anterior homeobox 2 (vax2)* mRNA overexpression in *Xenopus* causes a marked expansion in other ventral markers such as *pax2* and a reduction in the dorsal marker *vent2* (Barbieri et al., 1999). Ventralization of the retina is also associated with aberrant RGC projection, where nearly all dorsal RGCs misproject (Sakuta et al., 2001; Schulte et al., 1999). Conversely, alterations of dorsal markers can also influence the ventral retina. Reduction in the dorsally expressed *growth and differentiation factor 6a (gdf6a)* characteristically causes ventralization, with a complete expansion of *vax2* into the dorsal-most region of the retina (French et al., 2009; Gosse and Baier, 2009). In addition, over-expression of the dorsal retina gene *bone morphogenic protein 4 (bmp4)* in mouse dorsalizes the retina and reduces

the expression domain of *vax2* (Behesti et al., 2006). Similarly, over-expression of *T-box 5 (tbx5)* mRNA dorsalizes the retina, but with more subtle changes in retinotopic mapping than *vax2*-induced retina ventralization (Koshiba-Takeuchi et al., 2000). Because ventralization causes more striking changes in RGC projection than dorsalization, it has been postulated that ventral markers may have more influence on retinotopic mapping.

Ventralization signals emanating from the ventral midline and/or the optic stalk are opposed by dorsalization signals from the dorsal optic cup and RPE. These patterning cues come from three main signaling pathways to specify the dorsal or ventral retina. The dorsal retina secretes a gradient of Bone Morphogenic Protein (BMP). Multiple *BMP* genes are expressed dorsally to cooperatively pattern the retina, including *bmp2*, *bmp4*, and *gdf6*. BMP signaling is important not only for initiation of dorsal markers, but also for their maintenance (Adler and Belecky-Adams, 2002; French et al., 2009; Gosse and Baier, 2009). In contrast, ventral retina identity comes from the secreted morphogen *shh*. Overexpression of *shh* in both chick and *Xenopus* expands the ventral retina (Ekker et al., 1995; Sasagawa et al., 2002; Zhang and Yang, 2001). There is also the hypothesis that retinoic acid (RA) signaling may influence ventral retina identity, based on expression patterns of RA synthesizing enzymes versus RA degrading enzymes; however, there is conflicting evidence that RA signaling actually influences changes in ventral gene markers (Golz et al., 2004; Molotkov et al., 2006).

1.5 Choroid Fissure Closure and Ocular Coloboma

In addition to affecting retinotopic mapping, dorsal-ventral mispatterning can also influence optic fissure closure. Mesenchymal cells that give rise to the intraocular hyaloid vasculature (transient vasculature during embryonic development that nourishes the early lens) and choroidal endothelium (vessels that feed the neural retina) enter the eye through a gap in the ventral retina called the choroid fissure. This fissure forms in the neural retina during invagination of the optic vesicle and extends down the length of the optic stalk. The gap persists

only transiently during development, with the fissure generally fusing between 24-48hpf (Kurita et al., 2004). There also exists a superior optic fissure, but its purpose and timing of formation/closure is not fully understood (Lehmann and Waskiewicz, unpublished). If either fissure fails to close it results in a disorder called ocular coloboma. Multiple tissues can be affected in addition to the retina, including the iris, ciliary body, choroid, and optic nerve (Chang et al., 2006). Coloboma can have varying degrees of severity, with the most detrimental cases causing optic nerve malformation and vision loss. In fact, ocular coloboma is one of the leading causes of childhood blindness, accounting for 5-10% of all cases of congenital blindness (Chang et al., 2006). Ocular colobomata are also frequently a part of a spectrum of disorders that may include microphthalmia anophthalmia, and other systemic abnormalities such as growth retardation, and ear and heart defects (Gregory-Evans et al., 2004). Zebrafish are an excellent model system for studying ocular coloboma because vertebrate eye development is highly conserved, the main structures of the eye are already formed by 24hpf, and they develop externally, making it easier to stage-match genetically modified embryos to controls.

1.6 Wnt Signaling

Wnts are secreted morphogens that set up short-range signaling gradients to pattern such tissues as the neural tube, neural crest, lung, and kidney [reviewed in (Logan and Nusse, 2004)]. The expression and function of *wnt* genes during eye development has been difficult to track. Vertebrate organisms such as zebrafish, mouse, and humans, contain a large number of *wnt* genes that often share overlapping expression patterns and partially redundant functions. Therefore, loss-of-function experiments involving single *wnt* genes are not always informative. Zebrafish, in particular, contain 25 known *wnt* genes. To complicate our understanding of Wnt signal transduction, the Wnt ligand is able to activate multiple pathways. There are three main Wnt signaling pathways: canonical, planar cell polarity (PCP), and calcium-based pathways. It is thought that these

different pathways are initiated based on the complex of receptors and co-receptors that are activated during Wnt ligand binding (Grumolato et al., 2010).

The canonical Wnt pathway, the most well studied pathway, is characterized by the absence or presence of the transcription factor, β -catenin, inside the nucleus. Without Wnt ligand present, the β -catenin degradation complex is active in the cell. This complex consists of a number of proteins including adenomatous polyposis coli (APC), AXIN, casein kinase 1 (CK1), and glycogen synthase kinase 3 (GSK3). When this complex is active, β -catenin is bound by APC, phosphorylated by GSK3, and subsequently ubiquitylated and targeted for destruction in the proteasome (Hayashi et al., 1997; Munemitsu et al., 1995). In the absence of β -catenin in the nucleus, Wnt target genes are left in a repressed state (Korinek et al., 1997). In the active canonical Wnt signaling pathway, the secreted Wnt ligand binds to a receptor on target cells called Frizzled (Fz). Once bound, Fz, and co-receptors, LRP5/6, recruit the protein, Dishevelled (Dsh), and together inhibit the β -catenin degradation complex (Bhanot et al., 1996; Noordermeer et al., 1994). This allows the transcription factor, β -catenin to build up within the cell and enter the nucleus. Nuclear-localized β -catenin forms heterodimers with other T-cell factor (Tcf) or lymphoid enhancer factor (Lef) transcription factors and initiates transcription of Wnt-target genes (Billin et al., 2000) (Figure 1.16.2).

The second Wnt pathway, the PCP pathway, also uses some components of the canonical Wnt pathway but has different downstream effectors and subsequent biological functions. PCP is important for convergence and extension, an early development process that coordinates migration of cells in order to elongate the embryo. In the PCP pathway, the Wnt ligand binds to the Fz receptor and activates Dsh, same as the β -catenin canonical pathway. However, Dsh instead can activate three alternative branches of the pathway through its complex association with Daam1 (disheveled associated activator of morphogenesis 1). The first branch involves activation of Rac GTPase, which, in turn, activates Jnk (c-Jun NH₂-terminal kinase) (Habas et al., 2001; Schlessinger et al., 2009). The

second path is activation of Rho GTPase, which, instead, activates ROCK (Rho-associated kinase) (Habas et al., 2001; Kohn and Moon, 2005). Finally, the PCP pathway can activate Profilin (Sato et al., 2006). All three of these branches are able to influence actin polymerization, a crucial process in cell polarization and migration.

In contrast, in the calcium-Wnt signaling pathway Wnt still binds the Fz receptor to activate Dsh but activates molecules such as inositol 1,4,5-triphosphate (IP3) and diacylglycerol (DAG). Once activated, IP3 diffuses in the cell and interacts with calcium channels on the endoplasmic reticulum to increase intracellular calcium levels. The increase in intracellular calcium and DAG then activates protein kinase C (PKC) (Sheldahl et al., 1999). The calcium, along with calmodulin protein, also activates the calcium-responsive calcium-calmodulin-dependent protein kinase II (CaMKII) (Kuhl et al., 2000). Activated CaMKII and PKC, in turn, induce transcription factors to alter transcription of target genes. Although this pathway is the least understood Wnt signaling pathway, it is known to play roles in inflammatory responses and neuropathfinding. In addition, down-regulation has been associated with certain cancers (De, 2011; Kohn and Moon, 2005)

1.7 Wnt Signaling and Eye Development

During eye formation, the canonical (β -catenin) pathway is the predominant Wnt signaling pathway. In the earliest stages of eye development, Rx inhibits canonical Wnt signaling to allow transition from forebrain to eye field tissue and prevent posteriorization (Martinez-Morales and Wittbrodt, 2009; Wilson and Houart, 2004). Canonical Wnts are also regulators of later eye development, including RPE and retinal patterning. Loss of Wnt signaling in chick and mouse RPE leads to microphthalmia and conversion of RPE into retinal tissue (Fujimura et al., 2009). Furthermore, chromatin immunoprecipitation has shown that the Wnt effectors, Tcf and Lef1, bind to *mitf* and *otx2* enhancers, two genes that are important for RPE development (Westenskow et al., 2009).

Initiation of ocular canonical Wnt signaling, as determined by the Wnt signaling transgenic, *Tg[TOP;GFP]^{w25}* (Dorsky et al., 2002), occurs after optic vesicle formation and initiation of dorsal-ventral eye patterning (Veien et al., 2008). To date, only three known *wnt* genes have specific expression in the developing eye, however other currently unidentified *wnts* may also be expressed in relevant structures. *wnt11r* has lens-specific expression and *wnt2* and *wnt8b* expression turns on in the RPE between 14-16hpf. Morpholino knockdown of *wnt2* and *wnt8b* does not reveal any overt eye phenotypes, supporting the idea that if *wnt* genes are required for retinal patterning, other *wnt* genes are likely sufficient (Veien et al., 2008).

Because of functional redundancy between Wnts, an alternate approach was used to study the potential role of non-canonical Wnt signaling in zebrafish eye development. Overexpression of the Wnt inhibitors *dickkopf* (*dkk1*) or dominant negative Tcf inhibited signaling from any potential Wnt source. In congruence with canonical Wnt activity turning on after dorsal-ventral retina axis initiation, loss of Wnt signaling did not affect expression of early dorsal or ventral retina markers. However, embryos at later stages showed severe defects in retinal gene maintenance including ablation of the dorsal eye markers, *bmp2b*, *bmp4*, and *gdf6a*. Interestingly, dorsal eye phenotypes could be rescued by overexpressing *bmp4*, a member of the Bone Morphogenic Protein (BMP) family. It was therefore concluded that Wnts must act upstream of BMP signaling during the retinal maintenance phase to help establish proper dorso-ventral patterning in the retina (Veien et al., 2008). Similarly, mutation of the mouse Fz co-receptor, LRP6, caused, among other developmental abnormalities, ocular defects including severe ocular coloboma and microphthalmia. Investigation of dorsal-ventral retinal patterning revealed that *Lrp6*^{-/-} mice have expansion of ventral markers (*vax2*) at the expense of dorsal ones (*tbx5* and *bmp4*) (Zhou et al., 2008; Zhou et al., 2010), further supporting the idea that Wnt signaling is important for dorsal retina specification.

1.8 Bone Morphogenic Protein (BMP) Signaling

Bone morphogenic proteins (BMPs) are a family of secreted signaling molecules that function in early embryonic development to establish dorsal and ventral axes in a dose-dependent manner. These molecules are first synthesized as larger precursor proteins that undergo cleavage at the carboxy-terminus to form the mature BMP ligand (Massague, 1990). They are part of a larger family of signaling molecules called transforming growth factor- β s (TGF- β s), which, in addition to BMPs, includes Activins, Inhibins, and the TGF- β s, themselves. The TGF- β supergroup is characterized by the presence of seven conserved cysteine residues, as well as dimerized binding to extracellular transmembrane receptors with serine/threonine kinase activity. There are two types of serine/threonine kinase receptors, type I (BMPR-1) and type II (BMPR-2). Mutations in type I and type II Decapentaplegic (Dpp; *Drosophila* orthologue of BMP) receptors have shown that both types are required for signaling (Ruberte et al., 1995). Activation of one of these receptors, typically type II BMP receptors, promotes the formation of heteromeric complexes with additional type I serine/threonine receptors, followed by subsequent auto-phosphorylation (Weis-Garcia and Massague, 1996; Wieser et al., 1995). The specific compositions of these type I and type II receptor complexes can be quite characteristic and are one of the identifying features of the subfamilies of the TGF- β group (Heldin et al., 1997; Wordinger and Clark, 2007).

Like other growth factors, the activation of the extracellular receptors initiates an internal signaling cascade that results in the expression of target genes. In the case of TGF- β signaling, the serine/threonine kinase receptors phosphorylate a group of proteins called SMADs, named for a combination of the names of its *C. elegans* (*Sma*) and *Drosophila* (*Mad*) homologs. SMADs are downstream effectors that remain in the cytoplasm until phosphorylated and subsequently translocate to the nucleus. There are multiple SMADs that mediate TGF- β signaling, sometimes with opposing functions. In BMP signaling, SMADs 1,5,8 seem to positively affect BMP target gene expression, whereas SMADs 6,7 act as inhibitors of the pathway (Heldin et al., 1997). Once receptor-associated

SMADs are phosphorylated, they bind to other “common-partner” SMADs (SMAD 4) to form heterocomplexes and enter the nucleus (Lagna et al., 1996; Packard et al., 2003). There, they act as transcription factors to initiate expression of target genes (Figure 1.16.3).

BMPs function in a variety of processes during embryonic development. One of the most well studied functions of BMP signaling is its role in the establishment of the early dorsal-ventral axis of the embryo, a process which greatly impacts subsequent patterning events. *BMP* expression is important for specifying the ventral axis of the gastrula. Mutations in zebrafish or *Xenopus* *bmp2b* and *bmp4* result in expansion of dorsal structures (eg. head, notochord, pharynx) at the expense of ventral structures (eg. heart, blood, posterior somites) (Gonzalez et al., 2000; Hammerschmidt et al., 1996; Schmidt et al., 1995). BMP signaling is also involved at early stages of development in the specification of neural versus non-neural ectoderm. More specifically, *Bmp4* and *Bmp7* induce the formation of epidermis and concurrently inhibit the transition of non-neural ectoderm to neural tissue (Tanabe and Jessell, 1996; Wilson and Hemmati-Brivanlou, 1995). At slightly later stages of development, *Bmp4* and *Bmp7* expression from the ectoderm also works antagonistically against *Shh* signaling (from the notochord) to induce dorsalization cell types in the underlying dorsal neural tube (Tanabe and Jessell, 1996). Additionally, BMPs can work to pattern other non-neural tissues such as the vertebrate limb and kidney, as well as promote osteogenesis (Bandyopadhyay et al., 2006; Cheng et al., 2003; Dudley et al., 1995)

Because of their extreme importance in development, BMP expression and signaling output is tightly regulated. This can be achieved via multiple routes: external regulation through inhibitors that promote ligand sequestration, internal inhibitors such as *Smad6* and *Smad7*, and self-regulation. For example, one aspect of BMP regulation involves the use of the extracellular modulator BAMBI (BMP and Activin Membrane Bound Inhibitor), a BMP pseudoreceptor. BMP-binding antagonists such as BAMBI sequester the BMP ligands and prevent them from

interacting with their receptors. Interestingly, although BAMBI is a BMP inhibitor, it is a signaling target that is activated during increased periods of BMP signaling, suggesting a self-regulating loop (Onichtchouk et al., 1999). In fact, further study of the BMP pathway has revealed multiple different negative feedback interactions. A great example of negative feedback regulation can be found in the study of BMP signaling during osteoblast differentiation, which has already unearthed at least four potential negative feedback regulators that function in different parts of the BMP pathway (Murakami et al., 2003; Nishimura et al., 2002; Nishimura et al., 2012; Yoshida et al., 2000; Zamurovic et al., 2004). The existence of multiple self-regulating pathways, therefore, further emphasizes the need for strict regulation of signaling pathways. As such, opposing gradients of BMPs and their secreted antagonists are used to pattern a variety of tissues. Maternally provided *bmp* genes, such as *gdf6a*, activate the zygotic transcription of other *bmp* genes (*bmp2b*, *bmp4*) in the anterior, ventral region of the early gastrula to specify the ventral axis (Sidi et al., 2003). Corresponding to the ventral BMPs, dorsalizing agents (and BMP antagonists) such as Chordin and Bozozok are secreted from the Spemann-Mangold organizer in the posterior, dorsal embryo set up the dorsal axis (Gonzalez et al., 2000; Sasai et al., 1995). These early contrasting gradients of expression therefore help to establish the initial dorso-ventral axis that will specify neural tissue and subsequently guide patterning events throughout the rest of development.

1.9 BMP Signaling and Eye Development

In addition to patterning brain, bone, and kidney, BMP expression is also important for eye patterning. BMP2, 4, and 7 are all expressed in the paraxial mesoderm during early eye morphogenesis and regulate eye vesicle size (Teraoka et al., 2009). As the eye continue to develop, BMP genes such as *bmp2*, *bmp4*, *bmp7*, and *gdf6a* become restricted to the dorsal retina where they both initiate and maintain dorsal retina identity (Belecky-Adams and Adler, 2001; French et al., 2009; Gosse and Baier, 2009). Misexpression, whether upregulation or downregulation, of any of the BMP ligands results in dorsal–ventral retinal

patterning defects. For example, BMP4 has been extensively studied for its role in dorsal retina specification; overexpression of *bmp4* mRNA in various organisms causes dorsalization of the retina (Koshiba-Takeuchi et al., 2000; Sasagawa et al., 2002; Trousse et al., 2001). Corresponding to the expression of BMP4 in the eye, two different known BMP antagonists, Chordin and Noggin, were found in chick ventral retina using mRNA in situ hybridization (ISH) (Belecky-Adams and Adler, 2001). Interestingly, a novel BMP4 antagonist called Ventroptin was also identified in chick due to its similarity to the cysteine repeat regions in Chordin. mRNA ISH revealed that *ventroptin* is expressed in the ventral retina, in the opposite pattern to *bmp4* expression. Binding assays, as well as rescue experiments following BMP overexpression supported the hypothesis that Ventroptin is a novel BMP antagonist (Sakuta et al., 2001). Surprisingly, *ventroptin* expression has not been identified in the retina of any other vertebrates. Researchers have continued to look for additional retinal BMP antagonists in other organisms, but have had little success. Antagonists have been found, however, in other ocular tissues. Mice express *noggin* during eye development, whose expression is required for proper formation of the ciliary body (Zhao et al., 2002). Noggin and Chordin have also been found to regulate lens formation in both mice and chick (Beebe et al., 2004; Belecky-Adams et al., 2002). The presence of BMP antagonists and their influence on ocular formation therefore highlight the importance of BMP regulation during eye morphogenesis.

In addition to BMP4, perturbation of other BMPs also influences eye patterning. For instance, targeted overexpression of mouse *bmp7* in the lens causes aberrant apoptosis in the retina, leading to severe retinal thinning (Hung et al., 2002). Retinal patterning is also impacted by BMP2 depletion, which causes down-regulation of dorsal markers such as *tbx5* and the axon guidance genes *ephrinB1* and *ephrinB2* in chick (Sakuta et al., 2006). Conversely, BMP2 misexpression creates dorsalization of the retina at the expense of ventral retina genes (Sakuta et al., 2006). Another BMP expressed in the dorsal retina is *bmp13*, better known as *gdf6*. Mutations in both human and zebrafish *gdf6* result in a spectrum of anomalies including ocular coloboma (Asai-Coakwell et al., 2007).

The role of *gdf6a* has been studied with regards to dorsal-ventral axis formation in the eye, with noted importance for both initiation and maintenance of dorsal gene markers (French et al., 2009; Gosse and Baier, 2009).

1.10 Secreted Frizzled-Related Proteins

As their name suggests, Secreted frizzled-related proteins (Sfrps) are secreted proteins that contain a domain that is homologous to the extracellular portion of the Wnt-binding receptor, Frizzled (Fz) (Uren et al., 2000). This Fz domain, characterized by an abundance of cysteine residues, has *in vitro* binding to the Wnt ligand and *in vivo* importance for Fz receptor function; protein constructs lacking the cysteine rich domain (CRD) have reduced Wnt signaling. Based on their structural similarity to the CRD of the Fz receptor, Sfrps were classically assumed to be Wnt inhibitors. This was based on the idea that Sfrps bind and sequester available ligand in the extracellular space. In support of this model of Sfrp function, original experiments investigating the relationship between Sfrps and Wnts showed that *Xenopus sfrp3 (frzb)* antagonizes Wnt8 activity; over-expression of *frzb* mRNA rescues the dorsalization phenotypes resulting from *wnt8* mRNA over-expression (Leyns et al., 1997; Wang et al., 1997). Similar conclusions were also obtained in zebrafish following rescue of *wnt8b* dorsalization phenotypes with *sfrp1a* mRNA over-expression (Kim et al., 2007). Conversely, over-expression of *wnt11* can also rescue foregut defects caused by *sfrp5* over-expression in *Xenopus* (Li et al., 2008).

Although early experiments dissecting Sfrp function revealed their role as potential Wnt antagonists, surprising discrepancies involving the relationship between Sfrps and Wnts have surfaced. In particular, there have been conflicting results regarding changes in Wnt signaling following inactivation of one or more *sfrp* genes. In direct contrast to the model of Sfrps acting as Wnt inhibitors, Sfrps have been shown to positively influence Wnt diffusion and consequently aid in Wnt signaling. Co-injection of fluorescently-tagged Wnt and Sfrp proteins (into a 4-cell stage embryo) increases the spread of Wnt in the *Xenopus* gastrula, as compared to Wnt expressed alone (Mii and Taira, 2011). Additional *in vivo*

experiments looking at *Drosophila* imaginal wing discs also suggest that co-expression of Wnts and Sfrps increase the distance travelled by Wnt away from its starting point; *sfrp1* expression was induced in the wing and diffusion of Wingless (Wg), the *Drosophila* Wnt homolog, was monitored with immunohistochemistry using a Wg antibody. Addition of *sfrp1* was sufficient to alter the extracellular diffusion of Wg (Esteve et al., 2011b). Conversely, inhibition of Sfrp function, as seen in *sfrp1a^{-/-}/sfrp2^{-/-}* mouse mutants, prevents proper diffusion of venus-tagged Wnt11 in retina explants; a phenotype that could be rescued by bathing retina cultures in medium supplemented with Sfrp1a (Esteve et al., 2011b). These latest findings, along with research that showed a positive relationship between Sfrps and β -catenin levels in hematopoietic stem cells of *sfrp1* knockout mice (Renstrom et al., 2009), suggest that Sfrps may be required for proper Wnt signaling. In support of this model, Sfrps contain both Wnt-binding and Fz-binding domains (Bovolenta et al., 2008; Lin et al., 1997; Lopez-Rios et al., 2008; Uren et al., 2000), which are hypothesized to aid Wnt-Fz interaction by bringing the receptor and ligand in close proximity (Bovolenta et al., 2008). It should be noted, however, that Sfrps may act in a dose dependent, biphasic manner. Overexpression experiments of Sfrp1 in *Drosophila*, a model system that does not endogenously express Sfrp, induced changes whereby higher concentrations of Sfrp inhibit Wnt signaling and lower concentrations promote Wnt signaling (Uren et al., 2000). Although these experiments were performed in an environment that does not typically interact with Sfrps, they may provide a potential explanation for the discrepancies between Sfrp functions both within and between different model species. Interestingly, the Sfrp cysteine-rich domain may also allow Sfrps to have signaling activity of their own independent of the Wnt ligand (Bafico et al., 1999).

1.11 Zebrafish Secreted Frizzled-Related Proteins

The zebrafish genome contains seven known *sfrp* genes: *sfrp1a*, *sfrp1b*, *sfrp2*, *sfrp3* (*frzb*), *sfrp5*, *sizzled*, and *tlc*. Sequence homology has shown that these genes can be broken down into sub-categories of relatedness; *sfrp1a*, *sfrp1b*, *sfrp2*, and *sfrp5* are all more closely related to each other than to the other *sfrp*

genes. Furthermore, *sfrp1a*, *sfrp1b*, and *sfrp5* form an even smaller sub-category of increased homology (Tendeng and Houart, 2006). Not surprisingly, this group of highly related *sfrp* genes has been shown to work cooperatively to pattern tissues in the developing embryo. Work done on the *lim homeobox 5* (*lhx5*) transcription factor identified it as a regulator of both *sfrp1a* and *sfrp5* and highlighted their joint role in patterning the zebrafish forebrain (Peng and Westerfield, 2006). In addition, studies in mice have shown that single *sfrp* mutants display few overt phenotypes as compared to double *sfrp* mutants. Such is the case with *sfrp1a*^{-/-}/*sfrp2*^{-/-} mice, which only showed defects in peripheral optic cup formation, retinal neurogenesis, and somitogenesis in the double mutant strain (Esteve et al., 2011a; Esteve et al., 2011b; Satoh et al., 2006). Therefore, functional redundancy seems to be a recurrent theme with regards to Sfrp activity.

Few zebrafish Sfrps have been studied in detail with regards to development. In addition to the role of Sfrp1a and Sfrp5 in forebrain patterning (Peng and Westerfield, 2006), we know that Sfrp1a plays an important role in eye field specification, as overexpression causes expansion of the optic primordium (Kim et al., 2007). Early embryonic dorsal-ventral development also requires Sfrp1a and Frzb (Sfrp3) as secreted antagonists to restrict the domain of the maternally provided dorsal determinant, Wnt8a (Lu et al., 2011). Similarly, TLC antagonizes early Wnt8b signaling to protect specification of the telencephalon (Houart et al., 2002). Additionally, zebrafish Sizzled has been linked to BMP signaling during early formation of the dorsal-ventral axis by regulating a modifier of the BMP inhibitor, Chordin (Yabe et al., 2003).

1.12 Sfrp Protein Structure and Function

Two functional domains are characteristic of secreted frizzled-related proteins, the netrin (NTR) domain and the cysteine-rich domain (CRD). The exact biological function of either domain for Sfrp activity are unknown; however expression of truncated forms of Sfrp proteins lacking the either the NTR domain or CRD can reduce their ability to activate Wnt signaling. Interestingly, these results are not always consistent and, depending on the particular Sfrp/Wnt

combination, certain domains seem to be more important for biological interaction than others. For instance, removal of the *Xenopus* Sfrp3 CRD domain prevents binding to Wnt1, whereas removal of the NTR domain produces only a mild reduction in activity (Lin et al., 1997). In contrast, truncated human Sfrp1 lacking the NTR domain was no longer able to bind the *Drosophila* Wnt homologue, Wg, but retained Wg binding ability without the CRD domain (Uren et al., 2000). Similarly, the NTR domain was found to be the biologically active domain for Sfrp1 Wnt inhibition in Medaka (Lopez-Rios et al., 2008). Together, these data suggest that Sfrp CRD and NTR domains can interact with Wnt ligands with different affinities, based on altered Sfrp-Wnt pairing or Sfrp conformation.

Variability between results of binding assays has made it difficult to fully understand the interaction of these protein domains. However, insight into the biological functions of the NTR domain and the CRD can be drawn from their appearance in other proteins. For example, NTR domains are found in proteins such as netrins and metalloproteases. Netrins are guidance molecules and function during neuronal migration. Interestingly, Sfrp1 has been shown to influence RGC axon guidance in both chick and *Xenopus* by acting directly with the Fz2 receptor to activate the calcium-mediated Wnt signaling pathway (Rodriguez et al., 2005). In contrast, metalloproteases function in the cleavage of metalloproteins. Metalloproteins are commonly found in the extracellular matrix (ECM) and are important for interactions between the ECM and various extracellular ligands. Sfrps interact with metalloproteins in the BMP signaling pathway. The metalloprotease, Tolloid (BMP1), cleaves the BMP inhibitor Chordin and reduces its ability to bind BMP. Multiple Sfrps, including Sizzled, Crescent, and Sfrp2 have been shown to interact with Tolloid, preventing Chordin cleavage and inducing BMP inhibition (Lee et al., 2006; Ploper et al., 2011).

1.13 Sfrp Interaction With Other Pathways

Although most studies have been done with regards to Sfrps and Wnt signaling, additional evidence is building that Sfrps influence other important signaling pathways. In particular, Sfrps have been linked to BMP signaling, as

well as Notch signaling. The first Sfrp to be identified as a BMP antagonist was Sizzled. The *sizzled* gene was identified as a dorsalizing factor in the *ogon* mutant zebrafish, which had striking ventralization phenotypes. Sizzled was proposed to be a BMP inhibitor and not a Wnt inhibitor because the misexpression defects were specifically dorsalization and not anteriorization, as seen in overexpression of other Sfrps or the Wnt antagonist, Dkk1. Additionally, *ogon* mutant phenotypes could be rescued by inhibiting BMP signaling. Interestingly, the phenotypes associated with *sizzled* overexpression required Chordin to be present; injection of *sizzled* mRNA into *chordino* mutants did not elicit the dorsalization phenotype. This, along with evidence that the *ogon* mutation does not synergize with the *chordino* mutation, suggested that Sizzled affects BMP signaling through interactions with Chordin (Yabe et al., 2003). As a follow-up to these results, it was found that, in *Xenopus*, Sizzled affects Chordin degradation through interference with an upstream tolloid chordinase, Xlr (Lee et al., 2006). More recently, an additional Sfrp was also found to inhibit BMP by competitive inhibition of Tolloid proteases. Crescent, a *Xenopus* Sfrp for which no zebrafish ortholog has been identified, was able to inhibit in a dose-dependent manner Tolloid digestion of Chordin (Ploper et al., 2011). In the same study, mammalian Sfrp2 was also found to bind Tolloid and potentially act as an inhibitor.

Sfrps were also recently linked to inhibition of another metalloprotease, a disintegrin and metalloprotease domain-containing protein 10 (ADAM10). ADAM10 has been given the description “shedase” because it functions to cleave domains of proteins present at the extracellular surface, mediating their diffusion or “shedding” into the extracellular space. Investigation of *sfrp1^{-/-}/sfrp2^{-/-}* mice revealed that double mutants have increased numbers of photoreceptors, indicating a defect in retinal neurogenesis. Since Notch signaling is a common mechanism to regulate cell differentiation, they chose to look at changes in the Notch pathway. They found Notch signaling to be down-regulated, based on lowered levels of the intracellular active form NICD. Further investigation revealed that Sfrp interacts with ADAM10 and that ADAM10 inhibition rescues *sfrp* mutant retinal neurogenesis phenotypes. Therefore, based

on these data, it was proposed that mouse *sfrp1* and *sfrp2* act as inhibitors of ADAM10 to mediate retinal neurogenesis (Esteve et al., 2011a).

1.14 Sfrps and Eye Development

Most of the work involving Sfrps and eye development has revolved around their role in earliest stages of eye morphogenesis, namely eye field specification. Previous studies have found that *sfrp1a* or *sfrp5* mRNA overexpression causes anteriorization of the embryo, including expansion of the optic primordium and forebrain markers such as *sine oculis homeobox homolog 3b* (*six3b*) and *empty spiracles homeobox 3* (*emx3*) (Kim et al., 2007) (Peng and Westerfield, 2006). Analogous results were also found in Medaka *sfrp1* studies, which induced forebrain expansion with overexpression and eye field reduction during morpholino knockdown (Lopez-Rios et al., 2008). These phenotypes are similar to those seen following overexpression of Wnt inhibitors, supporting the idea that *sfrp1a* and *sfrp5* may act as Wnt antagonists during development. The function of zebrafish *sfrp1a* has not been studied at any later stages, including retinal patterning. In contrast, *osfrp5* has been studied in *Medaka* during retinal patterning, a tissue where both zebrafish and Medaka orthologues have similar expression patterns. Morpholino knockdown of *osfrp5* causes loss of ventral identity and changes in both cell proliferation and apoptosis in the developing eye (Ruiz et al., 2009).

Although multiple studies of *sfrp1a* and *sfrp5* in teleosts support the idea that Sfrps act as Wnt antagonists (Kim et al., 2007; Leyns et al., 1997; Ruiz et al., 2009; Wang et al., 1997), recent experiments involving mouse *sfrp1/sfrp2* double knockouts support the idea that Sfrps are required for Wnt function during patterning of the peripheral optic cup (Esteve et al., 2011b). While informative, evidence for Sfrps as being Wnt facilitators in the formation of the peripheral optic cup suggests that either Sfrps have differing functions between vertebrates, Sfrps have very distinct, tissue-specific functions, or that each individual Sfrp may affect Wnt signaling in a different manor.

Compiling all of the data, there are currently four proposed mechanisms of Sfrp modulation of Wnt signaling. In the first model, Sfrps use both the CRD and NTR domains to sequester Wnts and inhibit signaling. Conversely, Sfrps may facilitate Wnt signaling by binding the CRD and NTR domains to the Wnt ligand and bringing it in close proximity to the Fz receptor. Additionally, based on its ability to directly bind Fz, Sfrps have also been proposed to act as dominant negative inhibitors that occupy the receptor site (Bafico et al., 1999). Finally, Sfrps have also been shown to activate Wnt-independent signaling through Fz binding, as seen during *Sfrp1* regulated retinal axon guidance (Drescher, 2005). Evidence has been collected to support each of these models, making it difficult to determine the exact mechanism behind Sfrp modulation of the Wnt signaling. Therefore, the lack of consistency between experimental results argues that more research needs to be conducted involving Sfrp activity and function.

1.15 Purpose of Research and Working Hypothesis

Based on the discrepancies involving the relationship between Sfrp function and Wnt signaling during eye development, we decided to study the role of zebrafish *sfrp1a* and *sfrp5* in the formation of the dorsal-ventral axis of the retina, a question that has not previously been examined. From our experiments, we hope to gain a better understanding of Sfrp regulation of Wnt signaling as well as how Wnt signaling interacts with other signaling cascades. Using the classical model of Sfrps as Wnt antagonists, we predicted that *sfrp1a* and *sfrp5* knockdown would cause defects in retinal specification consistent with increased Wnt resulting in an expansion of dorsal identity at the expense of ventral retina.

1.16 Figures

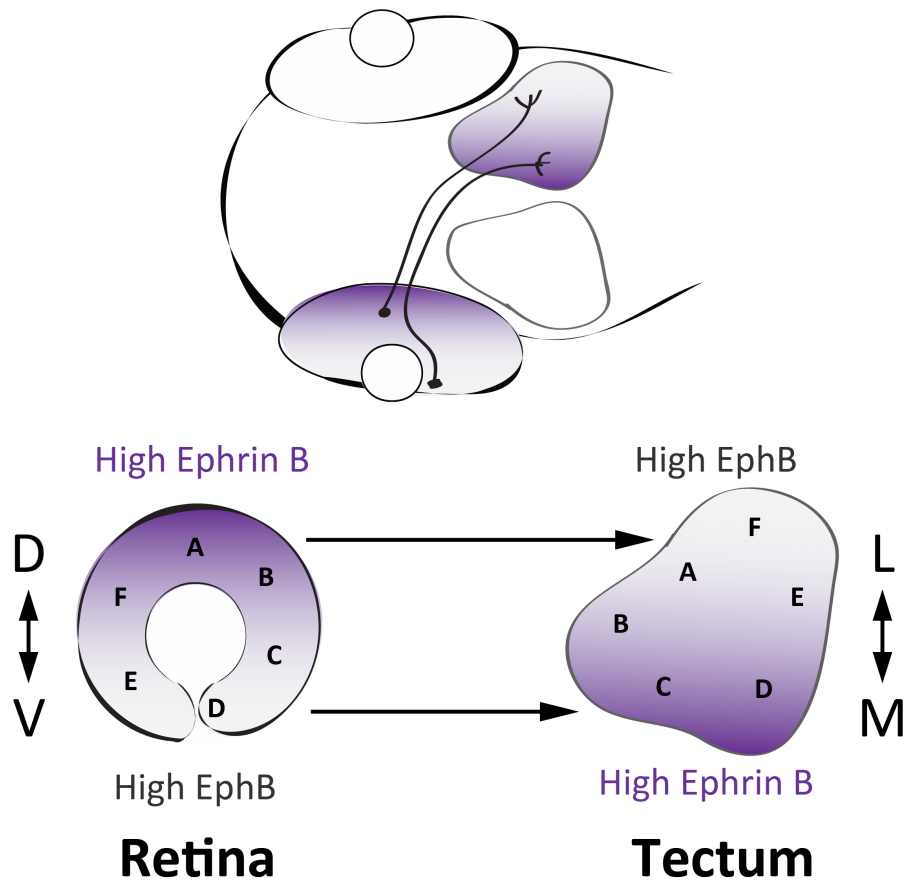


Figure 1.1. Dorsal-ventral retinotectal mapping in zebrafish. Retinal ganglion cells are given positional cues from the expression of Eph receptors and Ephrins ligands that guide innervation of the optic tectum. These positional cues are mediated by attractive interactions between EphB receptors and Ephrin B ligands. Ephrin B is expressed in a dorsal-high to ventral-low gradient in the retina. RGC axons from the dorsal retina express high levels of Ephrin B and are attracted to the lateral contralateral tectum, which expresses high levels of the EphB receptor. Conversely, the EphB receptor is expressed in a ventral-high to dorsal-low gradient. RGCs from the ventral retina instead project their axons to the medial contralateral tectum, which expresses higher levels of the Ephrin B ligand (Trowe et al., 1996).

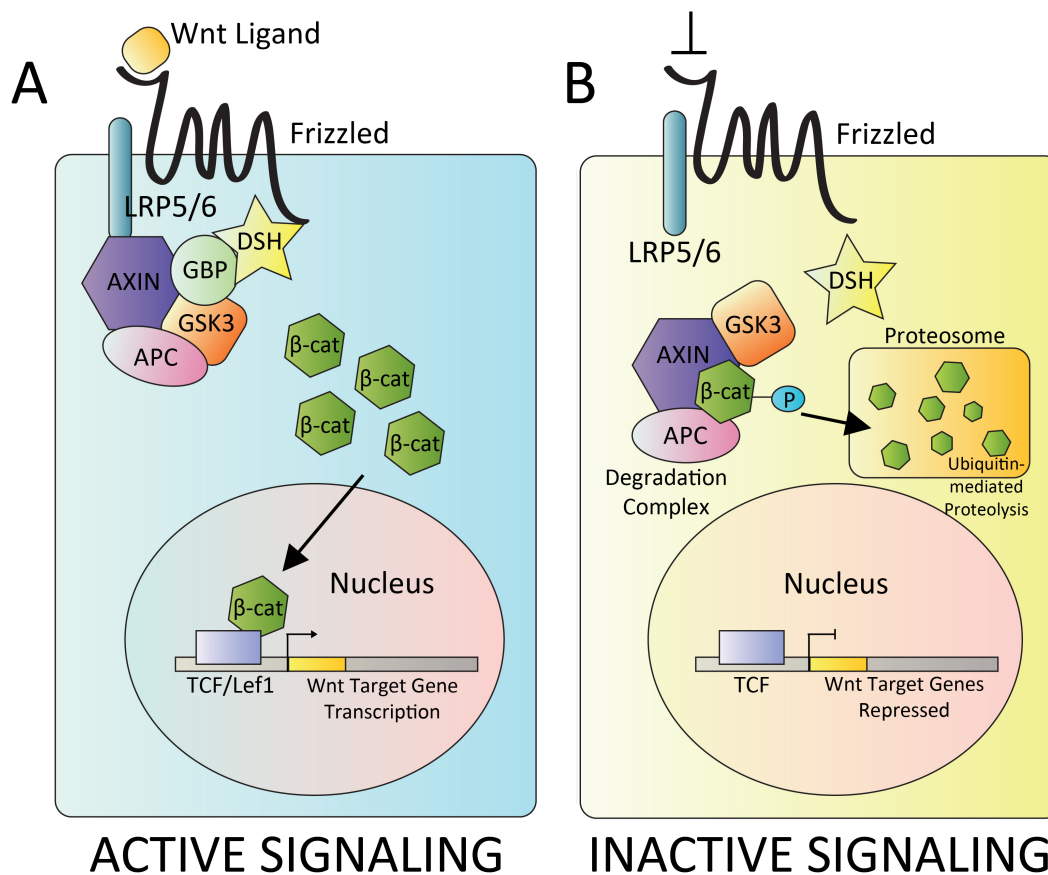


Figure 1.2. Overview of the canonical Wnt pathway. A) During active signaling, the Wnt ligand binds to the Frizzled receptor. This recruits co-receptors, such as LRP5/6 and the intracellular modulator DSH to bind and inhibit the β -catenin degradation complex. This complex contains the inhibitory proteins Axin, GBP, GSK3, and APC. With the complex inhibited, the β -catenin transcription factor builds up in the cytoplasm and enters the nucleus. Once in the nucleus, it binds to other co-factors such as TCF and Lef1 and activates target gene expression. B) When Wnt signaling is inhibited or no ligand is present, DSH is no longer recruited and the β -catenin degradation complex remains functional in the cytoplasm. APC binds β -catenin, allowing GSK3-mediated phosphorylation. Phosphorylation of β -catenin then targets it for ubiquitinylation and subsequent degradation in the proteasome. Without β -catenin present in the nucleus, TCF remains bound to the DNA and acts as a transcriptional repressor (Reviewed in

Moon et al., 2004). APC - adenomatous polyposis coli, DSH – dishevelled, GBP – GSK3 binding protein; GSK3 - glycogen synthase kinase 3, Lef – Lymphoid enhancer factor, P – phosphorylation, LRP5/6 – LDL-receptor-related proteins 5/6, Tcf – T-cell factor.

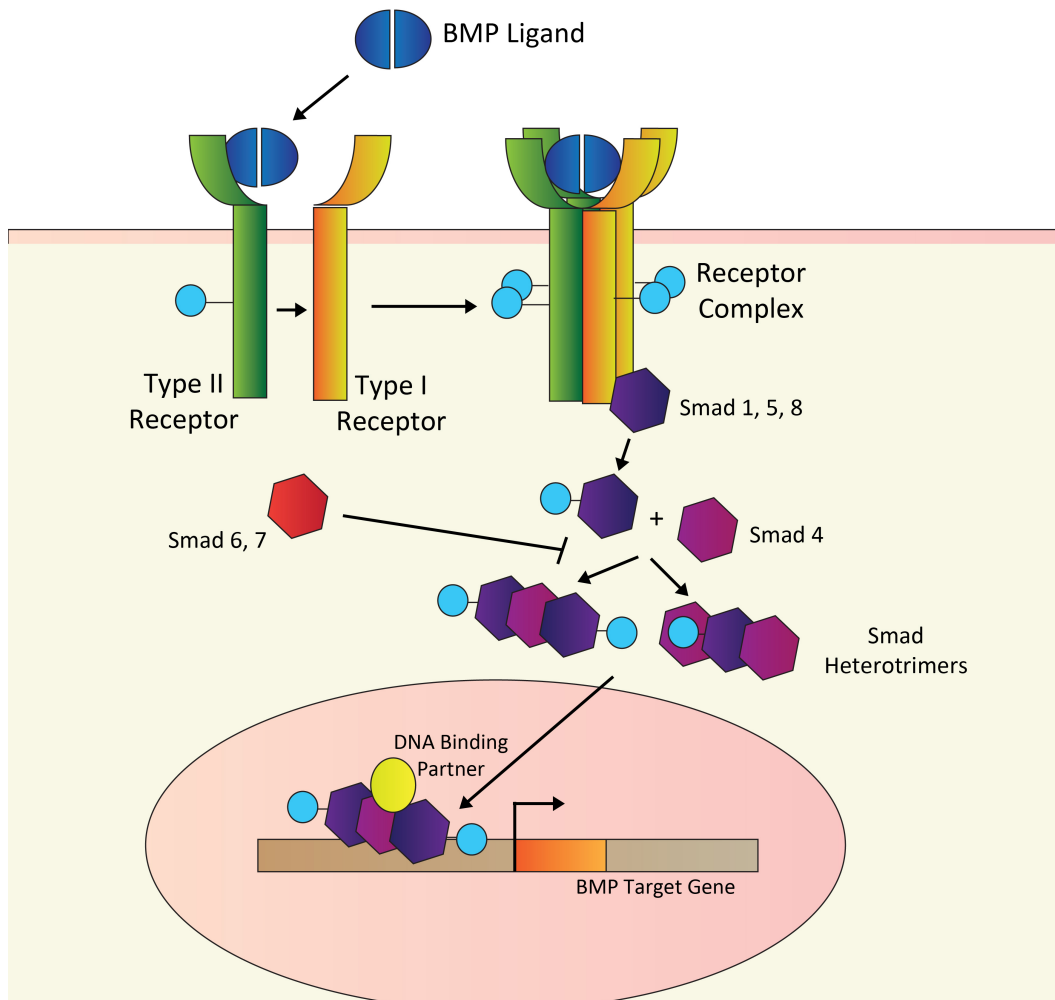


Figure 1.3. Overview of canonical bone morphogenic protein (BMP) signaling. Dimerized BMP ligand binds to a Type II serine threonine kinase receptor, which recruits a Type I serine threonine kinase receptor. Ligand binding induces the formation of a receptor complex of characteristic combinations of Type I and Type II receptors. Receptor-regulated Smads present in the nucleus (Smad 1,5,8) are activated by phosphorylation from the receptor complex. Activated Smads then bind to other “common” Smads (Smad 4) to form heterotrimers. This process is negatively regulated by the inhibitory Smads (Smad 6,7). The heterotrimers then enter the nucleus, bind to other cofactors, and activate BMP target gene transcription (Reviewed in Packard et al., 2003).

1.18 Literature Cited

- Acampora, D., Mazan, S., Lallemand, Y., Avantaggiato, V., Maury, M., Simeone, A., and Brulet, P. (1995). Forebrain and midbrain regions are deleted in *Otx2*^{-/-} mutants due to a defective anterior neuroectoderm specification during gastrulation. *Development* *121*, 3279-3290.
- Adler, R., and Belecky-Adams, T.L. (2002). The role of bone morphogenetic proteins in the differentiation of the ventral optic cup. *Development* *129*, 3161-3171.
- Andreazzoli, M., Gestri, G., Angeloni, D., Menna, E., and Barsacchi, G. (1999). Role of *Xrx1* in *Xenopus* eye and anterior brain development. *Development* *126*, 2451-2460.
- Andreazzoli, M., Gestri, G., Cremisi, F., Casarosa, S., Dawid, I.B., and Barsacchi, G. (2003). *Xrx1* controls proliferation and neurogenesis in *Xenopus* anterior neural plate. *Development* *130*, 5143-5154.
- Asai-Coakwell, M., French, C.R., Berry, K.M., Ye, M., Koss, R., Somerville, M., Mueller, R., van Heyningen, V., Waskiewicz, A.J., and Lehmann, O.J. (2007). *GDF6*, a novel locus for a spectrum of ocular developmental anomalies. *Am J Hum Genet* *80*, 306-315.
- Bafico, A., Gazit, A., Pramila, T., Finch, P.W., Yaniv, A., and Aaronson, S.A. (1999). Interaction of frizzled related protein (FRP) with Wnt ligands and the frizzled receptor suggests alternative mechanisms for FRP inhibition of Wnt signaling. *J Biol Chem* *274*, 16180-16187.
- Bailey, T.J., El-Hodiri, H., Zhang, L., Shah, R., Mathers, P.H., and Jamrich, M. (2004). Regulation of vertebrate eye development by *Rx* genes. *Int J Dev Biol* *48*, 761-770.
- Bandyopadhyay, A., Tsuji, K., Cox, K., Harfe, B.D., Rosen, V., and Tabin, C.J. (2006). Genetic analysis of the roles of *BMP2*, *BMP4*, and *BMP7* in limb patterning and skeletogenesis. *PLoS Genet* *2*, e216.
- Barbieri, A.M., Lupo, G., Bulfone, A., Andreazzoli, M., Mariani, M., Fougereuse, F., Consalez, G.G., Borsani, G., Beckmann, J.S., Barsacchi, G., *et al.* (1999). A homeobox gene, *vax2*, controls the patterning of the eye dorsoventral axis. *Proc Natl Acad Sci U S A* *96*, 10729-10734.
- Beebe, D., Garcia, C., Wang, X., Rajagopal, R., Feldmeier, M., Kim, J.Y., Chytil, A., Moses, H., Ashery-Padan, R., and Rauchman, M. (2004). Contributions by members of the TGFbeta superfamily to lens development. *Int J Dev Biol* *48*, 845-856.

- Behesti, H., Holt, J.K., and Sowden, J.C. (2006). The level of BMP4 signaling is critical for the regulation of distinct T-box gene expression domains and growth along the dorso-ventral axis of the optic cup. *BMC Dev Biol* 6, 62.
- Belecky-Adams, T., and Adler, R. (2001). Developmental expression patterns of bone morphogenetic proteins, receptors, and binding proteins in the chick retina. *J Comp Neurol* 430, 562-572.
- Belecky-Adams, T.L., Adler, R., and Beebe, D.C. (2002). Bone morphogenetic protein signaling and the initiation of lens fiber cell differentiation. *Development* 129, 3795-3802.
- Bhanot, P., Brink, M., Samos, C.H., Hsieh, J.C., Wang, Y., Macke, J.P., Andrew, D., Nathans, J., and Nusse, R. (1996). A new member of the frizzled family from *Drosophila* functions as a Wntless receptor. *Nature* 382, 225-230.
- Billin, A.N., Thirlwell, H., and Ayer, D.E. (2000). Beta-catenin-histone deacetylase interactions regulate the transition of LEF1 from a transcriptional repressor to an activator. *Mol Cell Biol* 20, 6882-6890.
- Bovolenta, P., Esteve, P., Ruiz, J.M., Cisneros, E., and Lopez-Rios, J. (2008). Beyond Wnt inhibition: new functions of secreted Frizzled-related proteins in development and disease. *J Cell Sci* 121, 737-746.
- Branchek, T., and Bremiller, R. (1984). The development of photoreceptors in the zebrafish, *Brachydanio rerio*. I. Structure. *J Comp Neurol* 224, 107-115.
- Carl, M., Loosli, F., and Wittbrodt, J. (2002). Six3 inactivation reveals its essential role for the formation and patterning of the vertebrate eye. *Development* 129, 4057-4063.
- Chang, L., Blain, D., Bertuzzi, S., and Brooks, B.P. (2006). Uveal coloboma: clinical and basic science update. *Curr Opin Ophthalmol* 17, 447-470.
- Cheng, H., Jiang, W., Phillips, F.M., Haydon, R.C., Peng, Y., Zhou, L., Luu, H.H., An, N., Breyer, B., Vanichakarn, P., *et al.* (2003). Osteogenic activity of the fourteen types of human bone morphogenetic proteins (BMPs). *J Bone Joint Surg Am* 85-A, 1544-1552.
- Cheng, H.J., Nakamoto, M., Bergemann, A.D., and Flanagan, J.G. (1995). Complementary gradients in expression and binding of ELF-1 and Mek4 in development of the topographic retinotectal projection map. *Cell* 82, 371-381.

- Cheyette, B.N., Green, P.J., Martin, K., Garren, H., Hartenstein, V., and Zipursky, S.L. (1994). The *Drosophila sine oculis* locus encodes a homeodomain-containing protein required for the development of the entire visual system. *Neuron* *12*, 977-996.
- Chow, R.L., Altmann, C.R., Lang, R.A., and Hemmati-Brivanlou, A. (1999). Pax6 induces ectopic eyes in a vertebrate. *Development* *126*, 4213-4222.
- Chuang, J.C., and Raymond, P.A. (2001). Zebrafish genes rx1 and rx2 help define the region of forebrain that gives rise to retina. *Dev Biol* *231*, 13-30.
- De, A. (2011). Wnt/Ca²⁺ signaling pathway: a brief overview. *Acta Biochim Biophys Sin (Shanghai)* *43*, 745-756.
- Del Bene, F., Tessmar-Raible, K., and Wittbrodt, J. (2004). Direct interaction of geminin and Six3 in eye development. *Nature* *427*, 745-749.
- Donner, A.L., Lachke, S.A., and Maas, R.L. (2006). Lens induction in vertebrates: variations on a conserved theme of signaling events. *Semin Cell Dev Biol* *17*, 676-685.
- Dorsky, R.I., Sheldahl, L.C., and Moon, R.T. (2002). A transgenic Lef1/beta-catenin-dependent reporter is expressed in spatially restricted domains throughout zebrafish development. *Dev Biol* *241*, 229-237.
- Drescher, U. (2005). A no-Wnt situation: SFRPs as axon guidance molecules. *Nat Neurosci* *8*, 1281-1282.
- Dudley, A.T., Lyons, K.M., and Robertson, E.J. (1995). A requirement for bone morphogenetic protein-7 during development of the mammalian kidney and eye. *Genes Dev* *9*, 2795-2807.
- Ekker, S.C., Ungar, A.R., Greenstein, P., von Kessler, D.P., Porter, J.A., Moon, R.T., and Beachy, P.A. (1995). Patterning activities of vertebrate hedgehog proteins in the developing eye and brain. *Curr Biol* *5*, 944-955.
- Esteve, P., Sandonis, A., Cardozo, M., Malapeira, J., Ibanez, C., Crespo, I., Marcos, S., Gonzalez-Garcia, S., Toribio, M.L., Arribas, J., *et al.* (2011a). SFRPs act as negative modulators of ADAM10 to regulate retinal neurogenesis. *Nat Neurosci* *14*, 562-569.
- Esteve, P., Sandonis, A., Ibanez, C., Shimono, A., Guerrero, I., and Bovolenta, P. (2011b). Secreted frizzled-related proteins are required for Wnt/beta-catenin signalling activation in the vertebrate optic cup. *Development* *138*, 4179-4184.

- French, C.R., Erickson, T., French, D.V., Pilgrim, D.B., and Waskiewicz, A.J. (2009). Gdf6a is required for the initiation of dorsal-ventral retinal patterning and lens development. *Dev Biol* 333, 37-47.
- Fujimura, N., Taketo, M.M., Mori, M., Korinek, V., and Kozmik, Z. (2009). Spatial and temporal regulation of Wnt/beta-catenin signaling is essential for development of the retinal pigment epithelium. *Dev Biol* 334, 31-45.
- Furukawa, T., Kozak, C.A., and Cepko, C.L. (1997). rax, a novel paired-type homeobox gene, shows expression in the anterior neural fold and developing retina. *Proc Natl Acad Sci U S A* 94, 3088-3093.
- Glaser, T., Walton, D.S., and Maas, R.L. (1992). Genomic structure, evolutionary conservation and aniridia mutations in the human PAX6 gene. *Nat Genet* 2, 232-239.
- Golz, S., Lantin, C., and Mey, J. (2004). Retinoic acid-dependent regulation of BMP4 and Tbx5 in the embryonic chick retina. *Neuroreport* 15, 2751-2755.
- Gonzalez, E.M., Fekany-Lee, K., Carmany-Rampey, A., Erter, C., Topczewski, J., Wright, C.V., and Solnica-Krezel, L. (2000). Head and trunk in zebrafish arise via coinhibition of BMP signaling by bozozok and chordino. *Genes Dev* 14, 3087-3092.
- Gosse, N.J., and Baier, H. (2009). An essential role for Radar (Gdf6a) in inducing dorsal fate in the zebrafish retina. *Proc Natl Acad Sci U S A* 106, 2236-2241.
- Gregory-Evans, C.Y., Williams, M.J., Halford, S., and Gregory-Evans, K. (2004). Ocular coloboma: a reassessment in the age of molecular neuroscience. *J Med Genet* 41, 881-891.
- Greiling, T.M., and Clark, J.I. (2009). Early lens development in the zebrafish: a three-dimensional time-lapse analysis. *Dev Dyn* 238, 2254-2265.
- Grumolato, L., Liu, G., Mong, P., Mudbhary, R., Biswas, R., Arroyave, R., Vijayakumar, S., Economides, A.N., and Aaronson, S.A. (2010). Canonical and noncanonical Wnts use a common mechanism to activate completely unrelated coreceptors. *Genes Dev* 24, 2517-2530.
- Gu, S.M., Thompson, D.A., Srikumari, C.R., Lorenz, B., Finckh, U., Nicoletti, A., Murthy, K.R., Rathmann, M., Kumaramanickavel, G., Denton, M.J., *et al.* (1997). Mutations in RPE65 cause autosomal recessive childhood-onset severe retinal dystrophy. *Nat Genet* 17, 194-197.

- Habas, R., Kato, Y., and He, X. (2001). Wnt/Frizzled activation of Rho regulates vertebrate gastrulation and requires a novel Formin homology protein Daam1. *Cell* 107, 843-854.
- Halder, G., Callaerts, P., and Gehring, W.J. (1995). Induction of ectopic eyes by targeted expression of the eyeless gene in *Drosophila*. *Science* 267, 1788-1792.
- Hammerschmidt, M., Pelegri, F., Mullins, M.C., Kane, D.A., van Eeden, F.J., Granato, M., Brand, M., Furutani-Seiki, M., Haffter, P., Heisenberg, C.P., *et al.* (1996). *dino* and *mercedes*, two genes regulating dorsal development in the zebrafish embryo. *Development* 123, 95-102.
- Hanson, I., and Van Heyningen, V. (1995). Pax6: more than meets the eye. *Trends Genet* 11, 268-272.
- Hayashi, S., Rubinfeld, B., Souza, B., Polakis, P., Wieschaus, E., and Levine, A.J. (1997). A *Drosophila* homolog of the tumor suppressor gene adenomatous polyposis coli down-regulates beta-catenin but its zygotic expression is not essential for the regulation of Armadillo. *Proc Natl Acad Sci U S A* 94, 242-247.
- Heitzler, P., Coulson, D., Saenz-Robles, M.T., Ashburner, M., Roote, J., Simpson, P., and Gubb, D. (1993). Genetic and cytogenetic analysis of the 43A-E region containing the segment polarity gene *costa* and the cellular polarity genes *prickle* and *spiny-legs* in *Drosophila melanogaster*. *Genetics* 135, 105-115.
- Heldin, C.H., Miyazono, K., and ten Dijke, P. (1997). TGF-beta signalling from cell membrane to nucleus through SMAD proteins. *Nature* 390, 465-471.
- Hindges, R., McLaughlin, T., Genoud, N., Henkemeyer, M., and O'Leary, D.D. (2002). EphB forward signaling controls directional branch extension and arborization required for dorsal-ventral retinotopic mapping. *Neuron* 35, 475-487.
- Holash, J.A., and Pasquale, E.B. (1995). Polarized expression of the receptor protein tyrosine kinase Cck5 in the developing avian visual system. *Dev Biol* 172, 683-693.
- Houart, C., Caneparo, L., Heisenberg, C., Barth, K., Take-Uchi, M., and Wilson, S. (2002). Establishment of the telencephalon during gastrulation by local antagonism of Wnt signaling. *Neuron* 35, 255-265.

- Hung, F.C., Zhao, S., Chen, Q., and Overbeek, P.A. (2002). Retinal ablation and altered lens differentiation induced by ocular overexpression of BMP7. *Vision Res* 42, 427-438.
- Jensen, A.M., and Westerfield, M. (2004). Zebrafish mosaic eyes is a novel FERM protein required for retinal lamination and retinal pigmented epithelial tight junction formation. *Curr Biol* 14, 711-717.
- Jordan, T., Hanson, I., Zaletayev, D., Hodgson, S., Prosser, J., Seawright, A., Hastie, N., and van Heyningen, V. (1992). The human PAX6 gene is mutated in two patients with aniridia. *Nat Genet* 1, 328-332.
- Kim, H.S., Shin, J., Kim, S.H., Chun, H.S., Kim, J.D., Kim, Y.S., Kim, M.J., Rhee, M., Yeo, S.Y., and Huh, T.L. (2007). Eye field requires the function of Sfrp1 as a Wnt antagonist. *Neurosci Lett* 414, 26-29.
- Kohn, A.D., and Moon, R.T. (2005). Wnt and calcium signaling: beta-catenin-independent pathways. *Cell Calcium* 38, 439-446.
- Korinek, V., Barker, N., Morin, P.J., van Wichen, D., de Weger, R., Kinzler, K.W., Vogelstein, B., and Clevers, H. (1997). Constitutive transcriptional activation by a beta-catenin-Tcf complex in APC^{-/-} colon carcinoma. *Science* 275, 1784-1787.
- Koshiba-Takeuchi, K., Takeuchi, J.K., Matsumoto, K., Momose, T., Uno, K., Hoepker, V., Ogura, K., Takahashi, N., Nakamura, H., Yasuda, K., *et al.* (2000). Tbx5 and the retinotectum projection. *Science* 287, 134-137.
- Kuhl, M., Sheldahl, L.C., Malbon, C.C., and Moon, R.T. (2000). Ca(2+)/calmodulin-dependent protein kinase II is stimulated by Wnt and Frizzled homologs and promotes ventral cell fates in *Xenopus*. *J Biol Chem* 275, 12701-12711.
- Kurita, R., Tabata, Y., Sagara, H., Arai, K., and Watanabe, S. (2004). A novel smoothelin-like, actin-binding protein required for choroidal fissure closure in zebrafish. *Biochem Biophys Res Commun* 313, 1092-1100.
- Lagna, G., Hata, A., Hemmati-Brivanlou, A., and Massague, J. (1996). Partnership between DPC4 and SMAD proteins in TGF-beta signalling pathways. *Nature* 383, 832-836.
- Lagutin, O.V., Zhu, C.C., Kobayashi, D., Topczewski, J., Shimamura, K., Puelles, L., Russell, H.R., McKinnon, P.J., Solnica-Krezel, L., and Oliver, G. (2003). Six3 repression of Wnt signaling in the anterior neuroectoderm is essential for vertebrate forebrain development. *Genes Dev* 17, 368-379.

- Lee, H.X., Ambrosio, A.L., Reversade, B., and De Robertis, E.M. (2006). Embryonic dorsal-ventral signaling: secreted frizzled-related proteins as inhibitors of tolloid proteinases. *Cell* 124, 147-159.
- Lemke, G., and Reber, M. (2005). Retinotectal mapping: new insights from molecular genetics. *Annu Rev Cell Dev Biol* 21, 551-580.
- Leyns, L., Bouwmeester, T., Kim, S.H., Piccolo, S., and De Robertis, E.M. (1997). Frzb-1 is a secreted antagonist of Wnt signaling expressed in the Spemann organizer. *Cell* 88, 747-756.
- Li, Y., Rankin, S.A., Sinner, D., Kenny, A.P., Krieg, P.A., and Zorn, A.M. (2008). Sfrp5 coordinates foregut specification and morphogenesis by antagonizing both canonical and noncanonical Wnt11 signaling. *Genes Dev* 22, 3050-3063.
- Lin, K., Wang, S., Julius, M.A., Kitajewski, J., Moos, M., Jr., and Luyten, F.P. (1997). The cysteine-rich frizzled domain of Frzb-1 is required and sufficient for modulation of Wnt signaling. *Proc Natl Acad Sci U S A* 94, 11196-11200.
- Logan, C.Y., and Nusse, R. (2004). The Wnt signaling pathway in development and disease. *Annu Rev Cell Dev Biol* 20, 781-810.
- Loosli, F., Staub, W., Finger-Baier, K.C., Ober, E.A., Verkade, H., Wittbrodt, J., and Baier, H. (2003). Loss of eyes in zebrafish caused by mutation of chokh/rx3. *EMBO Rep* 4, 894-899.
- Loosli, F., Winkler, S., Burgtorf, C., Wurmbach, E., Ansorge, W., Henrich, T., Grabher, C., Arendt, D., Carl, M., Krone, A., *et al.* (2001). Medaka eyeless is the key factor linking retinal determination and eye growth. *Development* 128, 4035-4044.
- Loosli, F., Winkler, S., and Wittbrodt, J. (1999). Six3 overexpression initiates the formation of ectopic retina. *Genes Dev* 13, 649-654.
- Lopez-Rios, J., Esteve, P., Ruiz, J.M., and Bovolenta, P. (2008). The Netrin-related domain of Sfrp1 interacts with Wnt ligands and antagonizes their activity in the anterior neural plate. *Neural Dev* 3, 19.
- Lu, F.I., Thisse, C., and Thisse, B. (2011). Identification and mechanism of regulation of the zebrafish dorsal determinant. *Proc Natl Acad Sci U S A* 108, 15876-15880.
- Martinez-Morales, J.R., Dolez, V., Rodrigo, I., Zaccarini, R., Leconte, L., Bovolenta, P., and Saule, S. (2003). OTX2 activates the molecular

- network underlying retina pigment epithelium differentiation. *J Biol Chem* 278, 21721-21731.
- Martinez-Morales, J.R., Signore, M., Acampora, D., Simeone, A., and Bovolenta, P. (2001). Otx genes are required for tissue specification in the developing eye. *Development* 128, 2019-2030.
- Martinez-Morales, J.R., and Wittbrodt, J. (2009). Shaping the vertebrate eye. *Curr Opin Genet Dev* 19, 511-517.
- Massague, J. (1990). The transforming growth factor-beta family. *Annu Rev Cell Biol* 6, 597-641.
- Mathers, P.H., Grinberg, A., Mahon, K.A., and Jamrich, M. (1997). The Rx homeobox gene is essential for vertebrate eye development. *Nature* 387, 603-607.
- Mii, Y., and Taira, M. (2011). Secreted Wnt "inhibitors" are not just inhibitors: Regulation of extracellular Wnt by secreted Frizzled-related proteins. *Dev Growth Differ* 53, 911-923.
- Molotkov, A., Molotkova, N., and Duester, G. (2006). Retinoic acid guides eye morphogenetic movements via paracrine signaling but is unnecessary for retinal dorsoventral patterning. *Development* 133, 1901-1910.
- Munemitsu, S., Albert, I., Souza, B., Rubinfeld, B., and Polakis, P. (1995). Regulation of intracellular beta-catenin levels by the adenomatous polyposis coli (APC) tumor-suppressor protein. *Proc Natl Acad Sci U S A* 92, 3046-3050.
- Murakami, G., Watabe, T., Takaoka, K., Miyazono, K., and Imamura, T. (2003). Cooperative inhibition of bone morphogenetic protein signaling by Smurf1 and inhibitory Smads. *Mol Biol Cell* 14, 2809-2817.
- Neumann, C.J., and Nüsslein-Volhard, C. (2000). Patterning of the zebrafish retina by a wave of sonic hedgehog activity. *Science* 289, 2137-2139.
- Nishida, A., Furukawa, A., Koike, C., Tano, Y., Aizawa, S., Matsuo, I., and Furukawa, T. (2003). Otx2 homeobox gene controls retinal photoreceptor cell fate and pineal gland development. *Nat Neurosci* 6, 1255-1263.
- Nishimura, R., Hata, K., Harris, S.E., Ikeda, F., and Yoneda, T. (2002). Core-binding factor alpha 1 (Cbfa1) induces osteoblastic differentiation of C2C12 cells without interactions with Smad1 and Smad5. *Bone* 31, 303-312.

- Nishimura, R., Hata, K., Matsubara, T., Wakabayashi, M., and Yoneda, T. (2012). Regulation of bone and cartilage development by network between BMP signalling and transcription factors. *J Biochem* *151*, 247-254.
- Noordermeer, J., Klingensmith, J., Perrimon, N., and Nusse, R. (1994). *dishevelled* and *armadillo* act in the wingless signalling pathway in *Drosophila*. *Nature* *367*, 80-83.
- Oliver, G., Mailhos, A., Wehr, R., Copeland, N.G., Jenkins, N.A., and Gruss, P. (1995). *Six3*, a murine homologue of the *sine oculis* gene, demarcates the most anterior border of the developing neural plate and is expressed during eye development. *Development* *121*, 4045-4055.
- Onichtchouk, D., Chen, Y.G., Dosch, R., Gawantka, V., Delius, H., Massague, J., and Niehrs, C. (1999). Silencing of TGF-beta signalling by the pseudoreceptor BAMBI. *Nature* *401*, 480-485.
- Packard, M., Mathew, D., and Budnik, V. (2003). Wnts and TGF beta in synaptogenesis: old friends signalling at new places. *Nat Rev Neurosci* *4*, 113-120.
- Pasquier, L., Dubourg, C., Blayau, M., Lazaro, L., Le Marec, B., David, V., and Odent, S. (2000). A new mutation in the six-domain of *SIX3* gene causes holoprosencephaly. *Eur J Hum Genet* *8*, 797-800.
- Peng, G., and Westerfield, M. (2006). *Lhx5* promotes forebrain development and activates transcription of secreted Wnt antagonists. *Development* *133*, 3191-3200.
- Ploper, D., Lee, H.X., and De Robertis, E.M. (2011). Dorsal-ventral patterning: *Crescent* is a dorsally secreted Frizzled-related protein that competitively inhibits Tollid proteases. *Dev Biol* *352*, 317-328.
- Quiring, R., Walldorf, U., Kloter, U., and Gehring, W.J. (1994). Homology of the *eyeless* gene of *Drosophila* to the *Small eye* gene in mice and *Aniridia* in humans. *Science* *265*, 785-789.
- Rashid, T., Upton, A.L., Blentic, A., Ciossek, T., Knoll, B., Thompson, I.D., and Drescher, U. (2005). Opposing gradients of ephrin-As and EphA7 in the superior colliculus are essential for topographic mapping in the mammalian visual system. *Neuron* *47*, 57-69.
- Rembold, M., Loosli, F., Adams, R.J., and Wittbrodt, J. (2006). Individual cell migration serves as the driving force for optic vesicle evagination. *Science* *313*, 1130-1134.

- Renstrom, J., Istvanffy, R., Gauthier, K., Shimono, A., Mages, J., Jardon-Alvarez, A., Kroger, M., Schiemann, M., Busch, D.H., Esposito, I., *et al.* (2009). Secreted frizzled-related protein 1 extrinsically regulates cycling activity and maintenance of hematopoietic stem cells. *Cell Stem Cell* 5, 157-167.
- Rodriguez, J., Esteve, P., Weigl, C., Ruiz, J.M., Fermin, Y., Trousse, F., Dwivedy, A., Holt, C., and Bovolenta, P. (2005). SFRP1 regulates the growth of retinal ganglion cell axons through the Fz2 receptor. *Nat Neurosci* 8, 1301-1309.
- Roskies, A.L., and O'Leary, D.D. (1994). Control of topographic retinal axon branching by inhibitory membrane-bound molecules. *Science* 265, 799-803.
- Ruberte, E., Marty, T., Nellen, D., Affolter, M., and Basler, K. (1995). An absolute requirement for both the type II and type I receptors, *punt* and *thick veins*, for *dpp* signaling in vivo. *Cell* 80, 889-897.
- Ruiz, J.M., Rodriguez, J., and Bovolenta, P. (2009). Growth and differentiation of the retina and the optic tectum in the medaka fish requires *olSfrp5*. *Dev Neurobiol* 69, 617-632.
- Sakuta, H., Suzuki, R., Takahashi, H., Kato, A., Shintani, T., Iemura, S., Yamamoto, T.S., Ueno, N., and Noda, M. (2001). *Ventropin*: a BMP-4 antagonist expressed in a double-gradient pattern in the retina. *Science* 293, 111-115.
- Sakuta, H., Takahashi, H., Shintani, T., Etani, K., Aoshima, A., and Noda, M. (2006). Role of bone morphogenic protein 2 in retinal patterning and retinotectal projection. *J Neurosci* 26, 10868-10878.
- Sasagawa, S., Takabatake, T., Takabatake, Y., Muramatsu, T., and Takeshima, K. (2002). Axes establishment during eye morphogenesis in *Xenopus* by coordinate and antagonistic actions of BMP4, *Shh*, and *RA*. *Genesis* 33, 86-96.
- Sasai, Y., Lu, B., Steinbeisser, H., and De Robertis, E.M. (1995). Regulation of neural induction by the *Chd* and *Bmp-4* antagonistic patterning signals in *Xenopus*. *Nature* 377, 757.
- Sato, A., Khadka, D.K., Liu, W., Bharti, R., Runnels, L.W., Dawid, I.B., and Habas, R. (2006). *Profilin* is an effector for *Daam1* in non-canonical Wnt signaling and is required for vertebrate gastrulation. *Development* 133, 4219-4231.

- Satoh, W., Gotoh, T., Tsunematsu, Y., Aizawa, S., and Shimono, A. (2006). *Sfrp1* and *Sfrp2* regulate anteroposterior axis elongation and somite segmentation during mouse embryogenesis. *Development* 133, 989-999.
- Schlessinger, K., Hall, A., and Tolwinski, N. (2009). Wnt signaling pathways meet Rho GTPases. *Genes Dev* 23, 265-277.
- Schmidt, J.E., Suzuki, A., Ueno, N., and Kimelman, D. (1995). Localized BMP-4 mediates dorsal/ventral patterning in the early *Xenopus* embryo. *Dev Biol* 169, 37-50.
- Schmitt, E.A., and Dowling, J.E. (1994). Early eye morphogenesis in the zebrafish, *Brachydanio rerio*. *J Comp Neurol* 344, 532-542.
- Schulte, D., Furukawa, T., Peters, M.A., Kozak, C.A., and Cepko, C.L. (1999). Misexpression of the *Emx*-related homeobox genes *cVax* and *mVax2* ventralizes the retina and perturbs the retinotectal map. *Neuron* 24, 541-553.
- Scicolone, G., Ortalli, A.L., and Carri, N.G. (2009). Key roles of Ephs and ephrins in retinotectal topographic map formation. *Brain Res Bull* 79, 227-247.
- Seo, H.C., Drivenes, O., Ellingsen, S., and Fjose, A. (1998). Transient expression of a novel *Six3*-related zebrafish gene during gastrulation and eye formation. *Gene* 216, 39-46.
- Sheldahl, L.C., Park, M., Malbon, C.C., and Moon, R.T. (1999). Protein kinase C is differentially stimulated by Wnt and Frizzled homologs in a G-protein-dependent manner. *Curr Biol* 9, 695-698.
- Sidi, S., Goutel, C., Peyrieras, N., and Rosa, F.M. (2003). Maternal induction of ventral fate by zebrafish radar. *Proc Natl Acad Sci U S A* 100, 3315-3320.
- Sperry, R.W. (1963). Chemoaffinity in the Orderly Growth of Nerve Fiber Patterns and Connections. *Proc Natl Acad Sci U S A* 50, 703-710.
- Tanabe, Y., and Jessell, T.M. (1996). Diversity and pattern in the developing spinal cord. *Science* 274, 1115-1123.
- Tendeng, C., and Houart, C. (2006). Cloning and embryonic expression of five distinct *sfrp* genes in the zebrafish *Danio rerio*. *Gene Expr Patterns* 6, 761-771.

- Teraoka, M.E., Paschaki, M., Muta, Y., and Ladher, R.K. (2009). Rostral paraxial mesoderm regulates refinement of the eye field through the bone morphogenetic protein (BMP) pathway. *Dev Biol* 330, 389-398.
- Ton, C.C., Hirvonen, H., Miwa, H., Weil, M.M., Monaghan, P., Jordan, T., van Heyningen, V., Hastie, N.D., Meijers-Heijboer, H., Drechsler, M., *et al.* (1991). Positional cloning and characterization of a paired box- and homeobox-containing gene from the aniridia region. *Cell* 67, 1059-1074.
- Trousse, F., Esteve, P., and Bovolenta, P. (2001). Bmp4 mediates apoptotic cell death in the developing chick eye. *J Neurosci* 21, 1292-1301.
- Trowe, T., Klostermann, S., Baier, H., Granato, M., Crawford, A.D., Grunewald, B., Hoffmann, H., Karlstrom, R.O., Meyer, S.U., Muller, B., *et al.* (1996). Mutations disrupting the ordering and topographic mapping of axons in the retinotectal projection of the zebrafish, *Danio rerio*. *Development* 123, 439-450.
- Uren, A., Reichsman, F., Anest, V., Taylor, W.G., Muraiso, K., Bottaro, D.P., Cumberledge, S., and Rubin, J.S. (2000). Secreted frizzled-related protein-1 binds directly to Wntless and is a biphasic modulator of Wnt signaling. *J Biol Chem* 275, 4374-4382.
- Veien, E.S., Rosenthal, J.S., Kruse-Bend, R.C., Chien, C.B., and Dorsky, R.I. (2008). Canonical Wnt signaling is required for the maintenance of dorsal retinal identity. *Development* 135, 4101-4111.
- Voronina, V.A., Kozhemyakina, E.A., O'Kernick, C.M., Kahn, N.D., Wenger, S.L., Linberg, J.V., Schneider, A.S., and Mathers, P.H. (2004). Mutations in the human RAX homeobox gene in a patient with anophthalmia and sclerocornea. *Hum Mol Genet* 13, 315-322.
- Wallis, D.E., Roessler, E., Hehr, U., Nanni, L., Wiltshire, T., Richieri-Costa, A., Gillissen-Kaesbach, G., Zackai, E.H., Rommens, J., and Muenke, M. (1999). Mutations in the homeodomain of the human SIX3 gene cause holoprosencephaly. *Nat Genet* 22, 196-198.
- Wang, S., Krinks, M., Lin, K., Luyten, F.P., and Moos, M., Jr. (1997). Frzb, a secreted protein expressed in the Spemann organizer, binds and inhibits Wnt-8. *Cell* 88, 757-766.
- Wargelius, A., Seo, H.C., Austbo, L., and Fjose, A. (2003). Retinal expression of zebrafish six3.1 and its regulation by Pax6. *Biochem Biophys Res Commun* 309, 475-481.

- Weis-Garcia, F., and Massague, J. (1996). Complementation between kinase-defective and activation-defective TGF-beta receptors reveals a novel form of receptor cooperativity essential for signaling. *EMBO J* 15, 276-289.
- Westenskow, P., Piccolo, S., and Fuhrmann, S. (2009). Beta-catenin controls differentiation of the retinal pigment epithelium in the mouse optic cup by regulating Mitf and Otx2 expression. *Development* 136, 2505-2510.
- Wieser, R., Wrana, J.L., and Massague, J. (1995). GS domain mutations that constitutively activate T beta R-I, the downstream signaling component in the TGF-beta receptor complex. *EMBO J* 14, 2199-2208.
- Wilson, P.A., and Hemmati-Brivanlou, A. (1995). Induction of epidermis and inhibition of neural fate by Bmp-4. *Nature* 376, 331-333.
- Wilson, S.W., and Houart, C. (2004). Early steps in the development of the forebrain. *Dev Cell* 6, 167-181.
- Wordinger, R.J., and Clark, A.F. (2007). Bone morphogenetic proteins and their receptors in the eye. *Exp Biol Med (Maywood)* 232, 979-992.
- Wyatt, A., Bakrania, P., Bunyan, D.J., Osborne, R.J., Crolla, J.A., Salt, A., Ayuso, C., Newbury-Ecob, R., Abou-Rayyah, Y., Collin, J.R., *et al.* (2008). Novel heterozygous OTX2 mutations and whole gene deletions in anophthalmia, microphthalmia and coloboma. *Hum Mutat* 29, E278-283.
- Yabe, T., Shimizu, T., Muraoka, O., Bae, Y.K., Hirata, T., Nojima, H., Kawakami, A., Hirano, T., and Hibi, M. (2003). Ogon/Secreted Frizzled functions as a negative feedback regulator of Bmp signaling. *Development* 130, 2705-2716.
- Yoshida, Y., Tanaka, S., Umemori, H., Minowa, O., Usui, M., Ikematsu, N., Hosoda, E., Imamura, T., Kuno, J., Yamashita, T., *et al.* (2000). Negative regulation of BMP/Smad signaling by Tob in osteoblasts. *Cell* 103, 1085-1097.
- Zamurovic, N., Cappellen, D., Rohner, D., and Susa, M. (2004). Coordinated activation of notch, Wnt, and transforming growth factor-beta signaling pathways in bone morphogenic protein 2-induced osteogenesis. Notch target gene Hey1 inhibits mineralization and Runx2 transcriptional activity. *J Biol Chem* 279, 37704-37715.

- Zhang, X.M., and Yang, X.J. (2001). Temporal and spatial effects of Sonic hedgehog signaling in chick eye morphogenesis. *Dev Biol* 233, 271-290.
- Zhao, X., Das, A.V., Thoreson, W.B., James, J., Wattnem, T.E., Rodriguez-Sierra, J., and Ahmad, I. (2002). Adult corneal limbal epithelium: a model for studying neural potential of non-neural stem cells/progenitors. *Dev Biol* 250, 317-331.
- Zhou, C.J., Molotkov, A., Song, L., Li, Y., Pleasure, D.E., Pleasure, S.J., and Wang, Y.Z. (2008). Ocular coloboma and dorsoventral neuroretinal patterning defects in *Lrp6* mutant eyes. *Dev Dyn* 237, 3681-3689.
- Zhou, C.J., Wang, Y.Z., Yamagami, T., Zhao, T., Song, L., and Wang, K. (2010). Generation of *Lrp6* conditional gene-targeting mouse line for modeling and dissecting multiple birth defects/congenital anomalies. *Dev Dyn* 239, 318-326.

Chapter 2

Materials and Methods

2.1 Zebrafish Lines & Animal Care

All zebrafish were cared for using the protocols presented in Westerfield et al. (2000), as approved by the Animal Care and Use Committee - Biosciences. Unless noted, experiments were performed using the AB strain of wildtype fish, with a few experiments taking advantage of transgenic lines of zebrafish including the *Tg(TOP:dGFP)^{w25}*, *Tg[BRE:eGFP]*, and *Tg[hsp701:dkk1-GFP]^{w32}** strains (Collery and Link, 2011; Dorsky et al., 2002; Veien et al., 2008). Transgene carriers were identified by performing incrosses and screening progeny for GFP fluorescence. Prior to GFP screening, the *Tg[hsp701:dkk1-GFP]^{w32}* line was heat shocked for two hours in a 39°C water bath and screened for fluorescence prior to fixation (Veien et al., 2008).

2.2 Morpholino Preparation/Injection and Embryo Treatment

Morpholino oligonucleotides, both splice blocking and translation blocking, were designed and ordered from GeneTools to knockdown gene function (Nasevicius and Ekker, 2000). The sequences for all morpholinos used are listed in Table 2.1. Stock solutions of morpholinos were prepared to a concentration of 10 mg/ml by dissolving the powdered morpholino in autoclaved milli-Q water. Further working stock dilutions were prepared by diluting the 10 mg/ml stock solution in danieau buffer (58mM NaCl, 0.7mM KCl, 0.4mM MgSO₄, 0.6mM Ca(NO₃)₂, 5.0mM HEPES (hydroxyethyl piperazineethanesulfonic acid) pH 7.6). Stock solutions were kept at either 4°C or -20°C for long-term storage.

Prior to injection, all working stock morpholino dilutions were heated at 65°C for 5-10 minutes and subsequently allowed to cool before injecting. Morpholinos were injected at concentrations ranging from 1ng to 6ng into 1-4 cell stage zebrafish embryos using a microinjection rig. All embryos were then raised in embryo media (EM) (15mM NaCl, 500nM KCl, 1mM CaCl₂, 150nM KH₂PO₄, 1mM MgSO₄, 715 nM NaHCO₃) supplemented with 10ml/L penicillin-

* Fish line obtained from ZIRC (Zebrafish International Resource Center)

streptomycin (Sigma) at temperatures of either 25.5°C, 28.5°C, or 33°C. Once embryos reached the appropriate developmental stage, they were fixed in 4% paraformaldehyde (PFA) in PBS (Phosphate Buffered Saline – 137mM NaCl, 2.7mM KCl, 10mM NaH₂PO₄, 1.75 mM KH₂PO₄, pH 7.4) at room temperature for 5 hours or overnight at 4°C on a rotating platform. Staging of embryos was based on distinct developmental characteristics as described in Kimmel et al. (1995). After completing fixation, embryos were either washed out of 4% PFA into PBST (Phosphate Buffered Saline, 0.1% Tween-20) and kept at 4°C for short-term storage (<1 week) or put into methanol and left at -20°C for long-term storage (>1 week). If embryos were allowed to reach stages of 28hpf or older, they were transferred to a solution of 0.003% 1-phenyl 2-thiourea (PTU) (Sigma) in EM at 24hpf to prevent pigment formation. PTU media was changed every 24 hours. Older embryos were also anesthetized in a 4% dilution of 0.4% tricaine stock solution prior to fixation or termination as required.

Embryos were dechorionated manually using Dumont No.5 forceps or chemically using Pronase E (Sigma). Chemical dechoriation involved bathing and swirling embryos in a solution of 1mg/ml Pronase E until the first chorion crumpled. All embryos were then washed three or more times in EM to remove any leftover Pronase E. Any chorions still intact following the washes were then gently removed by pipetting embryos up and down in EM. Chemical dechoriation was performed at embryos at stages of 50% epiboly or older.

2.3 Phusion High Fidelity PCR and TOPO Cloning

Generation of PCR products for cloning reactions was performed either through RT-PCR or Phusion High Fidelity PCR reactions. Gene-amplifying primers were designed to be between 23-28bp long, have a %GC content between 40-60%, and a T_m between 55°C-70°C. Primers for mRNA transcription inserts were designed to amplify the entire coding region and contained restriction enzyme sites for cloning into the pCS2+ vector. Forward primers also contained a kozac sequence (Kozak, 1986), chosen based on the gene sequence, followed by a stuffer sequence (caca) (Table 2.2). Each Phusion reaction was set up in a PCR

tube containing: 10 μ l 5X HF Buffer, 4 μ l of 2.5mM dTNP, 5 μ l Forward Primer (5 μ M), 5 μ l Reverse Primer (5 μ M), 1 μ l cDNA (1 μ g), 0.5 μ l Phusion® DNA Polymerase (New England Biolabs), and 24.5 μ l autoclaved Milli-Q. Reactions were run through a three temperature PCR reaction: 98°C for 20 seconds, 55-65°C[†] for 15 seconds, and 72°C for 30 seconds/kb. To obtain the appropriate sized product, all reactions were run on a 1-1.5% agarose/TAE (0.04M Tris-acetate, 0.001M Ethylenediaminetetraacetic acid (EDTA) buffer) gel. Correct size bands were excised and gel purified using the manufacturer's recommendations in the Fermentas GeneJet Gel Extraction kit.

Blunt end TOPO cloning was then used to transfer the PCR product in the pCR-4TOPO vector. An ExTaq (Takara) reaction was used to generate poly "A" tail on the end of the PCR product to allow for ligation with the "T" overhang on the TOPO vector. The reaction included 15 μ l of gel-purified product, 2 μ l 10X ExTaq Buffer, 1 μ l of 10mM dNTP, 1 μ l ExTaq, and 1 μ l of milli-Q. The reaction was mixed and incubated for 10 minutes at 72°C in a thermocycler. The PCR product was then diluted with 60 μ l for the "TA" ligation step. The ligation reaction itself combined 1 μ l of diluted product, 0.25 μ l of pCR-4TOPO vector, and 1.25 μ l of milli-Q, which was left at room temperature for five minutes.

The entire ligation reaction was then transformed into TOP10 chemically competent *E. coli* cells (Invitrogen). Tubes of TOP10 cells (50 μ l) were thawed on ice prior to transformation. During the transformation, 10 μ l of TOP10 cells were added to the ligation reaction. The tube was then placed back on ice and left for ten minutes to allow the DNA to enter the cells. This was followed by a heat shock at 42°C for exactly 45 seconds and a cool-down incubation on ice for two minutes. LB media (Per litre: 10g Bacto-Tryptone, 5g Bacto yeast extract, 10g NaCl, pH to 7.0 with 100 μ l NaOH) or SOC media (Per litre: 20g Bacto Tryptone, 5g yeast extract, 2ml 5M NaCl, 2.5ml 1M KCl, 10ml 1M MgCl₂, 10ml 1M MgSO₄, 20ml 1M glucose, fill to 1L with Milli-Q water) was then added (150 μ l) to each tube and the reaction was put at 37°C for 30-45 minutes. Using aseptic

[†] Annealing temperature was chosen to be 2-5°C below the lowest primer T_m.

technique, the reaction mix was plated on LB media containing 50µg/ml carbenicillin and left overnight at 37°C. Colonies were picked off of the plates and grown in liquid LB media with carbenicillin (1X) at 37°C to amplify the DNA. Liquid cultures were then mini-prepped using the recommended protocol in the Fermentas GeneJet™ Plasmid Miniprep kit to isolate the plasmid DNA. Sequencing using the M13 forward and reverse primers confirmed insertion of the proper PCR product. To transfer the insert into the pCS2+ vector for mRNA transcription, the product was cut out of the vector using a restriction digest containing 5µl of miniprep DNA, 1µl of Restriction Enzyme #1, 1µl of Restriction Enzyme #2 (Table 2.2, based on primers used), 2.5µl of Restriction Enzyme Buffer, and 15.5µl of milli-Q water. A similar restriction digest reaction was also used to digest the CS2+ plasmid prior to ligation to create compatible ends. The reaction was left at 37°C for ≥ 2hours and then run on a 1% agarose/TAE gel to excise the insert bands. Gel purified insert bands were then ligated into digest CS2+ vector in reactions containing 5µl vector, 10µl insert, 2µl 10X T4 Ligase Buffer, 1µl T4 DNA Ligase (Invitrogen), and 2µl of milli-Q. The reaction was left at room temperature for four hours or at 16°C overnight in the thermocycler. This was followed by transformation of the newly ligated plasmid/insert into TOP10 cells. The transformation followed the standard protocol with 2.5µl of ligation product mixed with 10µl of cells. Colonies were then cultured and plasmid isolated by mini-prep protocol. The correct insert was confirmed using M13 forward and reverse primer sequencing. CS2+ plasmids were stored at -20°C and used later on during mRNA in vitro transcription reactions.

Sequencing reactions contained 6µl Big Dye Buffer, 5µl miniprep DNA, 2µl Big Dye premix, 1µl of sequencing primer (usually M13 forward or reverse), and 6µl of autoclaved Milli-Q water to bring the total volume to 20µl. The reaction was then set on a three-temperature PCR program (96°C for 30 seconds, 50°C for 15 seconds, and 60°C for 90 seconds) for 25 cycles. DNA was precipitated by transferring the reaction to a 1.7ml microfuge tube and adding 2µl of 1.5M NaOAc/250mM EDTA and 85µl of 95% ethanol. The tubes were then vortexed and stored at -20°C for 15 minutes. This was followed by a 20-minute

spin at 14 800 rpm at 4°C. The ethanol was removed from the tube and 700µl of 70% ethanol was added. The tubes were then spun once more at 4°C for 10 minutes at 14 800 rpm. Following the final spin, all 70% ethanol was removed from the tubes, being careful to not disturb the DNA pellet. Tubes were left open to allow residual ethanol to evaporate before bringing the reactions to the Molecular Biology Service Unit (MBSU) for sequencing. Reactions were stored temporarily at -20°C before running sequencing reactions.

2.4 In vitro mRNA Transcription

All CS2+ plasmid templates were linearized and purified prior to mRNA synthesis. Each linearization reaction used 10µg of DNA, 4µl of restriction enzyme Buffer D (Promega), 2.5µl of NotI restriction enzyme (Promega), and diethylpyrocarbonate-treated water (depC) to bring the total volume up to 40µl. The reaction mix was then incubated at 37°C for \geq 2hrs. Following the linearization reaction, leftover enzyme and RNAses were removed using SDS/Proteinase K treatment. Per 40µl reaction, 5µl of 1µg/µl of Proteinase K, 1.25µl of 20% SDS (sodium dodecyl sulfate), and 4.75µl of depC-treated H₂O was added to each tube and incubated at 37°C for an additional 30 minutes.

To purify the linear DNA for mRNA synthesis, a phenol/chloroform extraction was performed. An additional 140µl of depC-treated H₂O was added to each reaction following RNase removal to top the volume up to 190µl, along with 10µl of NaOAc (pH 5.3). Equal volume of phenol (50%)/chloroform (49%)/isoamyl alcohol(1%) (200µl) (Fisher Bioreagents) was then added, followed by vortexing of each tube for 20 seconds. The tubes were then spun in the centrifuge for five minutes at 14 800 rpm to separate the layers. The top layer was carefully transferred over to a new 1.7ml microfuge tube. Equal volume of chloroform (Fisher Bioreagents) was added to the transferred solution and the tubes were again vortexed for 20 seconds. Following an additional five-minute spin, the upper layer was transferred to a new 1.7ml tube. To precipitate the DNA, 1/10 of the total volume of NaOAc (3M pH 5.2) and 3 volumes of 100% ethanol were added to each tube. The tubes were mixed and then left at -20°C for 15

minutes. Following precipitation, the tubes were spun at 4°C for 20 minutes (14 800 rpm) to pellet the DNA. The supernatant was removed and the pellet washed with 70% ethanol/depC, being careful not to disturb the pellet. Following a second, 10-minute spin at 14,800rpm, the supernatant was removed and the pellet left to air dry. Once all of the ethanol/depC had evaporated, the pellet was re-suspended in up to 10µl of depC. The purified, linear DNA was then run on a 1% agarose/TAE gel to confirm linearization and purification. The remaining DNA prep was stored at -20°C.

In vitro synthesis of capped mRNA transcripts was done using the SP6 mMessage mMachine kit (Ambion) as per the manufacturer's recommended protocol. The following components were added to an RNase-free 1.7ml microfuge tube on ice: 10µl 2X NTP/CAP, 2µl 10X Rxn Buffer, 2µl (approx. 2mg) linear, purified DNA, 2µl SP6 Enzyme Mix, 4µl nuclease-free water (from kit). The tubes were then incubated at 37°C for 2-2.5 hours. This was followed by a DNA digest using 1µl of DNase I (Ambion) and incubation for 15 minutes at 37°C. RNA recovery was performed using Amicom Microcon Columns. Reactions were run through three consecutive depC (400-480µl) washes in the columns and spun till the final concentrated volume was less than 50µl. Columns were spun at 3000 rpm for 15 minutes for each wash step. In between the second and third wash, the column was inverted into a new tube and spun at 3000 rpm for 3 minutes. The flow through was transferred to a fresh column for the third wash. Following the final depC wash, RNA was collected by inverting the column into a new, RNase-free 1.7ml tube, again spinning at 3000 rpm for 3 minutes. All mRNA synthesis preps were stored at -80°C.

2.5 Total RNA Extraction

Whole RNA preps were used for complementary DNA (cDNA) synthesis, and RT-PCR reactions for probe synthesis, cloning, or morpholino controls. Total RNA extraction was performed using the protocol given in the Ambion RNAqueous kit on live, dechorionated embryos. Groups of 25-40 embryos were placed into 1.7ml microfuge tubes with 300µl of Lysis/Binding Buffer (from kit).

The tubes were then vortexed until the embryos were completely homogenized. Tubes were occasionally stored short-term (1-2 days) in Lysis/Binding buffer at -20°C before continuing on with the rest of the protocol. Following Lysis/Binding Buffer treatment, 350µl of 64% ethanol (from kit) was added to each tube and the tubes were then vortexed for 30 seconds. The mixture was then transferred to a filter cartridge provided from the kit and spun in the centrifuge for 1 minute at 14 800 rpm. This was followed by one wash of 700µl of Wash #1 and two washes of 500µl of Wash #2/3. Each wash was accompanied by a spin of 1 minute at 14 800 rpm, with any flow through discarded after the spin. The carbon filter was then transferred to a new microfuge tube and 70µl (added in 40µl and 30µl aliquots each followed by a 30 second spin at 14 800 rpm) of pre-heated elution buffer (70°C) was added to the filter to elute the RNA. DNA was removed from the RNAqueous prep during a DNase I (RNAqueous) digest at 37°C for >1hr.

The RNA was further purified using the Qiagen RNeasy kit following the listed directions. Prior to starting the RNeasy protocol, 10µl of β-mercaptoethanol (BME) was added per ml of RLT lysis buffer provided in the kit. BME irreversibly denatures RNAses and prevent degradation of RNA products. Once combined, 350µl of the BME/RLT mixture was placed in each RNA prep, followed by the addition 250µl of 100% ethanol and gentle pipetting to mix the solution. Once mixed, the solution was transferred to a spin column provided in the kit. The tubes were spun for 15 seconds at 10 000 rpm and any flow through was discarded. The column was then placed in a new collection tube and 500µl of solution RPE was added. The tubes were spun again for 15 seconds at 10 000 rpm, followed by a second wash of RPE. The second wash was accompanied by a spin of two minutes at 10 000 rpm. The columns were then placed in new collection tubes and spun again for one minute at 14 800rpm. All columns were then placed in new 1.7ml microfuge tubes and 15µl of depC was added to elute the RNA. The tubes were left to sit for one minute and then spun for one minute at 10 000 rpm to collect the RNA. All purified RNA preps were stored at -80°C.

2.6 RT-PCR Reactions

Purified RNA extracts were used as a template in RT-PCR to generate PCR products for probe synthesis, cloning, or morpholino controls. The RT-PCR reaction was performed using the contents and directions presented in the SuperScript® III One-Step RT-PCR system with Platinum® Taq DNA Polymerase kit (Invitrogen). In an RNase-free PCR tube, 12.5µl 2X Rxn Mix, 1µl RNA, 1µl Superscript III Platinum® Taq DNA Polymerase, 8.5µl depC, and 1µl each of a forward and reverse primer (5µM) were combined. All primers used are listed in Table 2.2 or Table 2.3. The RT-PCR reaction was run according to a three temperature thermocycler program: 94°C for 15 seconds, 55-65°C for 30 seconds, and 68°C for 1 minute/kb. PCR cycles ranged from 25-40 cycles, depending on the RT-PCR reaction. Reaction products were run out on a 1-1.5% agarose/TAE gel. If required, bands of appropriate size were excised from the gel and gel extracted/purified using the manufacturer's recommended protocol in the Fermentas GeneJet Gel Extraction kit for use in probe synthesis or in vitro mRNA transcription.

2.7 cDNA Synthesis and Quantitative Real-Time PCR (qPCR)

Purified total RNA extracts were also used to generate complementary DNA (cDNA) for use in Phusion PCR reactions or quantitative real-time PCR (qRT-PCR) assays. cDNA was generated using the High Capacity cDNA Reverse Transcription kit (without RNase Inhibitor) (Applied Biosystems), following the manufacturer's recommendations. Per 20µl reaction, 2µl 10X RT Buffer, 0.8µl 25X dNTP Mix, 2µl 10X RT Random Primers, 1µl Multiscribe Reverse Transcriptase, and 3.2µl of nuclease-free water were added to each tube, in the specified order, on ice. The RNase inhibitor, RNase Out Recombinant Ribonuclease Inhibitor (Invitrogen) (1µl) was also added to each reaction and was not included in the kit. Between 2.5-3µg of RNA, depending on the experiment, was then added to each reaction, and topped up to 20µl with more nuclease-free water. Tubes were placed in the thermocycler and run on the cDNA synthesis program: 25°C for 5 minutes, 42°C for 30 minutes, and 95°C for 5 minutes. All

cDNA preps were stored at -20°C. Following the synthesis reactions, (if required) cDNA preparations were diluted in a 1:2 dilution series (with autoclaved milli-Q) to optimal dilutions determined during qPCR primer validation.

Prior to running qPCR experiments, all qPCR primers were validated by running reactions on cDNA dilutions ranging from 1:1 to 1:1024. Primers were designed using the Roche Universal Probe Library website. GFP and *sfrp1a* sequences were inputted into the program and primers were chosen that amplified short PCR products (\approx 100 bp) in the appropriate region of the gene. During qRT-PCR assays, experimental primers were compared to a universal control set of primers for the gene, *ef1 α* , which was used as the endogenous control in all experiments (Table 2.4). Primer validation was performed using the steps outlined in previously published papers (Livak and Schmittgen, 2001; Pillay et al., 2010). Reactions were carried out in a 96-well plate using the Brilliant® SYBR® Green QPCR Master Mix kit (Stratagene), as described below, on a cDNA dilution series of: 1/2, 1/4, 1/8, 1/16, 1/32, 1/64, 1/128, 1/256, using *ef1 α* forward and reverse primers. StepOne™ Software version 2.0 for StepOne™ Real-Time PCR Systems (Applied Biosystems) was used to eliminate any outliers and analyze the resulting standard curve/melting curve. Appropriate primers were chosen that contained R^2 values close to 98%, percent efficiency close to 100%, and a standard curve slope within 0.01 of the control group (*EF1 α*).

All qPCR reactions were run based on directions given in the Brilliant® SYBR® Green QPCR Master Mix kit (Stratagene). The following components were added, per reaction/well: 2.397 μ l autoclaved milli-Q, 5 μ l SYBR Master Mix, 0.003 μ l 1mM ROX, 0.3 μ l 5 μ M Forward Primer, 0.3 μ l 5 μ M Reverse Primer, and 2 μ l of cDNA. To try and maintain consistency between reactions, Master Mixes were created whenever possible and evenly distributed into each well. A buffer zone of unused wells was also created around the periphery of the reactions to prevent any artifacts caused by evaporation at the edge of the plate's seal. Prior to placing the plates (96-well) in the thermocycler, the reactions were vortexed thoroughly and spun for at least 2 minutes at 1500 rpm at 4°C. Plates (96-well)

were run on the Applied Biosystems StepOnePlus™ Real-Time PCR System thermocycler, with four to nine replicates per group. The qPCR thermocycler program was run as follows: 95°C for 30 seconds, 55°C for 1 minute, and 72°C for 30 seconds.

Results were again analyzed using the StepOne™ Software (Applied Biosystems), following removal of any outliers. Relative gene expression was determined with the comparative Ct method ($2^{-\Delta\Delta Ct}$ method). The StepOne™ provides the $2^{-\Delta\Delta Ct}$ (RQ) value, but still requires the user to manually calculate the standard deviation of the fold change (SD_{RQ}) for statistical purposes. Inputting the $SE_{\Delta Ct}$, $mean_{\Delta Ct}$, and the n value (number of replicates per group after omission) for both the control and experimental sets into an online calculator gives the standard deviation of ΔCt ($SD_{\Delta Ct}$). The $SD_{\Delta Ct}$ value was then used to calculate the SD_{RQ} using the formula: $SD_{RQ} = (\ln 2)(SD_{\Delta Ct})(RQ \text{ value})$. RQ values were graphed, using SD_{RQ} as a measurement for error bars. Fold changes in gene expression were then compared using an unpaired t-test to determine statistical significance for any observed changes, using EF1 α as the endogenous control. The t-test requires the following parameters for calculation: RQ, SD_{RQ} , and n (number of replicates per group after omission) values for both experimental and endogenous control groups.

2.8 mRNA In Situ Hybridization

2.8.1 Riboprobe Synthesis (Plasmid and PCR-based Approach)

In situ hybridization (ISH) requires digoxigenin (DIG) or fluorescein labeled antisense riboprobes. All riboprobes used during ISH were synthesized directly from a PCR product (Table 2.5) or from a linearized plasmid containing gene-specific sequence (Table 2.6). SP6, T3, or T7 RNA polymerase sites were used during the plasmid-based synthesis riboprobes as listed in Table 2.6. In the PCR-based approach, the 5' end of the reverse primer in the RT-PCR reaction contained a T3 or T7 RNA polymerase site (Thisse and Thisse, 2008) (Table 2.5). Primers were designed to be between 23-28bp long, have a %GC content between

40-60%, and a T_m between 55°C-70°C. Probe primers were designed to amplify regions in the 3' UTR (if possible). The 20µl synthesis reaction (for PCR or plasmid method) used 2µl 10X DIG RNA labeling mix (Roche)[‡], 1µl T3 RNA Polymerase (Roche), 2µl 10X Transcription Buffer (Roche), along with 200-400ng of pure, linear DNA. Reaction volume was topped up to 20µl with RNase-free water. The RNase inhibitor, RNase Out (Invitrogen) (1µL) was also added to the reaction to prevent degradation of the newly synthesized RNA products. The reaction mix was incubated at 37°C for one hour, an additional 1µl of RNA polymerase was added to the mix, and then incubated for another hour at 37°C. Then, following a 5-minute DNase I digest (Ambion) (1µl) at 37°C, the reaction was stopped using 2µl of 0.2M EDTA pH8.0. The reaction mix was then run through Roche Mini Quick Spin columns to purify the newly synthesized riboprobes. First the columns were spun (without any reaction product added) in the 2ml tube for 2 minutes at 2500rpm. The end of the column was then broken off and the column was spun again at 2500rpm for 2 minutes. The probe synthesis reaction was then transferred to the column in a clean 1.7ml tube and spun at 2500rpm for 4 minutes. RNase Out (Invitrogen) (0.5µl) was added to each probe preparation and put at -80°C for long-term storage. Working stocks of probes were created by diluting the probe reaction from 1:100 to 1:400 in hybridization solution (HYB) (50% formamide, 5X SSC [saline sodium citrate buffer], 50µg/ml heparin, 0.1% Tween-20, 0.092M citric acid, sterile H₂O). Working stocks were stored at -20°C in between use.

2.8.2 mRNA In Situ Hybridization Protocol

The mRNA in situ protocol used during experiments is based on previously described protocols by Gongal et al. (2011), Gongal and Waskiewicz (2008), and Thisse and Thisse (2008). If embryos were stored long-term in methanol, they were first rehydrated with successive washes of 70% methanol/PBST, 50% methanol/PBST, and 30% methanol/PBST before continuing on with the PBST washes. Embryos stored in PBST at 4°C began the

[‡] 10X Fluorescein Labeling Mix is substituted for fluorescein labeled probes

ISH with four 5 minute PBST washes. Staged, dechorionated embryos were then permeabilized during an incubation of 10µg/ml proteinase K in PBST for the following lengths of time: <10 hpf (no proteinase K treatment), 10-12hpf (30 seconds), 12-14hpf (1 min), 18-26 hpf (3-4 min), 28 hpf (7 min), 36 hpf (15 min), 2 dpf (20 min). Proteinase K-treated embryos were then refixed with 4% PFA for 20 minutes at room temperature on a rotating platform. Following re-fixation, embryos were washed out of 4% PFA with four additional 5 minute PBST washes. Embryos were then pre-hybridized for >2 hours at 65°C in HYB + tRNA solution (500µg/ml). Pre-warmed probe (200-500µl) was then added to each tube and embryos were left in the 65°C water bath overnight.

The following morning, embryos were washed at 65°C for 5 minutes (each) in [1] 66% HYB, 33% 2X SSC, [2] 33% HYB, 66% 2X SSC, and [3] 2X SSC. Twenty minute high stringency washes were carried out first with [1] 0.2X SSC + 0.1% Tween-20, followed by two consecutive washes in [2] 0.1X SSC + 0.1% Tween-20, all at 65°C. Embryos were then put into 5 minute washes of [1] 66% 0.2X SSC 33% PBST, 33% [2] 0.2X SSC 66% PBST, and [3] PBST at room temperature on a shaker. After the washes were complete, embryos were transferred into blocking solution containing 2% sheep serum and 2mg/ml bovine serum albumin (BSA) in PBST and allowed to incubate for >1hr at room temperature. Once blocking was complete, embryos were put into a 1:1000 dilution of sheep anti-DIG-AP FAB fragments (Roche) in blocking solution. The antibody incubation was put at room temperature for 2hrs or overnight at 4°C on a rotating platform.

Embryos were washed out of antibody for at least five 15-minute PBST washes at room temperature on a shaker and then put into Alkaline Tris colouration buffer (100mM Tris-HCl pH 9.5, 50mM MgCl₂, 100mM NaCl, 0.1% Tween-20, and sterile water) for four 5 minute washes. A 500µl aliquot of 0.45% nitroblue tetrazolium (NBT), 0.35% bromo-chloro indoyl phosphate (BCIP) in colouration buffer was then added to each tube of embryos, which were allowed to incubate in the dark for the duration of the colouration reaction. Embryos were

periodically monitored underneath a stereomicroscope to check the status of the colouration reaction. When the embryos were deemed sufficiently coloured, they were rinsed twice in milli-Q H₂O, followed by two quick washes of stop solution (PBST, pH 5.5)[§]. Afterwards, the embryos were put into two 10-minute washes in stop solution, with the embryos still sheltered from any light. Embryos were stored short-term (<2 days) in stop solution at 4°C and transferred to PBST for longer storage (>2 days).

During two color ISH reactions, the colouration reaction was followed by two washes in sterile H₂O, and a 10min wash in 0.1M Glycine, pH 2.2. Embryos were then put through 4X 5min washes of PBST. Once the washes were complete, the embryos were incubated in block solution (2% sheep serum, 2mg/ml BSA in PBST) for >1hr at room temperature and then placed back in primary antibody (1:10 000 dilution of anti-fluorescein-AP FAB fragments (Roche)) for 2 hrs at room temperature or overnight at 4°C. Similar to the first colouration reaction, the embryos were then washed out of antibody with at least five 15minute PBST washes, and then run through four 5 minute washes of colouration buffer. Embryos were then incubated in the dark in a solution of 0.175% INT Red and 0.0175% BCIP in colouration buffer. When the colouration reaction was complete, embryos were run through two colouration buffer washes, followed by two H₂O washes and four 5-minute PBST washes. Colored embryos were stored in 4% PFA at 4°C.

For high quality photographs, embryos were manually deyolked underneath the microscope using 2% methyl cellulose (a viscous substance used to hold the embryos in place) and an insect pin. Deyolked embryos were then washed in PBST to remove any leftover methylcellulose and run through successive washes of 30%, 50%, and 70% glycerol in PBS. Glycerol-cleared embryos were then carefully mounted on glass slides and photographed on a Zeiss

[§] Embryos photographed on the yolk were transferred directly from coloration solution into 100% methanol + 0.1% Tween-20 and photographed on the stereomicroscope using the Olympus SZX12 stereoscope fitted with a QImaging micropublisher camera.

Axiomager.Z1 scope using Axiovision SE64 Rel.4.8 Software. All figures were assembled in Photoshop CS4.

2.9 Whole Mount Immunohistochemistry (Laminin Staining)

Immunohistochemistry was performed in 1.7ml microfuge tubes with approximately 20 embryos/tube. Fixed, dechorionated embryos were washed out of 4% PFA fix through four 5-minute PBST washes. Permeabilization of 2dpf embryos was done during a five-minute incubation of 10 μ g/ml proteinase K in PBST at room temperature. Permeabilized embryos were then re-fixed in 4% PFA for 20 minutes at room temperature. PFA was washed off the embryos during another four 5-minute PBST washes. This was followed by two quick rinses with H₂O and a second permeabilization reaction with acetone at -20°C for seven minutes. The acetone was rinsed off during two quick H₂O washes and four 5-minute PBST washes. Afterwards, a block solution of 1x PBST, 1% BSA, and 5% Goat Serum was added to each tube and the embryos were allowed to incubate at room temperature for >1hr on a rotating platform. Embryos were then placed in a 1:200 dilution of anti-laminin (Sigma) in 1x block solution and left overnight at 4°C.

The following morning, the primary antibody was washed off the embryos during five 15-minute washes of PBS DTT (PBST, 1% DMSO, 0.1% Triton X100) on a nutator. Embryos were then re-blocked in a solution of 1% BSA, 5% goat serum in PBS DTT (1-2hr at room temperature). An additional overnight incubation at 4°C (or 2hrs at room temperature) was done in a 1:500 dilution of Alexafluor 488nm or 586nm goat anti-rabbit secondary antibody (Invitrogen) in block. Due to the light-sensitivity of the secondary antibody, all embryos were kept in the dark from this stage in the protocol onward.

Secondary antibody was rinsed off the next morning during four 15-minute PBS DTT washes at room temperature. To prepare embryos for photographing, all embryos were deyolked and cleared in 70% glycerol in PBST.

Mounted embryos were then photographed on using the Zeiss Axio Imager.Z1 camera and Zeiss Zen software.

2.10 mNRA and DNA Construct (*rx3:gdf6a*) Injection

The *rx3:gdf6a* BMP overexpression construct was designed and created using the techniques discussed in French et al. (2009). For insertion into the genome, DNA constructs were co-injection with Tol2 transposon mRNA (Urasaki et al., 2006). Immediately prior to injection, cocktails of 50pg/nl of *rx3gdf6a*, 250pg/nl of Tol2 mRNA were prepared using depC-treated H₂O and kept on ice for the duration of injections. Additionally, per 10µl DNA/Tol2 preparation, 1µl of 0.1M KCl to decrease the toxicity of injections. Similar to morpholinos, *rx3:gdf6a/Tol2* was injected into 1-cell stage embryos using a microinjection rig. For better integration, care was taken during injections make sure that DNA/mRNA material was placed into the single stage and not the surrounding yolk. Post-injection embryonic care was performed as previously described.

2.11 Live Imaging

Prior to imaging, if required, embryos were injected with 3ng/ea of *sfrp1a* and *sfrp5* morpholino into the *Tg[Rx3:GFP]* strain of zebrafish. All embryos, regardless of morpholino injection or not, were allowed to grow for approximately 18 hours at 28.5°C in embryo media. Once embryos reached the appropriate stage, they were dechorionated, laterally mounted in low-melting point agarose in a 35mm x 10mm petri dish, and submerged in embryo media. The dish was then secured to a glass slide using a generous amount of vacuum grease applied to the bottom of the dish. Embryos were photographed on a Zeiss Axio Imager.Z1 camera using a water-emersion 20X objective lens. To prevent evaporation of media during imaging, a layer of parafilm was used to create a seal around the petri dish and objective lens. In order to keep embryos developing at a normal rate, the imaging room was also heated to 28.5°C using a space heater. The Zeiss Zen program was set to take confocal images every 10 minutes over a span of 24 hours.

2.12 Tables

Morpholino Name	Sequence 5' - 3'	Concentration (ng)
<i>hhat MO</i>	ATG AAA GAA TCC AGT AAG CCA CCA T	up to 15
<i>hhatNOL</i>	ACA AAC AAA AAA CTC TCG CGC CCG C	7
<i>hhatlaMO</i>	TAA CCT TGT ATC TGC CTT TCA CAG C	up to 10
<i>hhatlbMO</i>	TCG GTA GAG CTG CTT TGA CCC CCA T	3 (with 3ng P53)
<i>hhatlbNOL</i>	TAT CCA CCT TGA GCA CAG AAA TTC T	up to 15
<i>hhatlb splice</i>	AAA CAC CTG TTT ACT AAC CTT GAG C	up to 15
<i>p53 MO</i>	GCG CCA TTG CTT TGC AAG AAT TG	3 (with 3ng hhatlbMO)
<i>sfrp1a TB</i>	GGA CAA AGA TGC AAG GGA CTT CAT T	1
<i>sfrp1a SB</i>	TAG TCA TTT AGA CTT ACC GTT GGG T	3 (with 3ng sfrp5 SB)
<i>sfrp1a-001/002 splice</i>	TGT CCT GAA AGA GAG AAA ATG CTG T	1 (with 3ng sfrp5 SB)
<i>sfrp1a 002 tln</i>	GGT GTC CCA TTC TTG ACG CAA ATG A	3
<i>sfrp5 TB</i>	ACA CCT GCC TCT TCA GCT CCG CCA T	1
<i>sfrp5 SB</i>	TGA GTG CTG TAG ATA GAA CAA AAG A	3 (with 3ng sfrp1a SB or 1ng sfrp1a-001/002)

Table 2.1: Morpholino oligonucleotide sequences

Gene	Primer Sequence	Restriction Site	Size (bp)	T(m)
hhat for BamHI	CAC AGG ATC CAC CAT GGT GGC TTA CTG GAT TCT TTC ATT C	BamHI		65.4
hhat rev XbaI	CAC ATC TAG ACA CTG AGT GGT GTT GTC ATC TCA TGT	XbaI	1500	62.8
hhatla for BamHI	CAC AGG ATC CAC CAT GGG GAT CAA G...	BamHI		71.4
hhatla rev EcoRI	CAC AGA ATT CCT CAA TGA CCT CTC TCT GT....	EcoRI	1500	61.8
hhatlb for BamHI	CAC AGG ATC CAC CAT GGG GGT CAA AAG CAG CTC TAC CG	BamHI		69.4
hhatlb rev EcoRI	CAC AGA ATT CCT ACT CTG CCT TTT GCT TGC TGG TCT CAG	EcoRI	1600	65.6

Table 2.2: mRNA overexpression primer sequences

Gene	Primer Sequence	Size (bp)	T(m)
sfrp1a for Exon1A (RT)	TCA ACA CAC CCA ATG ATA CTT CCA C	1181	56.6
sfrp1a rev Intron1A (RT)	TGA TAA CTC CAG ATG AAA ACC CCC		57.1
sfrp1a for Exon1C (RT)	TGG TTC TAC TCA CTT CAG CCT CTT C	496	55.0
sfrp1a rev Exon2C (RT)	GGT GGA CAC ACT TTG GAA ACT GG		57.1
sfrp5 for Intron 2C (RT)	TCA TTC GCT TCA GGG AAC AGC CAG	557	63.2
sfrp5 rev Exon3C (RT)	AGG TTG TCC AGT TGT GAG CAG GGG		62.2

Table 2.3: RT-PCR primer sequences for morpholino controls

Gene	Forward Primer (5'-3')	Reverse Primer (5'-3')
<i>ef1a</i>	CTT TCG TCC CAA TTT CAG G	CCT TGA ACC AGC CCA TGT
<i>GFP</i>	GTG GTG CCC ATC CTG GTC G	AGC TTG CCG TAG GTG GCA T
<i>sfrp1a</i> (Ex-Int)	TGT GCA TCA ACA CAC CCA AT	GAA TTA GTC ATT TAG ACT TAC CGT TGG
<i>sfrp1a</i> (Ex-Ex)	GCA TCA ACA CAC CCA ATG AT	CAA GGG GGA CAA ACT GGA G

Table 2.4: Quantitative Real Time PCR (qRT-PCR) primer sequences

Gene	Forward Primer (5'-3')	Reverse Primer (5'-3')	T3 or T7 Site	Size (bp)	T(m)
<i>bmp4</i>	GCC GCT AAA CGG AGA CTC TTA CC	TAA TAC GAC TCA CTA TAG GGG GGT CGC TTG GCT ATG TGT TTC	T7	1278	52.0
<i>eya2</i>	ATG GCA GCT TAC GGA CAG	TAA TAC GAC TCA CTA TAG GGG TTC TTG TAT GTG TTG TAG ATC TCT TTA	T7	1000	
<i>foxd1</i>	AGG CAA CTA CTG GAC GCT AGA CCC TG	CAT TAA CCC TCA CTA AAG GGA ACA GAC CGT GTA AAA ATA TCA CAC TCC	T3		
<i>foxd1</i>	AAA TGG CTT GAG TGT TGA CAG ACT CG	CAT TAA CCC TCA CTA AAG GGA AAG AAT GTG ACC TGC ATG GTG GTG AC	T3	1164	55.0
<i>nlz2</i>	GGG GAC AAG TTT GTA CAA AAA AGC AGG CTC CAT GAT	TAA TAC GAC TCA CTA TAG GGA GGG CTT GAG CCA GCT TTA CT	T7	1000	
<i>sfrp2*</i>	GGT GTG TTT GGA TGA CCT GGA CG	AAT TAA CCC TCA CTA AAG GGA CTG AAG TTT GCG AAT GCT GCG AG	T3	583	58.0
<i>tbx5</i>	GAG GGA AGT TCG CTA TCA ACC G	TAA TAC GAC TCA CTA TAG GGT CCA TTG TTT TCA TCC GCC TTG	T7	713	52.0
<i>vax1*</i>	CAC GGC AAC ATT CTT TAC ATT CTC AG	AAT TAA CCC TCA CTA AAG GGA CAC TCA TAC CAC GGT TCA CAA ACT TC	T3	876	54.5
<i>wnt2*</i>	AAC CCG TAG ACA AGT GCC TGA ACG	AAT TAA CCC TCA CTA AAG GGA GTA TTT TTT GCG AAG ATA GTC ACC CGT C	T3	759	58.1
<i>wnt2ba*</i>	AAA AAA AAT CGC AAA CTG ACC GC	AAT TAA CCC TCA CTA AAG GGA AAA GTC CCC GTC TTC ATC GCT CG	T3	911	53.5
<i>wnt2bb*</i>	ATC TAA AGC CCA AAC TTC AGC AGG	AAT TAA CCC TCA CTA AAG GGA CAT TCT TCC ACA GCG ATT GTT ATG	T3	803	55.4
<i>wnt8b*</i>	TGG TGA CTT TGA TAA CTG TGG ATG TG	AAT TAA CCC TCA CTA AAG GGA TTC TTG ACC CGT TTG CTT CTC TTC	T3	708	55.0
<i>wnt11r*</i>	TCT CAC TCG GAC TTC ACA CAA ACG G	AAT TAA CCC TCA CTA AAG GGA GAA TGG AGC AGG AAC CAG AAA CAC C	T3	651	63.1
<i>zic2a</i>	CCA ACA ACC ACA GCA GTT TAT CGT C	GCC AGA GTC AAG TTC AAG TTC ACG GCA TTA ACC CTC ACT AAA GGG AA	T3	1292	

Table 2.5: PCR-based probe primer sequences

* Probe construction by author

Gene	Vector	Antibiotic	Linearize	RNA Pol.	Made by VH
<i>aldh1a2</i>	pSPORT	Carbenicillin	EcoR1	Sp6	no
<i>aldh1a3</i>	pCR4-TOPO	Carbenicillin	Not1	T3	no
<i>bambi</i>	pCR4-TOPO	Carbenicillin	Not1	T3	no
<i>ephB2 (c11)</i>	pCR4-TOPO	Carbenicillin	Not1	T3	no
<i>ephB3 (c8)</i>	pCR4-TOPO	Carbenicillin	Pme1	T7	no
<i>efnB2a</i>	pCR-4TOPO	Carbenicillin	Not1	T3	no
<i>eGFP</i>			Not1	T3	no
<i>gdf6a</i>	pBSKII	Carbenicillin	Not1	T7	no
<i>pax2a</i>		Carbenicillin	BamH1	T7	no
<i>sfrp1a</i>		Carbenicillin	Not1	T3	no*
<i>sfrp5</i>		Carbenicillin	Not1	T3	no*
<i>vax2</i>	pCR4-TOPO	Carbenicillin	Not1	T3	no

Table 2.6: mRNA in situ hybridization probe plasmids

* Made in the Houart lab

2.13 Literature Cited

- Collery, R.F., and Link, B.A. (2011). Dynamic smad-mediated BMP signaling revealed through transgenic zebrafish. *Dev Dyn* 240, 712-722.
- Dorsky, R.I., Sheldahl, L.C., and Moon, R.T. (2002). A transgenic Lef1/beta-catenin-dependent reporter is expressed in spatially restricted domains throughout zebrafish development. *Dev Biol* 241, 229-237.
- French, C.R., Erickson, T.E., French, D.V., Pilgrim, D.B., and Waskiewicz, A.J. (2009). Gdf6a is required for the initiation of dorsal-ventral retinal patterning and lens development. *Dev Biol* 333, 37-47.
- Gongal, P.A., March, L.M., Holly, V.L., Pillay, L.M., Berry-Wynne, K.M., Kagechika, H., and Waskiewicz, A.J. (2011). Hmx4 regulates Sonic hedgehog signaling through control of retinoic acid synthesis during forebrain patterning. *Dev Biol* 355, 55-64.
- Gongal, P.A., and Waskiewicz, A.J. (2008). Zebrafish model of holoprosencephaly demonstrates a key role for TGIF in regulating retinoic acid metabolism. *Hum Mol Genet* 17, 525-538.
- Kozak, M. (1986). Point mutations define a sequence flanking the AUG initiator codon that modulates translation by eukaryotic ribosomes. *Cell* 44, 283-292.
- Livak, K.J., and Schmittgen, T.D. (2001). Analysis of relative gene expression data using real-time quantitative PCR and the $2^{-\Delta\Delta C(T)}$ Method. *Methods* 25, 402-408.
- Nasevicius, A., and Ekker, S.C. (2000). Effective targeted gene 'knockdown' in zebrafish. *Nat Genet* 26, 216-220.
- Pillay, L.M., Forrester, A.M., Erickson, T., Berman, J.N., and Waskiewicz, A.J. (2010). The Hox cofactors Meis1 and Pbx act upstream of gata1 to regulate primitive hematopoiesis. *Dev Biol* 340, 306-317.
- Thisse, C., and Thisse, B. (2008). High-resolution in situ hybridization to whole-mount zebrafish embryos. *Nat Protoc* 3, 59-69.
- Urasaki, A., Moryan, G., and Kawakami, K. (2006). Functional dissection of the Tol2 transposable element identified the minimal cis-sequence and a highly repetitive sequence in the subterminal region essential for transposition. *Genetics* 174, 639-649.

Veien, E.S., Rosenthal, J.S., Kruse-Bend, R.C., Chien, C.B., and Dorsky, R.I. (2008). Canonical Wnt signaling is required for the maintenance of dorsal retinal identity. *Development* 135, 4101-4111.

Westerfield, M. (2000). *The zebrafish book. A guide for the laboratory use of zebrafish (Danio rerio)*. 4th ed., Univ. of Oregon Press, Eugene.

Chapter 3

Results & Discussion

3.1 Zebrafish *sfrp1a* and *sfrp5* are expressed during early eye development

The expression patterns of zebrafish *secreted frizzled-related protein 1a* (*sfrp1a*), *sfrp1b*, *sfrp2*, *sfrp3*, and *sfrp5* at a variety of stages between 40% epiboly and 48hpf have been published (Tendeng and Houart, 2006). Based on their data, only *sfrp1a*, *sfrp2*, and *sfrp5* are expressed in the developing eye. To investigate the expression of *sfrp* genes during eye morphogenesis, we performed whole mount *in situ* hybridization for *sfrp1a*, *sfrp2*, and *sfrp5*.

Congruent with previous results, whole mount *in situ* hybridization revealed that both *sfrp1a* and *sfrp5* are expressed in the anterior forebrain at the time of optic vesicle formation (6ss) (Figure 3.1-A,B; M,N). Within the presumptive eye, *sfrp1a* expression is found throughout the budding optic vesicle, with exception of a small dorsal region (Figure 1-C,D). *sfrp5* is also expressed in the anterior, ventral optic vesicle during early eye development, but with a more restricted domain of expression than *sfrp1a* (Figure 1-O,P). As the optic vesicles invaginate, expression of both genes persists in the developing optic cup through to 25hpf (Figure 3.1-E-H; Q-T). Micro-dissection of eyes at 25hpf revealed that *sfrp1a* expression encompasses a large portion of the ventral retina, with only the dorsal-most region lacking expression. *sfrp1a* is also expressed in the lens at this stage of development (Figure 3.2-A). In contrast, although it is expressed strongly during earlier eye morphogenesis, *sfrp5* at 25hpf has low levels of expression in the ventral-to-mid retina and the lens (Figure 3.2-G). At 36hpf, *sfrp1a* continues to have strong expression in the majority of the retina, but expression in the lens is now absent (Figure 3.1-I,J; Figure 3.2-B). *sfrp5* expression at this time is nearly abolished, save for a small stripe of expression in the temporal retina (Figure 3.1-U,V; Figure 3.2-H). By 2dpf, *sfrp5* expression is undetectable and *sfrp1a* expression exists only as a single line adjacent to the fusing choroid fissure (Figure 3.1-K,L,W,X; Figure 3.2-C,I).

Past experiments have revealed that *sfrp1a* and *sfrp2* in other organisms can work in concert to pattern tissues (Esteve et al., 2011). However, zebrafish *sfrp1a* and *sfrp2* are not expressed in overlapping patterns and stages to work

cooperatively during eye development. In contrast to *sfrp1a*, *sfrp2* expression does not turn on in any eye structures until around 22hpf (Tendeng and Houart, 2006), and has very faint, transient expression in the retina at 25hpf (Figure 3.1-Y,Z; Figure 3.2-D). By 36hpf and 48hpf, its expression in the retina is undetectable (Figure 3.1-A'-D'). In contrast to previously published data demonstrating that *sfrp2* is expressed strongly in the lens (Tendeng and Houart, 2006), our *sfrp2* probe only weakly labels this tissue (Figure 3.2-D,E). Our experiments also detect expression of *sfrp2* in the retinal pigmented epithelium (RPE), a detail that has not been previously documented. Low levels of expression can be found throughout the RPE at all three stages of development (25hpf, 36hpf, 48hpf) (Figure 3.2-D-F). Proper RPE formation has been found to alter proper eye morphogenesis, however, because of the lack of significant expression at earlier stages of eye morphogenesis and extremely low levels of expression in the retina at later stages, I chose to focus solely on the roles of *sfrp1a* and *sfrp5* in retinal patterning for the remainder of this thesis.

Based on the observed expression patterns and previous research, we can conclude that *sfrp1a* and *sfrp5* are expressed in tissues at stages that are consistent with the hypothesis that these genes play a role in eye morphogenesis and retinal patterning. In continued support of this idea, zebrafish *sfrp1a* mRNA overexpression has already been linked to expansion of the optic primordium and has continued expression in later ocular tissues (Kim et al., 2007). This makes it reasonable to predict that *sfrp1a* knockdown may show additional roles for specification of ocular tissues. In addition, *osfrp5*, the *Medaka* ortholog of *sfrp5*, has a similar expression pattern to zebrafish *sfrp5* and, through morpholino knockdown, has been shown to cause dorsalization of the retina and changes in both cell proliferation and apoptosis in the developing eye (Ruiz et al., 2009). Furthermore, *sfrp1a/sfrp2* double knockouts in mice cause defects in peripheral optic cup patterning (Esteve et al., 2011). However, from our expression pattern analysis in zebrafish, we can see that *sfrp1a* and *sfrp5* genes, and not *sfrp1a* and *sfrp2*, have overlapping expression in the eye. We hypothesize that *sfrp2* may have alternative functions in zebrafish development and, based on shared tissue

expression, *sfrp1a* and *sfrp5* may instead work cooperatively during eye development. Compiling all of the data, we have strong support that both *sfrp1a* and *sfrp5* are expressed in the presumptive eye at stages when the optic vesicle is patterning, and are therefore good candidates to play roles in zebrafish retinal patterning.

3.2 Zebrafish *sfrp1a* & *sfrp5* have potential alternative transcripts

In order to investigate retinal patterning following knockdown of *sfrp1a* or *sfrp5*, we designed both translation-blocking and splice-blocking morpholinos to inhibit proper protein formation. Using the ENSEMBL database for sequence analysis, we were surprised to learn that both *sfrp1a* and *sfrp5* have predicted alternative transcripts that have not been previously addressed in the literature. The alternative transcript, *sfrp1a-002*, contains the same last two exons as *sfrp1a-001*, along with an alternative 4 bp first exon (Figure 3.3-A-C). Investigation of functional domains within either sequence showed that both *sfrp1a-001* and *sfrp-002* contain the netrin domain, but only *sfrp1a-001* contains the CRD domain. Independent experiments have had conflicting results on which domain is more important for Sfrp activity; however, Medaka Sfrp1 containing only the NTR domain is able to reproduce all of the phenotypes of the full-length transcript, suggesting that the NTR may be required for Sfrp1 activity (Lopez-Rios et al., 2008).

ESTs are short regions of DNA, typically between 200-500bp, that are found within the gene sequence that can act as identifiers for expressed transcripts. Gene mRNA or cDNA sequences can be analyzed using large online databases that can quickly identify any ESTs present. EST analysis of the alternative *sfrp1a-002* transcript reveals that its unique sequence is encoded by 3 independent ESTs. This suggests that the *sfrp1a-002* transcript is expressed *in vivo*. Therefore, because *sfrp1a* has two different (potentially) coding alternative-splice transcripts, multiple morpholinos were designed to target each sequence separately. In addition, a third morpholino was designed to target both sequences simultaneously (Figure 3.4-A).

A similar analysis of ESTs was also performed on both potential *sfrp5* transcripts. The predicted alternative transcript, *sfrp5-201*, contains a portion of the *sfrp5-001* first exon but uses a separate transcription start site. Both transcripts then share the second exon, but have completely different 3' exon sequences (Figure 3.3-D-F). Interestingly, although both transcripts contain each of the known functional domains (the CRD domain and the netrin domain), EST analysis suggests that only *sfrp5-001* is expressed in the embryo as no ESTs were found in the unique coding sequence of *sfrp5-201*. Based on this analysis, we have chosen to focus only on *sfrp5-001* and designed morpholinos to target this single transcript (Figure 3.4-A).

3.3 Confirmation of morpholino specificity

Morpholinos are anti-sense oligonucleotides that are designed to bind specific mRNA sequences and prevent gene expression (Nasevicius and Ekker, 2000). The name morpholino comes from the morpholine modification, which replaces the ribose sugar present in a typical oligo backbone (Summerton and Weller, 1997). There are two varieties of morpholinos: translation blocking and splice blocking. Translation blocking morpholinos sit on or near the AUG translation start site of the mRNA and prevent the transcription machinery from binding and translating the mRNA into protein (Nasevicius and Ekker, 2000; Summerton, 1999). In contrast, splice blocking morpholinos bind to exon-intron boundaries and prevent spliceosome machinery from removing introns from the pre-mRNA (Draper et al., 2001; Morcos, 2007). Even in the presence of splice-blocking morpholinos, splicing can still utilize cryptic splice sites; however, retained intronic sequences can result in changes to protein structure. Additionally, alternative splicing can cause excision of internal exons or deleterious frame-shift mutations (Morcos, 2007). Morpholinos provide a quick, convenient method for knocking down gene function but like any technology, come with drawbacks. Morpholino injection can cause phenotypes associated with toxicity or mistargeting, especially at higher doses (Robu et al., 2007; Sumanas and Larson, 2002)). For example, morpholinos have been known to produce non-specific

defects such as activation of the p53 apoptotic pathway. This results in widespread cell death and necrosis, most often in neural tissue. Co-injecting with a p53-targeted morpholino can diminish these defects, but does not always eliminate them (Robu et al., 2007). Other mistargeting artefacts include phenocopy of *bozozok* mutations causing notochord, trunk length and muscle abnormalities (Miller and Kimmel, 2001; Nasevicius and Ekker, 2000). Unfortunately, these additional phenotypes can be difficult to decipher and there is currently no easy way to prevent their occurrence. Therefore, because of knockdown technologies' notorious off-target effects, controls are essential to ensure that the morpholinos are specifically inhibiting the correct mRNAs.

Specificity of *sfrp1a* (*S2*) and *sfrp5* (*S*) splice-blocking morpholinos was confirmed using RT-PCR with primers spanning intron-exon and/or exon-exon boundaries (Figure 3.4-B,C). *Sfrp5* morphants have reduced levels of the 557bp exon-exon band (Figure 3.4-B). Although we do not detect a second PCR product band following splice-blocking morpholino injections, the targeted *sfrp5* intron is over 20kb in size and may create products too large for RT-PCR amplification. Similarly, *sfrp5* morphants may have decreased exon-exon products due to nonsense-mediated decay of alternatively spliced transcripts containing a premature stop codon. In addition to having changes to exon-exon products, *sfrp5* morphants also had increased levels of the 631bp exon-intron RT-PCR product, indicating improper splicing in morphant embryos (Figure 3.4-B). *Sfrp1a* (*S2*) morphants also have decreased 496bp exon-exon RT-PCR product, as seen by a decrease in band intensity (Figure 3.4-C). Similar to *sfrp5* morphants, a second splice product could not be detected on the gel due to large intron size. Exon-intron PCR was also attempted on *sfrp1a* (*S*) morphants, which show an increase in intronic products (496bp) formed.

qRT-PCR was used to confirm morpholino specificity for *sfrp1a* (*S2*). Targeting both exon-exon spanning products and exon-intron spanning products reveals a decrease in mRNA transcript in *sfrp1a* splice-blocking morphants (Figure 3.4-D,E). Exon-intron qRT-PCR showed that *sfrp1a* (*S2*) morphants have

a 1.52 fold decrease in PCR product levels (Figure 3.4-D). Similarly, morphants have a 2.85 fold decrease in exon-exon products (Figure 3.4-E). These findings can be explained by morpholino-induced degradation of mRNAs. For example, frame shift mutations caused by improper splicing can result in premature stop codons that activate the nonsense mediated decay pathway. Additionally, splice-blocking morpholinos may also cause retention of pre-mRNA products in the nucleus due to binding of only one snRNP (small nuclear ribonucleoproteins) to the remaining unblocked splice site on the transcript and cause them to experience increased rates of degradation.

3.4 Survey of phenotypes caused by *sfrp1a* & *sfrp5* morpholino knockdown

Morpholino knockdown of *sfrp1a* (*S*) and *sfrp5* (*S*) results in a suite of defects including open choroid fissures (ocular coloboma) (M = 59.1%, SD = 0.4%), ventral retina thinning (M = 25.7%, SD = 1.0%), misshapen somites and downward tail curving (M = 60.7%, SD = 2.6%), and cardiac edema (M = 62.3%, SD = 9.1%) (n = 66) (Figure 3.5-A-D). *sfrp1a/sfrp5* morphants do not exhibit high levels of necrosis, indicating that our morpholinos do not overtly cause non-specific activation of the p53 apoptotic pathway. Our *sfrp1a/sfrp5* morphants do, however, have minor developmental delays in addition to gross morphological changes. Because choroid fissure closure is a timed event, open fissures can persist due to developmental delays. To ensure that the ocular coloboma phenotypes I observed were not just a result of delayed fissure closing, embryos were screened at later stages. The ventral fissure typically closes between 24-48 hpf (Morris, 2011). Morphant embryos have obvious open choroid fissures that persist at 3dpf, well past the time of choroid fissure fusion, indicating that the ocular coloboma phenotype is not just a delayed developmental event.

To ensure that observed phenotypes were due to specific gene knockdown, we examined phenotypes resulting from injection of distinct non-overlapping morpholinos targeting each *sfrp* gene. Combinations of *sfrp1a* and *sfrp5* including translation-blocking morpholinos (*sfrp1a* (*T*)/*sfrp5* (*T*)) and splice-blocking morpholinos (*sfrp1a* (*S*)/*sfrp5* (*S*); *sfrp1a* (*S2*)/*sfrp5* (*S*)) (Figure 3.4-A) result in

similar phenotypes (Figure 3.6-A-D). Interestingly, based on single morpholino injections, *sfrp1a* (S2) seems to be more toxic than *sfrp1a* (S) and gives phenotypes at lower doses but does not translate to additional defects. Because *sfrp1a* (S2) targets both *sfrp1a* transcripts, it is possible that the increase in effectiveness of the morpholino is due to knockdown of two *sfrp1a* transcripts that have similar functions in development. Supplementing the RT-PCR and qRT-PCR data (Figure 3.4-A-E), these results support that the morpholinos are correctly targeting our chosen transcripts.

To gain a better understanding of the eye defects we see in our *sfrp1a/sfrp5* morphant embryos, we took live images of *sfrp1a/sfrp5*-depleted embryos from the *Tg[Rx3:GFP]* zebrafish strain. *rx3* is expressed in the early eye field and retains expression throughout eye morphogenesis (Chuang et al., 1999). The *Tg[Rx3:GFP]* line is useful because the GFP fluorescence provides a visual marker for changes in eye morphology during live imaging. Through comparing live imaging, we conclude that early eye morphogenesis and optic vesicle evagination is unchanged between *sfrp1a/sfrp5* double morphants and wildtype embryos. However, later stages reveal that *sfrp1a/sfrp5*-depletion causes thinning of the ventral retina, a phenotype also observed during assessments of gross morphology (Figure 3.5-C,D; Figure 3.7-A,B). In particular, our time course shows thinning of the ventral temporal lobe of the retina as compared to wildtype eyes (Figure 3.7-A,B).

Although we see embryos with obvious coloboma, some fissure defects are too subtle to easily identify. We were able to examine fissure defects further using immunohistochemistry (IHC) with an anti-laminin antibody on 2dpf embryos. Laminins are extracellular scaffolding proteins that aid in tissue structure, cell adhesion, cell differentiation, and cell migration (Scheele et al., 2007). Laminin forms a meshwork surrounding the outside of the eye, providing an outline of the developing retina. Laminin protein persists along the choroid fissure line, disappearing only when the two ventral lobes of the retina have completely joined; therefore, Laminin IHC is an additional assay for coloboma

that can identify even mild fissure closure defects. Comparison of uninjected embryos at 2dpf to stage-matched *sfrp1a/sfrp5* double morphants reveals the presence of coloboma phenotypes. Interestingly, *sfrp1a/sfrp5*- depleted embryos show distinct degrees of severity of open fissures. Some morphant eyes have a single stripe of Laminin left along the ventral fissure (n = 4/9), whereas others have a large, open gap and overall “horseshoe” shaped neural retina (n = 5/9) (Figure 3.5-E,F). Together, Laminin IHC and observation of gross eye morphology confirm that *sfrp1a/sfrp5* morphants fail to properly close the ventral choroid fissure. Additionally, Laminin IHC was able to identify more subtle defects than just those identified through general eye morphology, suggesting that more *sfrp1a/sfrp5* morphants may have fissure defects than initially observed (M = 59.1%, SD = 0.4%, n =66). Based on their expression patterns, it is not surprising that knockdown of *sfrp1a* and *sfrp5* causes fissure defects; both genes are expressed in the retina in restricted ventral regions at stages when dorso-ventral retinal patterning influences the ability of the ventral fissure to close. In addition, *sfrp1a* is expressed specifically along the fissure line during the final stages of choroid fissure closing.

3.5 *sfrp1a* and *sfrp5* act synergistically during eye development

Next, we wanted to determine if *sfrp1a* and *sfrp5* act cooperatively during eye morphogenesis. Based on injections during experiments aimed towards surveying morpholino phenotypes, single morpholino injections produced milder phenotypes; therefore, we predicted that *sfrp1a* and *sfrp5* work synergistically to pattern the eye. In order to assess this further, we compared single morphants to double morphants, using the same total morpholino concentration. Injection of 6ng each of either *sfrp1a* or *sfrp5* splice-blocking morpholinos into 1-cell staged zebrafish produces mild phenotypes at low frequencies. Morphants display ocular defects including open choroid fissure (ocular coloboma), ventral retina thinning, and, in some cases, microphthalmia at 2dpf. *Sfrp1a* morphants display ocular coloboma (2.6%; SD = 3.6%; n = 75), whereas for *sfrp5* we observe small eyes (17.8%; SD = 9.0%; n = 64) and coloboma (2.9%; SD = 4.0%; n = 64). In contrast,

combination of the two morpholinos results in much higher prevalence of observed ocular phenotypes. Furthermore, experiments comparing phenotypes of single morpholino (*sfrp1a* or *sfrp5*) injections versus double morpholino injections showed stronger phenotypes including severely reduced eye size and increased appearance of ocular coloboma. Double morphants (*sfrp1a/sfrp5*), co-injected with 3ng of each morpholino, show 57.2% (SD = 12.2%; n = 76) of embryos with severely smaller eyes and 43.1% (SD = 4.5%; n = 76) with open choroid fissures (adj. p < 0.0006, Fisher's Exact Test, cumulative counts of two independent experiments) (Figure 3.8-A-F). Because double morphants injected with equal amounts of total morpholino are more strongly affected than single morphants, our data suggest that *sfrp1a* and *sfrp5* share at least partial functional redundancy during eye development. Evidence of *sfrp1a* and *sfrp5* redundancy is not surprising due to the fact that they have also been found to work together during zebrafish forebrain development and share, at least in part, certain regulatory factors such as *lhx5* (Peng and Westerfield, 2006). Sfrps also have a history of functional redundancy during eye development, as *sfrp1* and *sfrp2* double mutants cause peripheral optic cup defects in mice (Esteve et al., 2011).

3.6 Knockdown of *sfrp1a/sfrp5* does not cause changes in nasal/temporal gene expression

Nasal/temporal patterning relies on different signaling pathways and is generally independent of changes in dorsal/ventral patterning (Picker and Brand, 2005). Both *sfrp1a* and *sfrp5* are expressed ventrally during retinal patterning. In contrast, Wnts and BMPs, two postulated Sfrp ligands, are found in the dorsal retina. Based on this dorsal-ventral dynamic, we predicted that our *sfrp1a/sfrp5* morphants would not exhibit changes in nasal/temporal markers. To investigate any alterations in nasal/temporal retinal patterning, we examined the expression domains of *foxd1* and *foxd1*, that respectively form distinct nasal and temporal boundaries in the developing retina (Takahashi et al., 2009; Takahashi et al., 2003; Zhao et al., 2009). Experiments revealed that at 28hpf *foxd1* and *foxd1* are generally unchanged in *sfrp1a/sfrp5* morphants as compared to uninjected

controls, even in the most severely affected embryos ($n_{\text{foxG1}} = 17/17$; $n_{\text{foxD1}} = 14/14$) (Figure 3.9-A-D). Taken together, these data demonstrate that *sfrp1a/sfrp5* do not regulate nasal/temporal retinal patterning in zebrafish.

3.7 *sfrp*-depleted embryos have mild defects in ventral retina markers (*ephB2*, *ephB3*, *zic2a*) at 28hpf

Based on the previously published results that *Sfrp1a* and *Sfrp5* act as Wnt antagonists during early teleost eye development (Kim et al., 2007; Lopez-Rios et al., 2008; Ruiz et al., 2009), we hypothesized that *sfrp*-depleted eyes would exhibit a Wnt-induced expansion of dorsal identity at the expense of ventral identity. In addition, both *sfrp1a* and *sfrp5* are expressed in the ventral retina; therefore, we predict that *sfrp* depletion causes defects in ventral specification, similar to phenotypes seen in morpholino knockdown of Medaka *sfrp5* (Ruiz et al., 2009). To test this hypothesis, we examined expression of ventral retina markers in both uninjected (control) and *sfrp1a/sfrp5* double morphant eyes at 28 hpf to assess any changes in dorso-ventral axis patterning. I chose to use multiple markers, including *eph receptor B2* (*ephB2*) and *ephB3*, which are known to be Wnt-responsive in other tissues such as the mouse gastrointestinal tract (Batlle et al., 2002). *EphB2* and *EphB3* are critical for proper ventral retina cell identity, functioning as retinal ganglion cell receptors for retinotopic mapping (Hindges et al., 2002); hence, these markers can give additional information about the biological implications of knocking down *sfrp1a/sfrp5*. Surprisingly, ventral markers such as *ephB2* ($n=12/12$), *ephB3* ($n=20/20$), and *zic2a* ($n=17$) are all still expressed in *sfrp* morphant eyes (Figure 3.10-A-D). This is in contrast to Medaka *osfrp5* data, which shows that morpholino knockdown of *osfrp5* causes a near complete loss of *ephB2* and *ephB3* in the ventral retina (Ruiz et al., 2009). A decrease in *ephB2* expression and domain is also expected because previous findings show that its gene expression in the retina is negatively regulated by Wnt signaling (Veien et al., 2008). Instead, we observe a partially penetrant mild expansion in the domains of all three genes (*ephB2* $n=3/6$; *ephB3* $n=2/5$; *zic2a* $n=4/7$) (Figure 3.10-A-D).

3.8 Ventral retina markers *aldh1a3* and *vax2* are expanded in *sfrp1a/sfrp5* double morphants at 2dpf

A survey of additional ventral markers, *aldh1a2* and *vax2*, at 28hpf also did not show any detectable changes between control (uninjected) and *sfrp1a/sfrp5* morphants (n = 17/18; n = 19/20, respectively) (Figure 10-G-J); however, striking changes were seen in these two markers from 2dpf embryos. Both *vax2* ($M_{sfrp} = 26.7\%$, $SD_{sfrp} = 22.9\%$, n = 33) and *aldh1a3* ($M_{sfrp} = 44.5\%$, $SD_{sfrp} = 17.9\%$, n = 36) have embryos severely expanded domains of expression in *sfrp*-depleted eyes, with phenotypes ranging from expansion only around the lens to complete expansion encompassing the entire retina (Figure 3.10-K-P; Table 3.1). These phenotypes were not observed in uninjected, control embryos ($n_{aldh1a3} = 34/34$; $n_{vax2} = 36/36$). Together, these data suggest that *sfrps* are not required for early ventral retina gene expression in zebrafish, but play an important role in the maintenance of gene expression boundaries in the larval 2dpf retina. *Vax2* and its orthologues are also notoriously responsive to changes in dorsal markers and displays significant expansion in a variety of models with attenuated dorsal retina identity. For instance, inhibition of BMP signaling through over-expression of dominant-negative BMP receptors in chick causes abrogation of dorsal markers and a marked expansion in *VAX* (Adler and Belecky-Adams, 2002). Similarly, mutations in mouse BMP receptors, *Bmpr1a* and *Bmpr1b*, also cause expansion of *Vax2* (Murali et al., 2005). Other case studies, such as zebrafish BMP ligand (*gdf6a*) mutants also display *vax2* expansion in the retina (French et al., 2009; Gosse and Baier, 2009). In addition to changes in BMP signaling, comparable changes in ventral markers are also seen when the Wnt pathway is inhibited; mutations in the co-receptor, *Lrp6*, cause reduction in a variety of dorsal markers and expansion of ventrally expressed *Vax2* and *Aldh1a3* (Zhou et al., 2008). Given the expansion of *vax2* and *aldh1a3* in our morphants, we hypothesize that there are also alterations in expression of dorsal markers.

3.9 *Sfrp*-depleted embryos have reduction in multiple dorsal retina markers (*aldh1a2*, *bambia*, *tbx5*)

Although *sfrp*-depleted embryos do not show overt changes in early ventral retina markers, investigation of markers at 2dpf shows strong ventralization of the retina. Because expansion of ventral retina tissue generally happens at the expense of dorsal retina, we predicted our *sfrp* morphants to have defects in dorsal retina specification. Again, to investigate changes in dorsal patterning, we examined gene expression of relevant marker genes. In comparison to uninjected control embryos, we observed a moderate reduction in the expression of a number of dorsal retina markers in *sfrp1a/sfrp5* double morphants at 28hpf. The domain and expression levels of *bambi* ($t(8) = 5.50, p = 0.006$), *aldh1a2* ($t(4) = 3.14, p = 0.035$), and *tbx5* ($t(2) = 11.899, p = 0.007$), are all consistently and significantly decreased in morphant eyes (Figure 3.11-A-F; Table 3.1). In addition, preliminary investigation of the dorsal markers, *aldh1a2* and *tbx5*, also shows moderate decreases in expression at 2dpf ($n_{aldh1a2} = 6/23$; $n_{tbx5} = 7/23$) (Figure 3.11-G-L). Interestingly, we also observed large amounts of ectopic *aldh1a2* expression in a small number of morphants ($n_{aldh1a2} = 2/23$), but without an increase in retinal expression (Figure 3.11-I). Based on the decrease in dorsal markers at multiple stages, our data suggest that *sfrp1a/sfrp5* morphant retinas are ventralized. There are two known signaling pathways that are important for dorsal retina specification that could account for the changes we see in our morphants. The first pathway is Wnt signaling, which has been shown through overexpression of the *dkk1* inhibitor or mutation of the Wnt co-receptor, *Lrp6*, to attenuate dorsal retina specification (Veien et al., 2008; Zhou et al., 2008). Another pathway that may be affected in our *sfrp1a/sfrp5* morphants is the BMP pathway. BMP signaling is the most well studied pathway with regards to dorsal retina patterning.

The first dorsal marker, *bambi* (*BMP and activin membrane-bound inhibitor*), codes for a BMP pseudoreceptor that, in addition to being a negative regulator of BMP signaling, is also an indicator of the level of BMP signaling in the embryo (Onichtchouk et al., 1999; Sekiya et al., 2004). Our observation of decreased *bambi* in the retina suggests that BMP signaling may be affected in *sfrp1a/sfrp5*-depleted embryos. *tbx5* is also a downstream target of BMP

signaling and serves as further evidence that BMP may be affecting on our *sfrp1a/sfrp5* morphants (French et al., 2009; Gosse and Baier, 2009). Interestingly, numerous ocular coloboma models, such as *gdf6a* zebrafish mutants (Asai-Coakwell et al., 2007; French et al., 2009), *Lrp6* or *Bmp7* mutant mice ((Morcillo et al., 2006; Zhou et al., 2008), and BMP antagonist (*gremlin*) overexpression experiments in chick (Huillard et al., 2005), have attenuated dorsal gene expression and BMP signaling that coincides with fissure defects; Therefore, the open fissures we observe, in combination with down-regulated dorsal retinal markers, may be explained by a change in BMP signaling.

3.10 *Sfrp*-depleted embryos have increased *BMP* gene expression but reduced BMP signaling

BMP signaling is important both for initiation and maintenance of dorsal retina markers, as well as the restriction of ventral retina markers to the ventral portion of the eye. We have data to suggest that the zebrafish retina is ventralized in the absence of *sfrp1a* and *sfrp5*, and also that BMP downstream targets (*bambi* and *tbx5*) have reduced expression. Based on these data, we predicted that *sfrp*-depleted embryos have reduced BMP signaling in the dorsal retina. To investigate changes in BMP signaling, we used a transgenic zebrafish strain, the *Tg[BRE:eGFP]* line, which contains a binding site (a BMP Responsive Element) for phosphorylated SMADs (pSMAD), the active version of transcription factors within the BMP signaling pathway. When pSMADs bind they activate expression of eGFP, giving a visual readout of BMP signaling within the embryo (Collery and Link, 2011). We utilized an anti-sense GFP probe to determine changes in BMP signaling in our *sfrp* morphants. ISH is advantageous when analyzing GFP transgenics because it provides a more sensitive detection of signal than, for example, confocal microscopy. Not surprisingly, analysis of our morphants revealed a decrease in intensity of BMP signaling ($t(2) = 8.77, p = 0.0128$) (Table 3.1), changes that were observed both in ISH and less sensitive confocal microscopy methods (Figure 3.12-G-J). These data are consistent with the decreased expression of the dorsal retina markers, *tbx5* and *bambi*, which, as

mentioned previously, are signaling targets of the BMP pathway and often provides insight into the levels of BMP signaling (French et al., 2009; Gosse and Baier, 2009; Sekiya et al., 2004).

One of the simplest explanations of the observed decrease in BMP signaling is a decrease in the amount of BMP ligand within the embryo. To investigate changes in BMP ligand, we used ISH to look at three different BMP markers in the dorsal retina, *bmp2b*, *bmp4*, and *gdf6a*. Despite the fact that BMP signaling is reduced, all three genes are up-regulated in *sfrp1a/sfrp5* double morphants as compared to uninjected control embryos [*bmp2b*: $t(4) = 14.64$, $p < 0.0001$]; *bmp4*: ($t(4) = 6.48$, $p = 0.0029$); *gdf6a*: ($t(4) = 28.12$, $p < 0.0001$)] (Figure 3.12-A-F; Table 3.1). Such changes could be observed in single morphants, as injection with either *sfrp1a* or *sfrp5* increases expression of both *bmp4* and *gdf6a* (Figure 3.12-L,M,P,Q), though double morphants have a more severe up-regulation of *BMP* expression (Figure 3.12-K-R

Increases in *BMP* expression could be explained by a negative feedback loop if BMP signaling targets normally downregulate ligand expression. If there is a block in the pathway downstream of *BMP* gene expression that decreases signaling output, it is plausible that the retina may try to up-regulate *BMP* expression as compensation. BMP-signaling target BAMBI has been previously implicated in a negative feedback inhibition loop (Onichtchouk et al., 1999); however, there have not been any studies that link decreased BMP signaling with an increase in *BMP* gene expression. In fact, loss of BMP signaling is correlated with a loss of *BMP* gene expression; zebrafish *gdf6a* mutants have abolished *bmp4* in the retina (French et al., 2009; Gosse and Baier, 2009). Similarly, loss of BMP signaling as a result of Wnt inhibition is concurrent with a reduction of a number of *BMP* genes, including *bmp2b*, *bmp4*, and *gdf6a* (Veien et al., 2008). This suggests that, in contrast to a feedback loop, there may be other Sfrp-mediated methods of regulating *BMP* gene expression.

3.11 *Sfrp1a/sfrp5* double morphants have increased *wnt* gene expression but decreased Wnt signaling

Although we observe altered BMP signaling in *sfrp1a/sfrp5* morphants, changes in dorsal retina markers can also be explained by decreased Wnt signaling. The Wnt pathway does not influence initiation of retinal markers, as abrogation of Wnt signaling still allows for BMP-dependent initiation of dorsal retina markers such as *tbx5* (Veien et al., 2008). However, dorsal identity is lost at later stages of eye development as a result of Wnt inhibition (Veien et al., 2008; Zhou et al., 2008). Therefore, Wnt is postulated to act upstream of BMP signaling during the maintenance phase of retinal patterning and may provide an enhanced explanation for the modifications we see in BMP gene expression and output.

Wnt signaling can be difficult to assess in an embryo because of a lack of understanding of how far the diffusible Wnt ligand can act cell non-autonomously. This is due in part to incomplete information regarding where exactly Wnt genes are expressed in the embryos, as well as limited Wnt antibodies available to survey where protein is present. In zebrafish, we have alternative, indirect methods of determining where Wnts are actually signaling within the body. The *Tg[*TOP:GFP*]^{w25}* zebrafish line has a transgene insertion that contains four binding sites for the transcription factor, Lef1, which is activated during canonical Wnt signaling. The Lef1 binding sites, once bound by Lef1 and its cofactor, β -catenin, uses a minimal promoter to drive expression of GFP in the embryo and provides a visual readout of where Lef1/ β -catenin signaling is active in the embryo (Dorsky et al., 2002). Although Lef1/ β -catenin signaling can be detected earlier, it becomes concentrated in neural tissue at the 6-somite stage, where it is found in both the hindbrain and midbrain-hindbrain boundary. At 18hpf, expression is maintained in the midbrain and appears, at low levels, in the forebrain. By 24hpf, GFP fluorescence can continue to be detected in the midbrain and forebrain and also first appears in the eye (Dorsky et al., 2002). Using a fluorescent stereomicroscope, strong GFP signal is detectable in the midbrain, in contrast to low levels of GFP in the eye using confocal microscopy. Due to the weak ocular signal, we employed ISH using an anti-GFP riboprobe because of its increased sensitivity.

Historically Sfrps have been widely accepted as secreted Wnt inhibitors, therefore we hypothesized that morpholino knockdown of *sfrp1a/sfrp5* should cause an increase in Wnt signaling (Kim et al., 2007; Li et al., 2008; Lopez-Rios et al., 2008; Ruiz et al., 2009). Our initial examination of dorsal retinal patterning was more consistent with a loss of Wnt signaling, which contrasts this traditional model. ISH comparing *sfrp1a/sfrp5* double morphants to wildtype embryos revealed that Wnt signaling is decreased throughout the embryo at 28hpf, including the eye ($t(4) = 6.87, p = 0.0023$) (Figure 3.13-G,H; Table 3.1);. This result was also recapitulated using qRT-PCR, which showed that morphants at 28hpf had a 1.36 fold decrease in GFP expression as compared to uninjected control morphants ($t(15) = 5.711, p < 0.001$) (Figure 3.13-I). Although our data disagrees with the classical Sfrp model, comparison with more recent publications shows these results are not so surprising.

There is increasing evidence that certain Sfrps, in certain situations, can act as Wnt facilitators (Esteve et al., 2011; Mii and Taira, 2011; Uren et al., 2000). The latest model places Sfrps as promoters of Wnt diffusion, allowing them to reach further targets in the body. In fact, Sfrps have been shown to increase the distance of Wnt diffusion in *Drosophila* wing discs and *Xenopus* gastrulas (Mii and Taira, 2009). Conversely, mutations in Sfrps, such as *sfrp1a/sfrp2* mutant mice, cause reduction in Wnt diffusion distance in retinal explants (Esteve et al., 2011). It is therefore plausible that zebrafish *sfrp1a* and *sfrp5* act in concert to promote Wnt diffusion in the retina. To further complicate the Sfrp-Wnt model, Sfrps have also been shown to act in a biphasic manner. For instance, although *Drosophila* do not actually express *sfrps*, over-expression of *sfrp1* in the model system can produce positive or negative impacts on Wnt signaling, depending on dose. These assays demonstrated that high levels of Sfrp inhibit Wnt signaling and low levels promote Wnt signaling (Uren et al., 2000). In fact, many assays that support the model of Sfrps as Wnt inhibitors use mRNA over-expression of Sfrps to showcase their negative impact on Wnt signaling. This makes it much more difficult to interpret the biological relevance of such experiments (Kim et al.,

2007; Leyns et al., 1997). Perhaps endogenous levels of Sfrp expression in the dorsal retina are conducive to Wnt facilitation, as opposed to Wnt inhibition.

In addition to observing an overall decrease in Wnt signaling, there is a stronger reduction of signaling in the ventral portion of the retina as compared to the dorsal retina (Figure 3.13-H). When considering the model where Sfrps aid in Wnt diffusion, we can justify that Wnt signaling is more strongly down-regulated in the ventral retina because the Wnt ligand is no longer able to reach long distance signaling targets. Furthermore, the ISH staining, in both wildtype and *sfrp*-depleted eyes, created an atypical expression pattern that made it difficult to determine if Wnt signaling was present in the retina or in the overlying RPE; typically, genes expressed in the retina have a uniform staining pattern, however, TOP:GFP expression is present in a only subset of cells. We were able to use live imaging on the TOP:GFP strain to view the GFP-expressing cells and concluded that they have the general morphology and behavior of retinal cells, as expected.

Similar to the changes we saw in BMP signaling, decreases in TOP:GFP expression can also be explained by decreased levels of Wnt ligand. To determine if there are alterations in Wnt levels, I investigated changes in *wnt* gene expression in the eye using ISH. There are three main Wnt genes that are expressed specifically in ocular tissues: *wnt11r* is expressed in the lens and *wnt2* and *wnt8b* are both expressed in the RPE (Thisse and Thisse, 2004) (Kelly et al., 1995; Veien et al., 2008). ISH of *wnt2* ($t(4) = 8.23, p = 0.0012$), *wnt8b* ($t(4) = 3.91, p = 0.0174$), and *wnt11r* ($n = 10/12$) show increased levels of transcript in *sfrp*-depleted embryos (Figure 3.13-A-F; Table 3.1). Because we do not observe decreased *wnt* gene expression, our data support the idea that Sfrp-dependent effects on Wnt signaling act upon a later step in the pathway. It is plausible that *wnt* gene expression could be increased due to a negative feedback loop coupled with decreased Wnt signaling. Up-regulation of Wnt signaling in colorectal and liver tumors has been linked to an increase in expression of the inhibitor, conductin (*axil, axin2*) (Lustig et al., 2002). Similarly, the Wnt inhibitor, *dkk1*, was also found to be a signaling target of β -catenin/TCF, identifying an

independent negative feedback loop (Niida et al., 2004). Analogous to BMPs, these studies have not examined changes in Wnt expression following decreases in signaling output. Therefore, we are only able to tell that Sfrps are affecting both BMP and Wnt signaling downstream of either *bmp* or *wnt* gene expression. Alternatively, Sfrps may regulate *wnt* gene expression through other pathways.

3.12 Altered Wnt signaling does not account for Sfrp-dependent changes in BMP gene expression

An additional method to assay Wnt signaling involves the use of transgenics that overexpress Wnt signaling inhibitors, such as *dickkopf-related protein 1* (*dkk1*) and dominant negative *T-cell factor* (*dntcf*), in order to assess the role of canonical Wnt signaling during development (Veien et al., 2008). *Dkk1* is an inhibitor that binds the Wnt co-receptor, Low density lipoprotein receptor-related protein 6 (Lrp6) and prevents signal transduction into the target cell (Bafico et al., 2001). Previous research using *dkk1* transgenics (*Tg[hsp701:dkk1-GFP]^{w32}*) have highlighted the roles of Wnt signaling in dorsal retina specification, as well as swim bladder development and ciliogenesis (Caron et al., 2012; Veien et al., 2008; Yin et al., 2011). Therefore, transgenics such as the heat shock inducible *dkk1* line can be very useful in gaining information about the role of canonical Wnt signaling in development. Heat-shock transgenics are an excellent tool for studying Wnt signaling because they enable timed expression experiments that allow researchers to bypass early stages of development where Wnt signaling is required for survival. For our experiments, we chose to activate *dkk1* expression at 10hpf, during the beginning stages of eye development. Because investigation of the *Tg[TOP:GFP]^{w25}* zebrafish line revealed that Wnt signaling output is reduced in *sfrp1a/sfrp5* morphants, we predicted that we would see similar changes in morphant eye gene expression as compared to the *Tg[hsp701:dkk1-GFP]^{w32}* heat-shocked embryos.

Abrogation of Wnt signaling by over-expressing *dkk1* resulted in an almost complete reduction in *bmp2*, *bmp4*, and *gdf6a* expression at 28hpf (n=19/19; n=17/20; n=19/19, respectively) (Figure 3.14-A-F). This data neatly

recapitulates data previously published (Veien et al., 2008). Importantly, this does not match up with changes in gene expression that we observe in our *sfrp1a/sfrp5* morphants. In fact, we see the opposite in *sfrp*-depleted embryos; expression levels of all three of the same *BMP* genes in the dorsal retina, *bmp2b*, *bmp4*, and *gdf6a*, are increased (Figure 3.12-A-F). This is surprising because Wnt signaling is hypothesized to act upstream of *BMP* gene expression to specify dorsal retina identity and, therefore, we would expect to see congruent changes (Veien et al., 2008; Zhou et al., 2008). In fact, overexpression of *BMPs*, a situation we see in our morphants with increased *bmp2b*, *bmp4*, and *gdf6a*, is sufficient to rescue defects in dorsal retina specification seen in heat-shock:*dkk1* (*hs:dkk1*) embryos. Misexpression of *bmp4* mRNA is able to almost fully rescue expression of the dorsal marker, *tbx5*, following heat shock treatment (Veien et al., 2008). Additionally, we have shown that *gdf6a* overexpression driven by the *Rx3* promoter (to target eye expression), is also able to partially rescue *bambi* expression in *hs:dkk1* embryos. Although it was not a full rescue of *hs:dkk1* phenotype, we no longer saw any embryos with severely reduced *bambi* ($n_{\text{uninj};hs} = 5/22$; $n_{\text{gdf6a};hs} = 0/40$) and fewer embryos with moderately reduced *bambi* ($n_{\text{uninj};hs} = 8/22$; $n_{\text{gdf6a};hs} = 4/40$) when injected with *Rx3:gdf6a* (Figure 3.14-G-J). Because we see increased expression of *bmp4* and *gdf6a* but still have defects in dorsal retina specification, it argues that the situation we see in our *sfrp1a/sfrp5* morphants is not simply a linear relationship in which a change in Wnt signaling accounts for all the developmental alterations we see in retinal patterning. Instead, there appears to be an additional break in the pathway, whereby *Sfrps* are acting downstream of *BMP* gene expression to regulate retinal development.

3.13 Figures

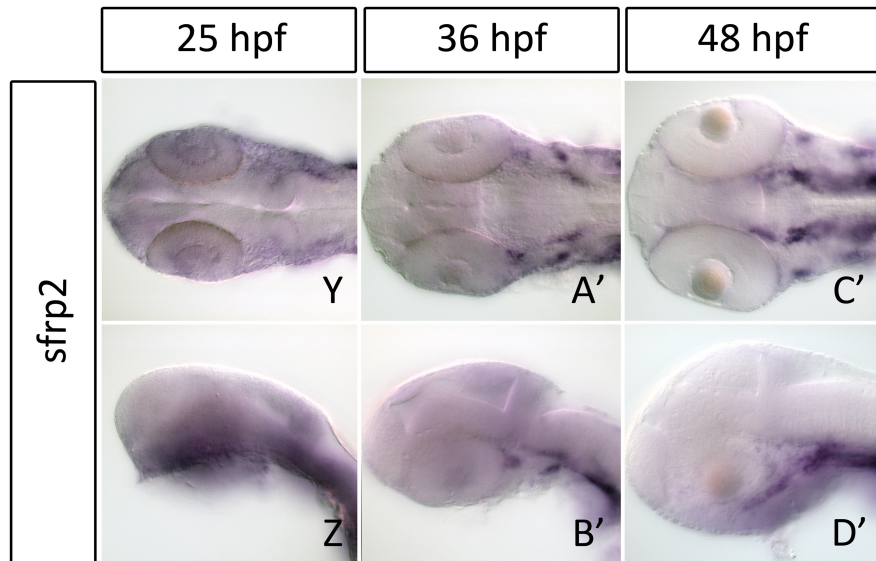
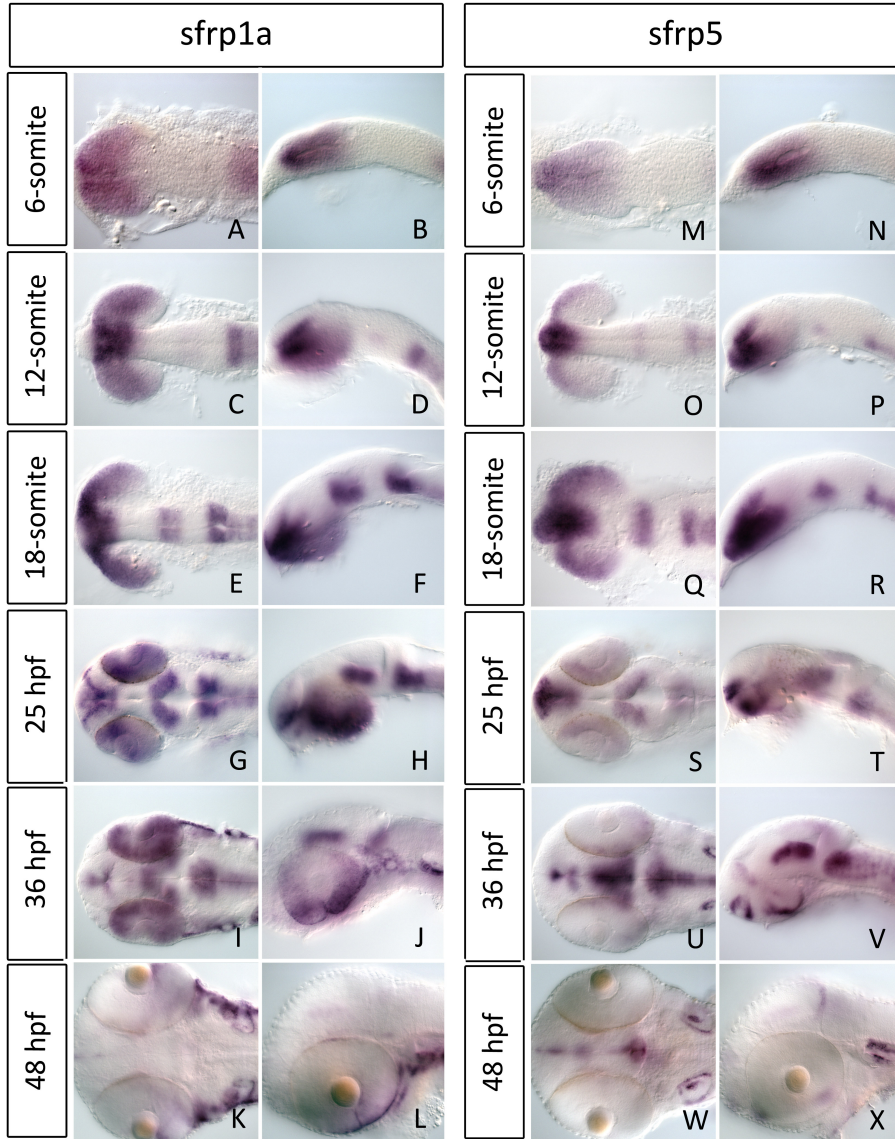


Figure 3.1. mRNA in situ hybridization expression of *sfrp1a*, *sfrp2*, and *sfrp5* in the developing zebrafish embryo. All stages of expression have been photographed in both a dorsal and lateral mount. (A-J) *sfrp1a* is expressed in the eye field as early as 6 somites and has continued expression in the out-budding optic vesicle (12-18 somites). As the optic cup forms, *sfrp1a* expression persists in the ventral and mid retina, encompassing all but the dorsal-most region (25 hpf). At this time point, *sfrp1a* also begins to regionalize in the brain, with specific areas of expression in the telencephalon and midbrain. Gene expression continues to persist in the ventral eye through 36 hpf, but becomes restricted by 48hpf to a single stripe of expression along the closing choroid fissure. (M-X) *sfrp5* has overlapping expression patterns with *sfrp1a* in early eye development, having robust expression in the developing eye anlage (6 somites). Expression is continued in the optic vesicle, similar to *sfrp1a*, but in a more restricted dorsal domain (12-18 somites). By 25hpf, expression in the eye becomes more reduced and is almost completely gone by 36hpf. Similar to *sfrp1a*, *sfrp5* expression exists in the developing midbrain and telencephalon. At 48hpf, *sfrp5* is no longer expressed in the eye, but maintains expression in restriction areas of the brain. (Y-D') *sfrp2* is expressed almost ubiquitously during zebrafish development, including low levels of expression in the retina and lens. At 36hpf, this expression is decreased and, by 48hpf, *sfrp2* is no longer expressed in the eye.

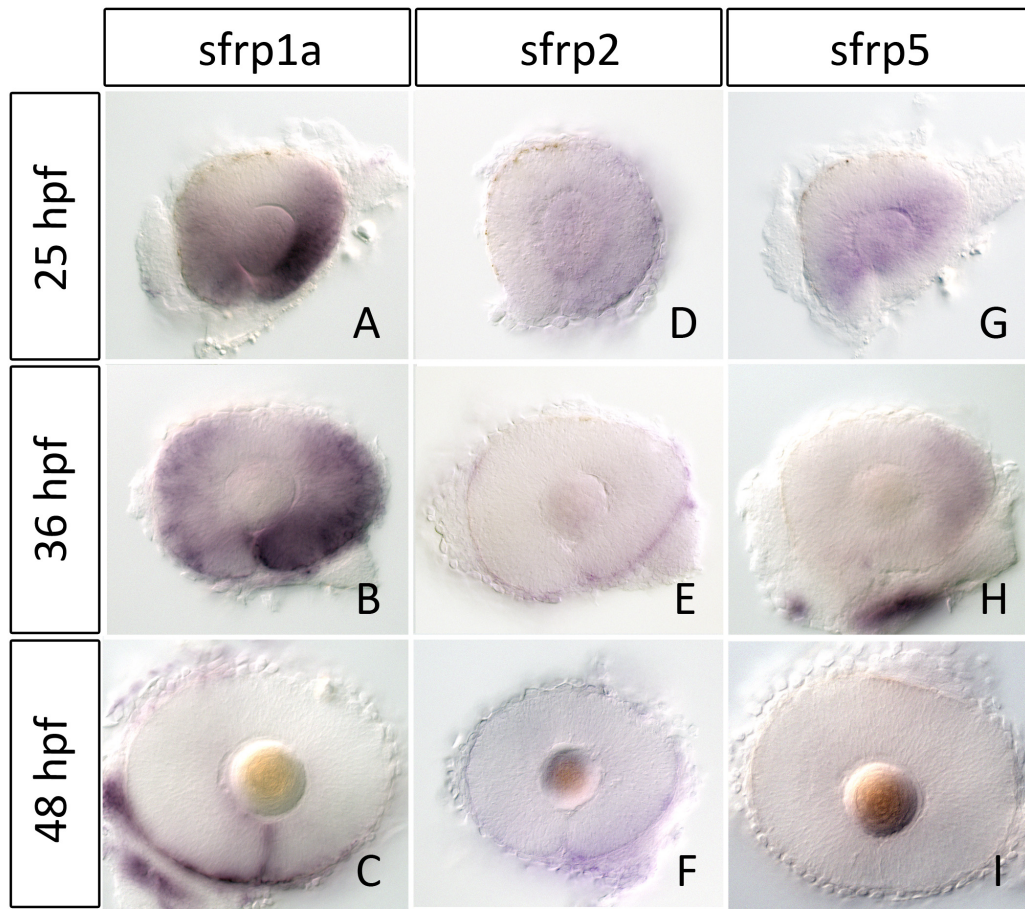


Figure 3.2. *sfrp1a*, *sfrp2*, and *sfrp5* expression in the zebrafish eye. (A) Expression of *sfrp1a* is robust in the lens and ventral/mid retina at 25hpf. (B) At 36hpf, lens expression is absent but retinal expression of *sfrp1a* remains. (C) By 48hpf, almost all *sfrp1a* mRNA is absent from the retina, save for a single stripe of expression along the ventral fissure. (D) *sfrp2* is expressed at low levels in the retina and lens at 25hpf. (E-F) At 36hpf, expression of *sfrp2* is absent from the retina but may have low levels in the lens. At this stage, *sfrp2* also has expression in the RPE, which persists to at least 48 hpf. (G) *sfrp5* has mid-retina and lens expression at 25hpf. (H) By 36hpf, *sfrp5* is almost gone from the eye, with the exception of a faint domain in the temporal retina. (I) At 48 hpf, *sfrp5* mRNA can no longer be detected in the eye. RPE – retinal pigmented epithelium.

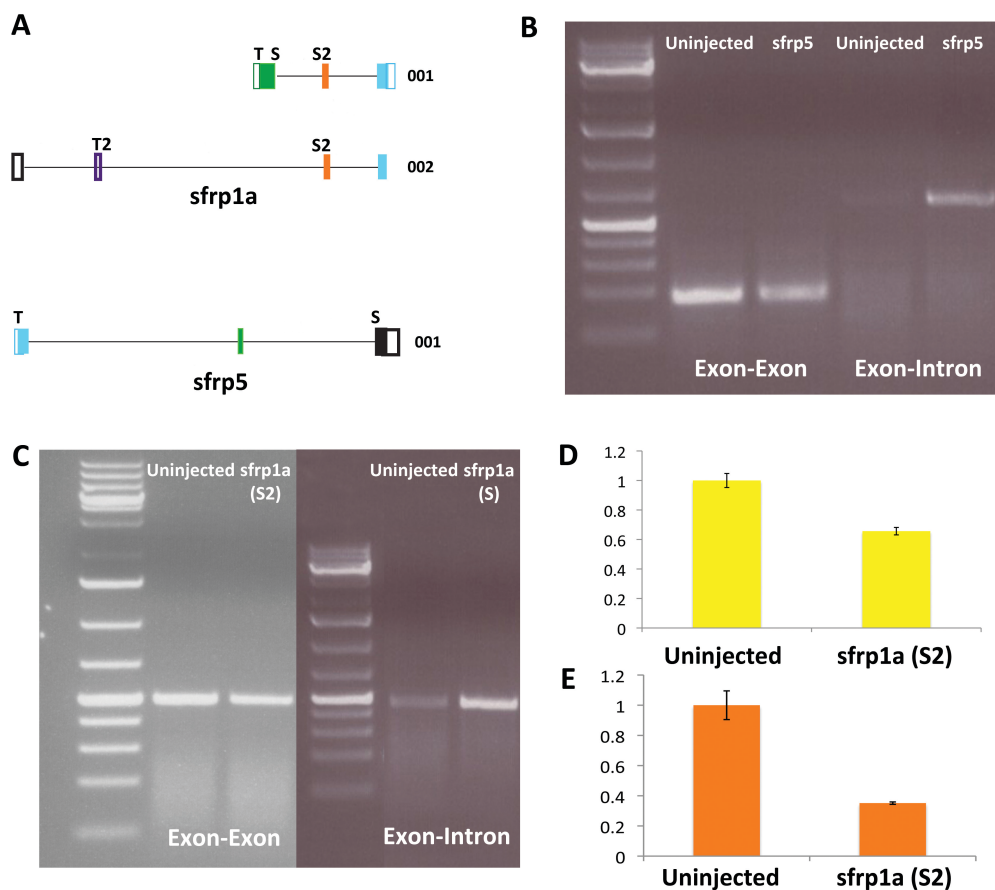


Figure 3.4. Morpholino design and specificity controls. (A) Placement of *sfrp1a* and *sfrp5* splice-blocking and translation-blocking morpholinos. S- splice; T- translation. (B) *sfrp5* exon-exon and exon-intron RT-PCR reactions. Injection of *sfrp5* morpholino results in decreased exon-exon and increased intron-exon PCR product. (C) *sfrp1a* (S) and *sfrp1a* (S2) morpholino control RT-PCR reactions. Exon-exon RT-PCR causes decreased *sfrp1a* (S2) morphant PCR product. Exon-intron RT-PCR creates only a strong PCR band in the *sfrp1a* (S) morphants. (D) qRT-PCR using exon-intron spanning primers. *sfrp1a* (S2)-depletion results in a 1.52 fold decrease in PCR product. (E) Exon-exon spanning *sfrp1a* (S2) qRT-PCR shows a 2.85 fold reduction of *sfrp1a* (S2) product. RNA was isolated from both uninjected control and *sfrp* morphant embryos at 28hpf prior for use in the RT-PCR and qRT-PCR reactions.

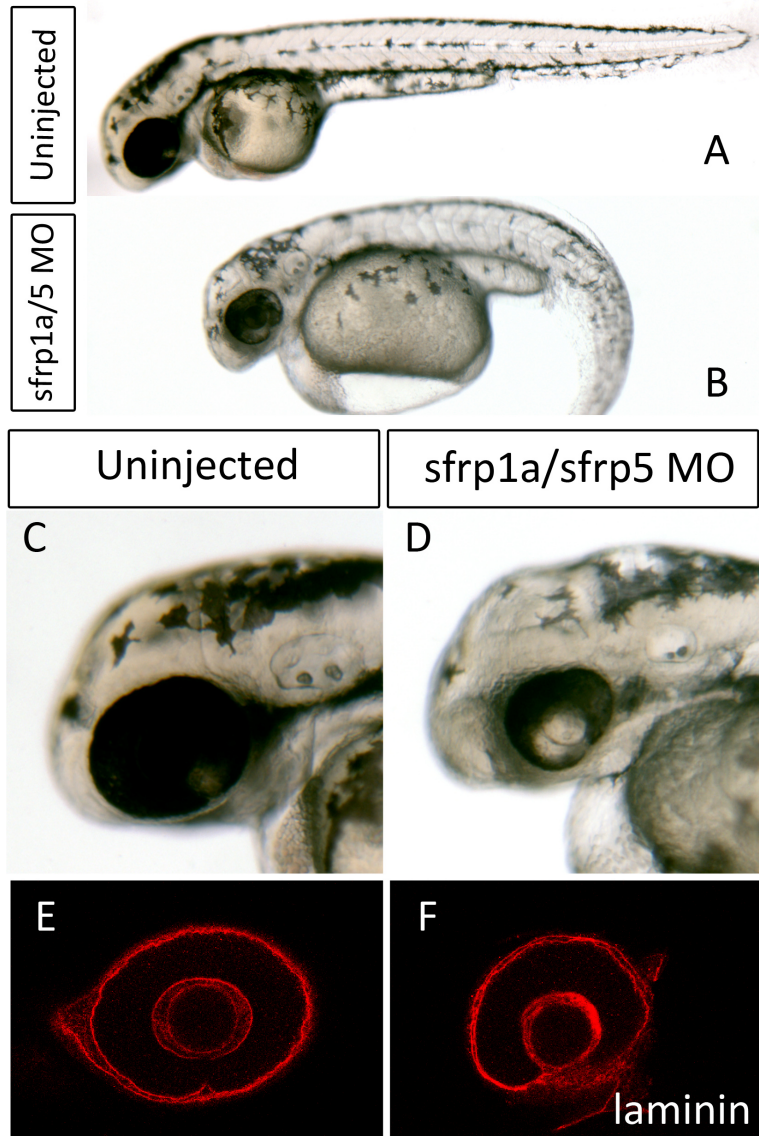


Figure 3.5. Phenotypic survey of *sfrp1a/sfrp5*-depletion. (A-B) Injection of both *sfrp1a* and *sfrp5* morpholino causes a suite of morphological defects including heart edema (M = 62.3%, SD = 9.10%), malformed somites, and a curved tail (M = 60.66%, SD = 2.60%). (C-D) Ocular phenotypes of *sfrp1a/sfrp5* morpholino injection comprise smaller eyes, ventral retina thinning (M = 25.74%, SD = 1.04%), and ocular coloboma (M = 59.10%, SD = 0.39%). Live images were taken on 2dpf embryos. (E-F) Immunohistochemistry laminin stain at 2dpf further highlights choroid fissure closure defects in *sfrp*-depleted eyes (n = 9/9).

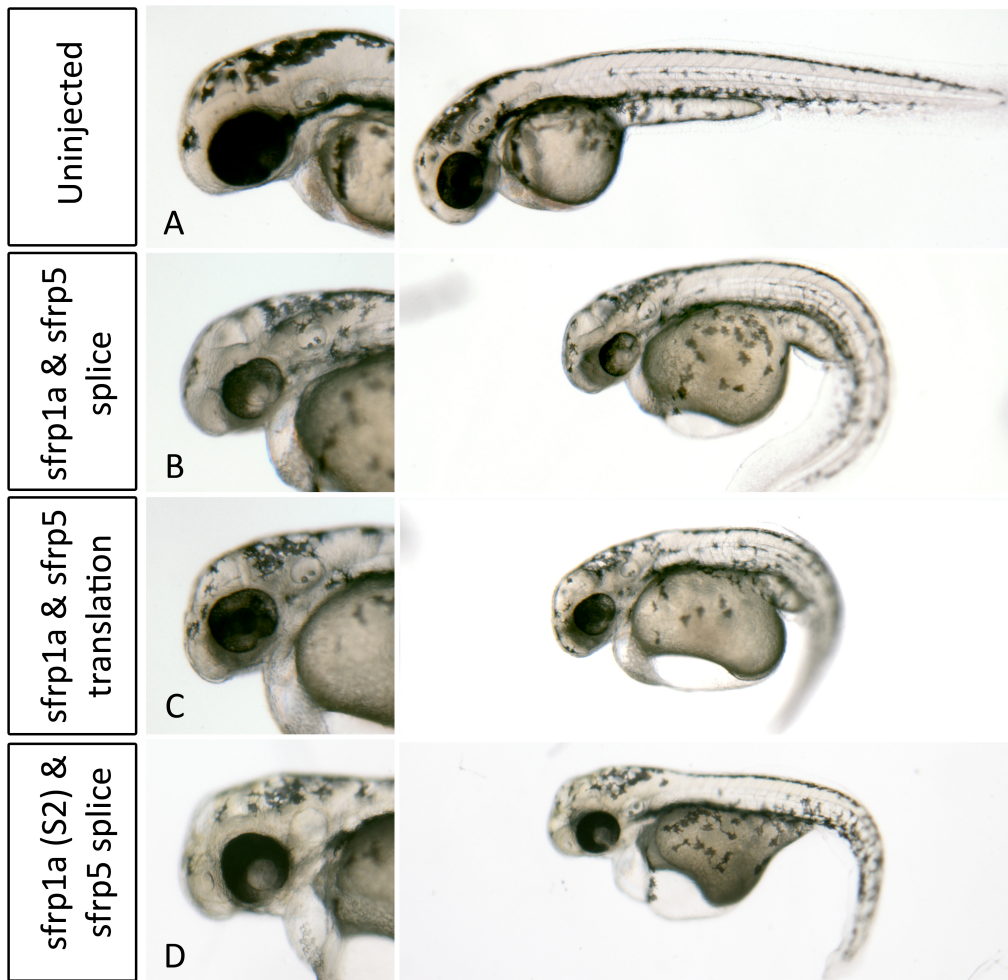


Figure 3.6. Phenocopy of morphological defects caused by multiple *sfrp1a* and *sfrp5* morpholino cocktails. (A-D) As compared to uninjected controls, *sfrp1a* and *sfrp5* splice-blocking and translation-blocking morpholino injections cause similar morphological defects such as tail kinking, somite malformation, heart edema, and ocular fissure defects. (B) *sfrp1a* (S) and *sfrp5* (S) morpholino injection. (C) *sfrp1a* (T) and *sfrp5* (T) morpholino injection. (D) *sfrp1a* (S2) and *sfrp5* (S) morpholino injection. Photographs of live embryos were taken at 2dpf.

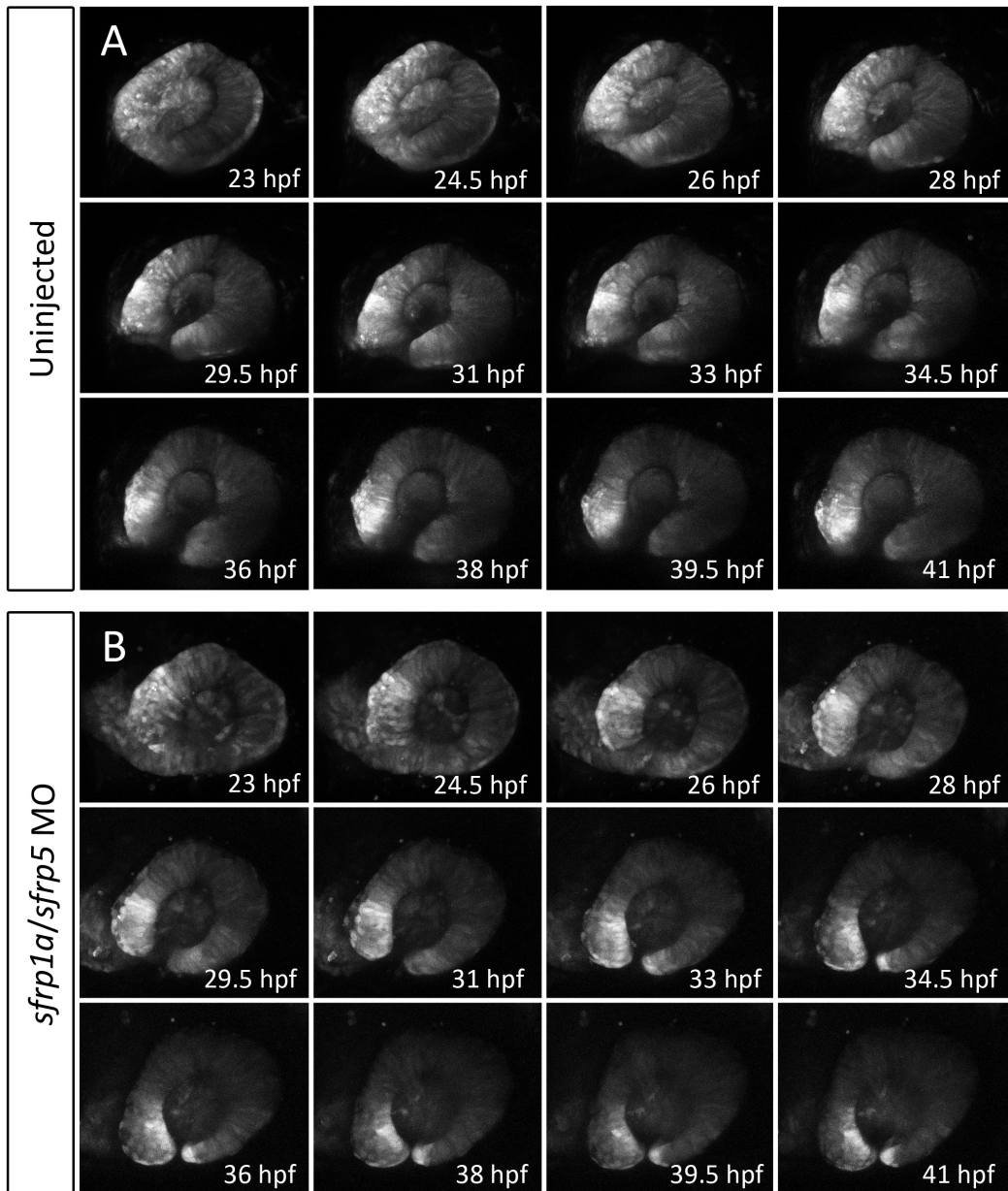


Figure 3.7. Survey of eye formation in *sfrp1a/sfrp5* morphants. (A-B) Early eye morphology is comparable between uninjected controls (A) and *sfrp*-depleted embryos (B). Ventral retina thinning can first be observed in *sfrp1a/sfrp5* morphants at around 31 hpf and becomes more pronounced as development continues. Live embryos from the *Tg[rx3:GFP]* transgenic strain were photographed over a period of almost 24 hours between 18hpf and 42 hpf.

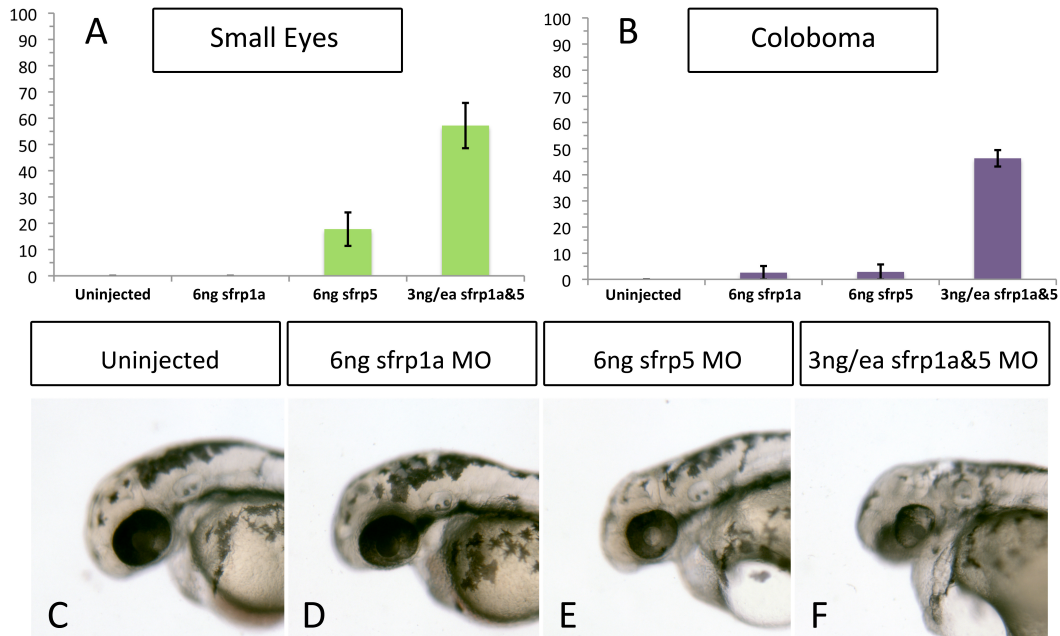


Figure 3.8. Sfrp1a and Sfrp5 share functional redundancy during ocular development. (A-B) Double *sfrp1a* and *sfrp5* morpholino injection causes an increased percentage of embryos showing both smaller eyes and ocular coloboma, as compared to uninjected controls and single morpholino injections. (A,B,C) Uninjected, wildtype control embryos do not exhibit any ocular defects. (A,B,D) Injection of *sfrp1a* morpholino does not cause changes in eye size and only a few embryos showed aberrant choroid fissure closure (M = 2.6%, SD = 3.6%). (A,B,E) Single morpholino injection of *sfrp5* causes a small percentage of embryos with either small eyes (M = 9.0%, SD = 17.8%) or ocular coloboma. (M = 2.9%, SD = 4.0%)(A,B,F) Double morpholino injection (to the same total morpholino dose) causes an increase in the number of embryos with microphthalmia (M = 57.2%, SD = 12.2%) and ocular coloboma (M = 43.1%, SD = 4.5%), as well as an increase in the severity of observed phenotypes. Live images and phenotypic surveys were taken on embryos at 2dpf.

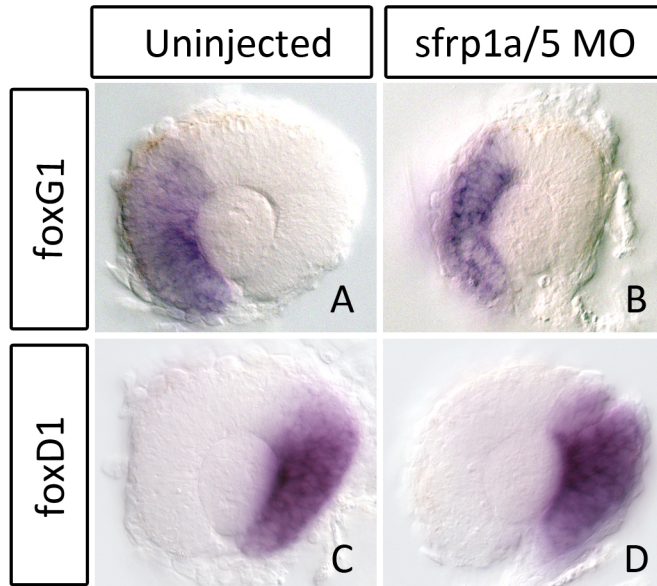


Figure 3.9. Depletion of *sfrp1a* and *sfrp5* does not cause changes in nasal or temporal retinal gene markers. (A-B) As compared to uninjected controls, ISH using the nasal marker *foxG1* was unchanged in *sfrp1a/sfrp5* morphants (n = 17/17). (C-D) Investigation of temporal gene expression using *foxD1* also did not reveal any changes in *sfrp*-depleted embryos as compared to wildtype embryos (n = 14/14). ISH was performed on control and morphant embryos staged to 28hpf.

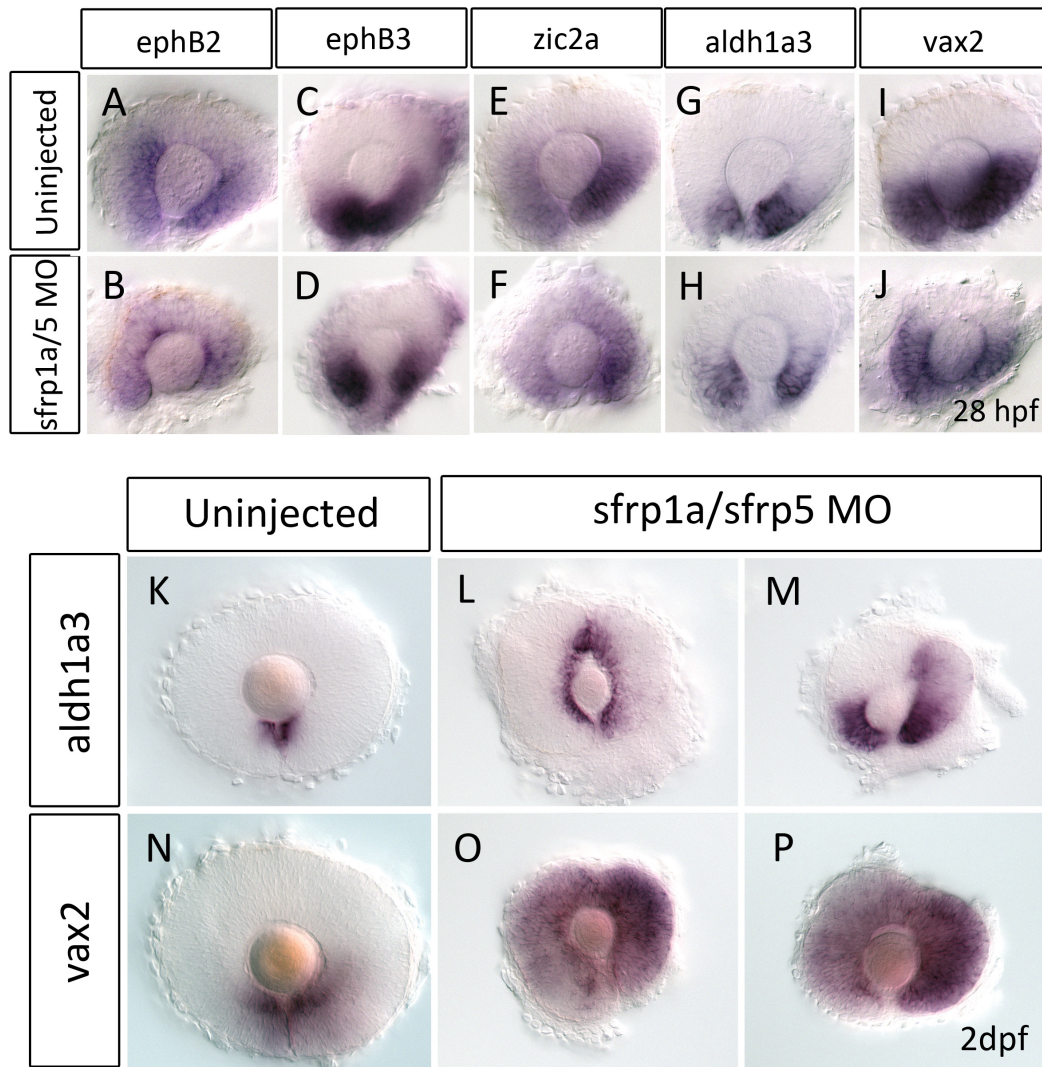


Figure 3.10. *sfrp1a/sfrp5* morphants show changes in ventral gene expression consistent with ventralization of the retina. (A-J) ISH of various ventral markers at 28hpf revealed that the ventral retina markers, *ephB2* (n = 12/12), *ephB3* (n = 20/20), *zic2a* (n = 17/17), *aldh1a3* (n = 17/18), and *vax2* (n = 19/20) are all still expressed in *sfrp*-depleted embryos, with only mild changes as compared to uninjected controls. A closer investigation of markers *ephB2* and *zic2a* reveals that *sfrp* morphants may have a slight expansion, however, the ventral markers at this stage of development were fairly variable in both morphant and control groups of

embryos. (K-P) ISH of ventral markers at 2dpf showed a significant expansion in a number of *sfrp1a/sfrp5* morphants as compared to wildtype embryos. (K-M) The marker *aldh1a3* is expanded around the lens in a portion of *sfrp* morphants ((M = 44.5%, SD = 17.9%), a phenotype never observed in uninjected embryos. Morphant eyes showed two different morphological phenotypes that correspond to change in ventral gene expression. The first morphological defect has fissure defects that separate the retina into two distinct lobes with a resulting expansion of *aldh1a3* in a line around the lens (L). The second phenotype has more of a “horseshoe” shaped retina, with a more general expansion of *aldh1a3* in the retina (M). (N-P) Expression of *vax2* is also expanded in *sfrp* morphants as compared to uninjected embryos (M = 26.7%, SD = 22.9%). Embryos also displayed the “lobed” (O) and “horseshoe” (P) morphology, but with similar changes in gene expression.

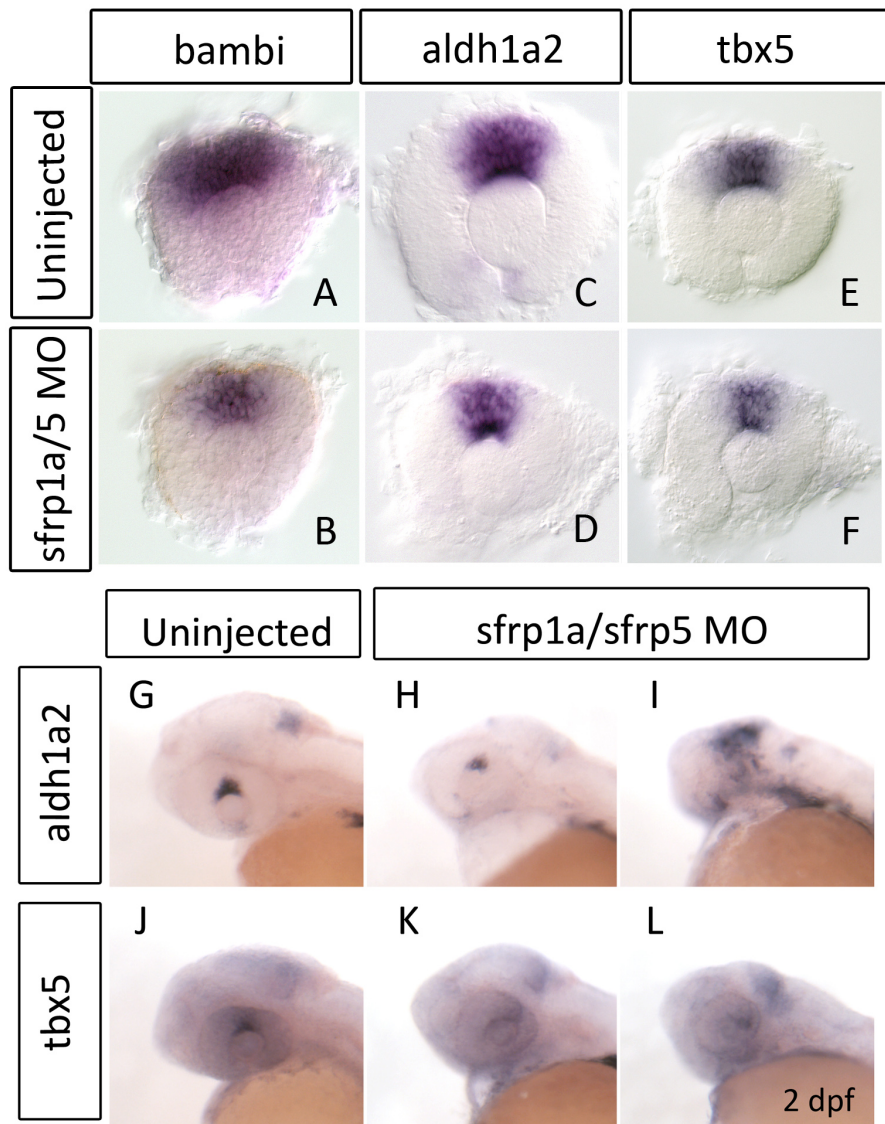


Figure 3.11. Depletion of *sfrp1a* and *sfrp5* causes decrease in dorsal markers at multiple stages (28hpf, 2dpf) consistent with ventralization of the retina. (A-F) *sfrp* morphants have reduced expression levels and domain of the dorsal markers *bambi* (M = 58.1%, SD = 20.7%), *aldh1a2* (M = 52.1%, SD = 28.8%), and *tbx5* (M = 88.7%, SD = 10.5%). (G-L) Defects in dorsal retina specification persist to 2dpf as the dorsal markers *aldh1a2* (n = 6/23) and *tbx5* (n = 7/23) are still reduced. A small percentage of *sfrp* morphant embryos also had ectopic expression of *aldh1a2* in the rest of the embryo, without an increase in retinal *aldh1a2* expression (n = 2/23) (I).

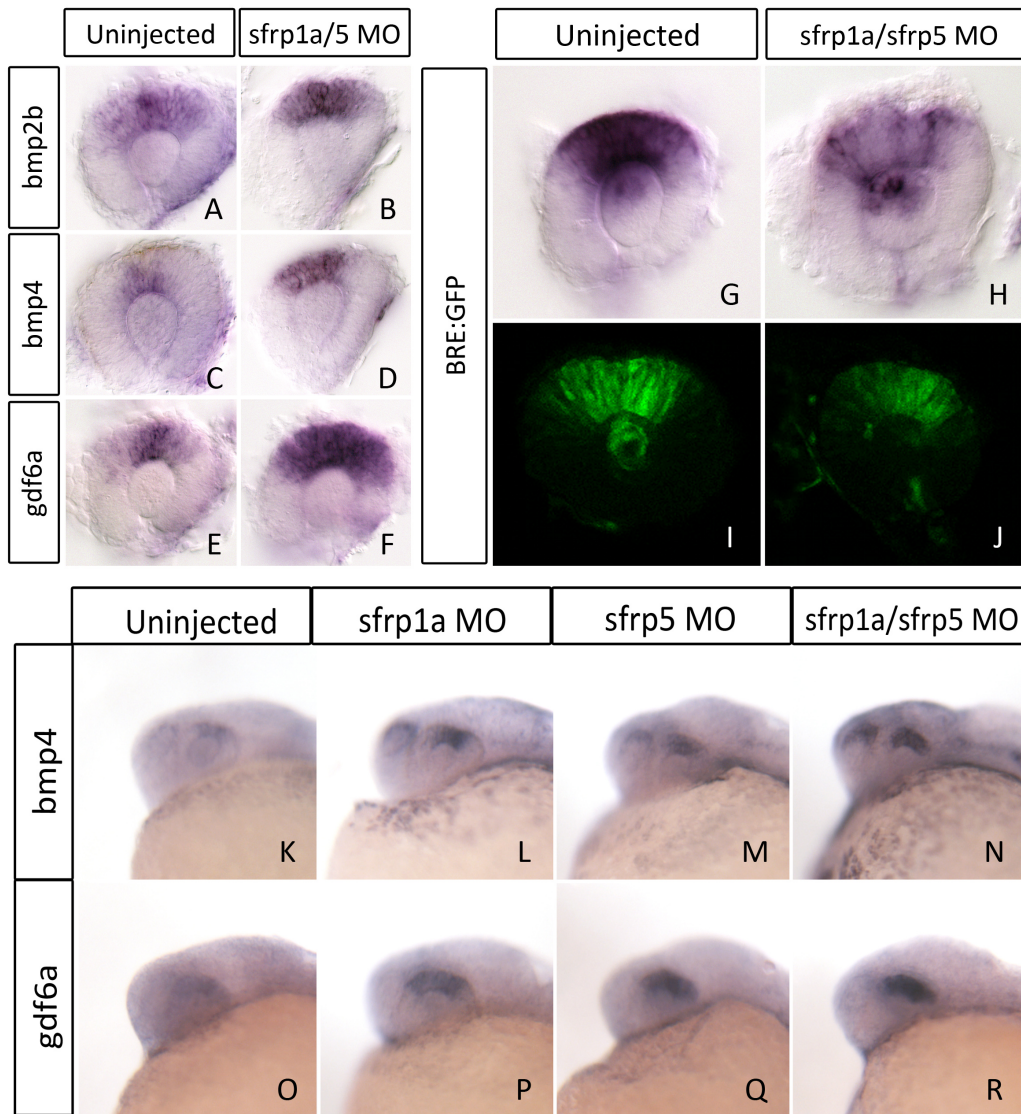


Figure 3.12. Embryos injected with *sfrp1a/sfrp5* morpholinos have defects in BMP signaling but increase in *BMP* gene expression. (A-F) *sfrp*-morphants have increased expression and domains of *bmp2b* (M = 90.9%, SD = 8.4%), *bmp4* (M = 70.3%, SD = 17.1%), and *gdf6a* (M = 94.2%, SD = 5.8%). ISH was performed on morphant and uninjected control embryos staged to 28hpf. (G-H) ISH against GFP on the BMP signaling transgenic, *Tg[BRE:eGFP]* revealed decreased expression in *sfrp*-depleted embryos (M = 51.9%, SD = 2.7%). (I-J) Changes in GFP ISH were also mimicked using confocal microscopy, with *sfrp* morphants showing decreased fluorescence. (K-R) Expression changes in

BMP genes at 28hpf synergize in *sfrp* double morphants, as shown using ISH with the markers *bmp4* and *gdf6a*. (K-N) Both single (L,M) morphants had increased *bmp4* expression that was further upregulated in *sfrp1a/sfrp5* double morphants. (O-R) Single *sfrp1a* (P) and *sfrp5* (Q) morphants had increased *gdf6a* expression that was exaggerated in *sfrp* double morphants (R).

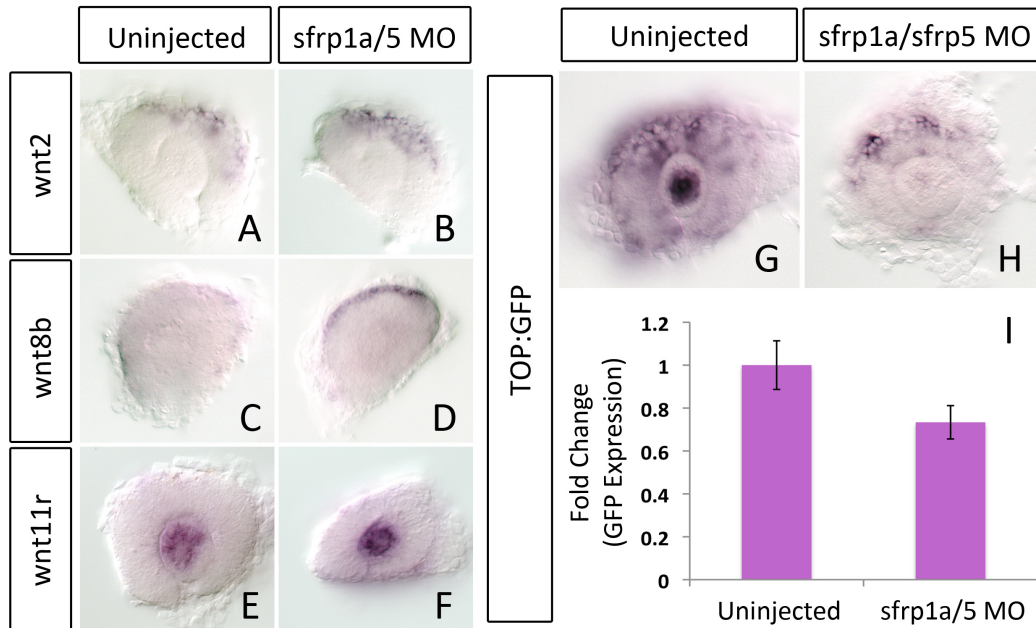


Figure 3.13. Reduction of *sfrp1a* and *sfrp5* results in a decrease in Wnt signaling but an increase in *wnt* gene expression. (A-F) ISH at 28hpf on *wnt* genes expressed in the eye reveal expansion of *wnt2* (M = 81.6%, SD = 2.2%), *wnt8b* (M = 58.6%, SD = 16.7%), and *wnt11r* (n = 10/12) markers. (G-I) Investigation of changes in Wnt signaling at 28hpf using the *Tg[TOP:GFP]^{w25}* strain shows decreased GFP expression using ISH (M = 81.6%, SD = 19.1%) (G-H) and qRT-PCR ($t(15) = 5.711, p < 0.001$) (I).

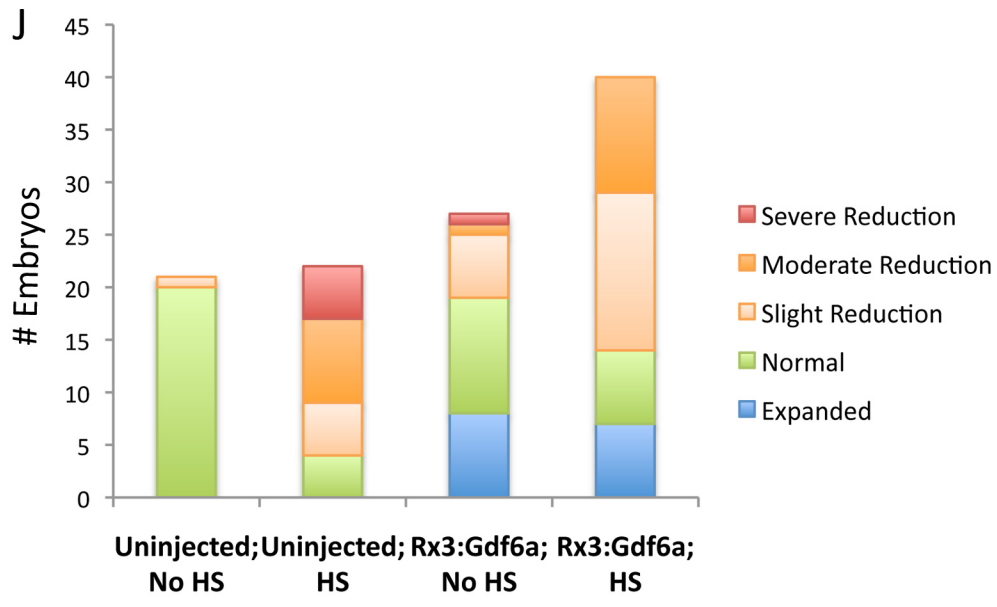
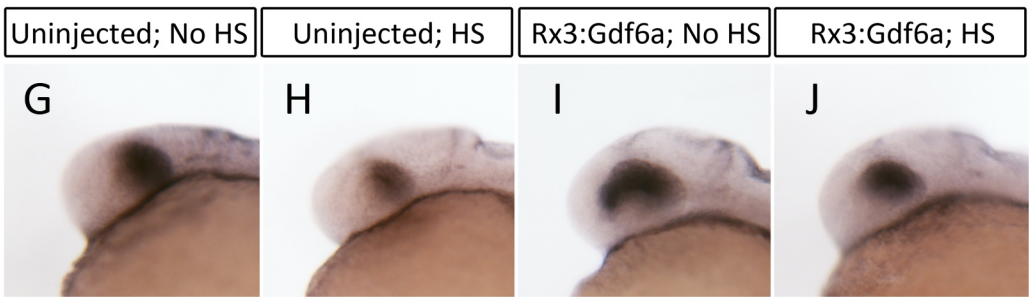
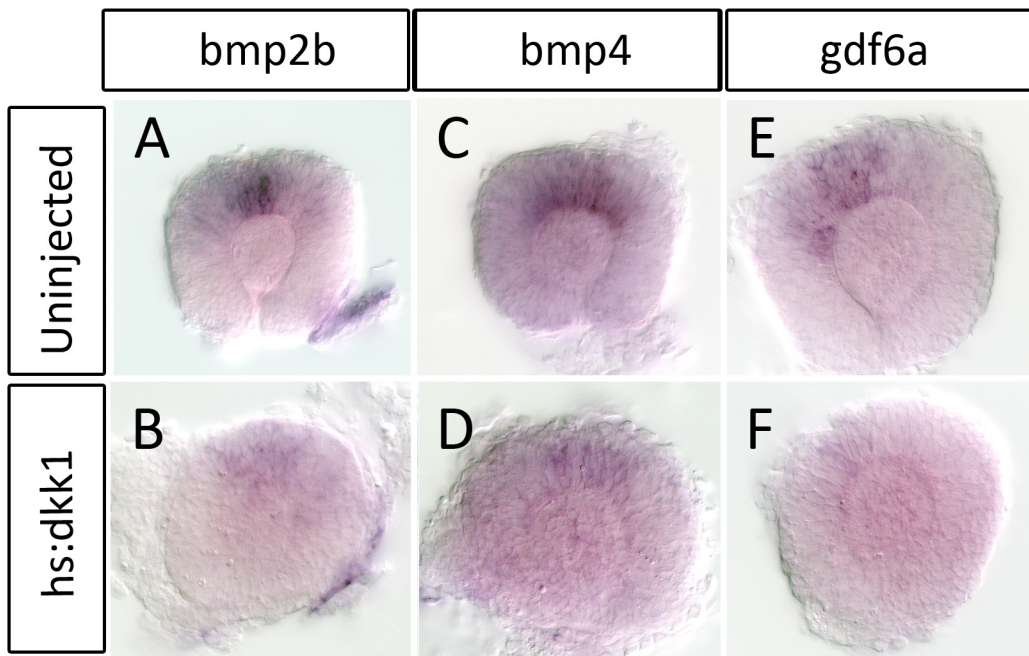


Figure 3.14. Changes in Wnt signaling cannot account for all of the changes seen in *sfrp1a/sfrp5* morphants. (A-F) Obstruction of Wnt signaling through overexpression of the inhibitor, Dkk1, in the *Tg[hsp701:dkk1-GFP]^{w32}* zebrafish strain resulted in completely abolished expression of the *BMP* genes, *bmp2b* (n = 19/19) (A-B), *bmp4* (n = 17/20) (C-D), and *gdf6a* (n = 19/19) (E-F). (G-J) Overexpression of the BMP ligand, Gdf6a, was able to rescue the most severely affected embryos following heat shock treatment to knockdown Wnt signaling. Heat shock, gdf6a-rescue embryos no longer have a severe reduction in *bambi* expression and an increased number of embryos have only a mild reduction in *bambi*. Overexpression of Gdf6a was accomplished by injection of 25pg of Tol2-*rx3:gdf6a-IRES GFP* DNA construct to target *gdf6a* expression to the developing eye. All heat-shock treated embryos were placed in a 39°C waterbath for two hours starting at 10hpf.

3.14 Tables

Group	Gene/Reporter	Stage (hpf)	Mean (%)	SD (%)	n	P Value*
Uninjected		28	0	0	54	
<i>sfrp1a/sfrp5</i> MO	<i>aldh1a2</i>	28	52.1	28.8	58	$p < 0.0001$
Uninjected		28	5.4	5.6	57	
<i>sfrp1a/sfrp5</i> MO	<i>bambi</i>	28	58.1	20.7	59	$p < 0.0001$
Uninjected		28	0	0	50	
<i>sfrp1a/sfrp5</i> MO	<i>tbx5</i>	28	88.7	10.5	48	$p < 0.0001$
Uninjected		28	5.0	7.1	94	
<i>sfrp1a/sfrp5</i> MO	BRE:GFP	28	51.9	2.7	81	$p < 0.0001$
Uninjected		28	6.1	5.4	65	
<i>sfrp1a/sfrp5</i> MO	<i>bmp2b</i>	28	90.9	8.4	61	$p < 0.0001$
Uninjected		28	3.2	5.5	57	
<i>sfrp1a/sfrp5</i> MO	<i>bmp4</i>	28	70.3	17.1	61	$p < 0.0001$
Uninjected		28	0	0	60	
<i>sfrp1a/sfrp5</i> MO	<i>gdf6a</i>	28	94.2	5.8	61	$p < 0.0001$
Uninjected		28	3.0	5.3	60	
<i>sfrp1a/sfrp5</i> MO	TOP:GFP	28	81.6	19.1	59	$p < 0.0001$
Uninjected		28	8.8	15.2	68	
<i>sfrp1a/sfrp5</i> MO	<i>wnt2</i>	28	81.6	2.2	59	$p < 0.0001$
Uninjected		28	11.4	12.7	64	
<i>sfrp1a/sfrp5</i> MO	<i>wnt8b</i>	28	58.6	16.7	63	$p < 0.0001$
Uninjected		48	0	0	34	
<i>sfrp1a/sfrp5</i> MO	<i>aldh1a3</i>	48	44.5	17.9	36	$p < 0.0001$
Uninjected		48	0	0	36	
<i>sfrp1a/sfrp5</i> MO	<i>vax2</i>	48	26.7	22.9	33	$p = 0.0017$

Table 3.1: mRNA in situ hybridization quantification and statistics

*Fisher's Exact Test, cumulative raw counts

3.15 Literature Cited

- Adler, R., and Belecky-Adams, T.L. (2002). The role of bone morphogenetic proteins in the differentiation of the ventral optic cup. *Development* *129*, 3161-3171.
- Asai-Coakwell, M., French, C.R., Berry, K.M., Ye, M., Koss, R., Somerville, M., Mueller, R., van Heyningen, V., Waskiewicz, A.J., and Lehmann, O.J. (2007). GDF6, a novel locus for a spectrum of ocular developmental anomalies. *Am J Hum Genet* *80*, 306-315.
- Bafico, A., Liu, G., Yaniv, A., Gazit, A., and Aaronson, S.A. (2001). Novel mechanism of Wnt signalling inhibition mediated by Dickkopf-1 interaction with LRP6/Arrow. *Nat Cell Biol* *3*, 683-686.
- Battle, E., Henderson, J.T., Beghtel, H., van den Born, M.M., Sancho, E., Huls, G., Meeldijk, J., Robertson, J., van de Wetering, M., Pawson, T., *et al.* (2002). Beta-catenin and TCF mediate cell positioning in the intestinal epithelium by controlling the expression of EphB/ephrinB. *Cell* *111*, 251-263.
- Caron, A., Xu, X., and Lin, X. (2012). Wnt/beta-catenin signaling directly regulates Foxj1 expression and ciliogenesis in zebrafish Kupffer's vesicle. *Development* *139*, 514-524.
- Chuang, J.C., Mathers, P.H., and Raymond, P.A. (1999). Expression of three Rx homeobox genes in embryonic and adult zebrafish. *Mech Dev* *84*, 195-198.
- Collery, R.F., and Link, B.A. (2011). Dynamic smad-mediated BMP signaling revealed through transgenic zebrafish. *Dev Dyn* *240*, 712-722.
- Dorsky, R.I., Sheldahl, L.C., and Moon, R.T. (2002). A transgenic Lef1/beta-catenin-dependent reporter is expressed in spatially restricted domains throughout zebrafish development. *Dev Biol* *241*, 229-237.
- Draper, B.W., Morcos, P.A., and Kimmel, C.B. (2001). Inhibition of zebrafish fgf8 pre-mRNA splicing with morpholino oligos: a quantifiable method for gene knockdown. *Genesis* *30*, 154-156.
- Esteve, P., Sandonis, A., Ibanez, C., Shimono, A., Guerrero, I., and Bovolenta, P. (2011). Secreted frizzled-related proteins are required for Wnt/beta-catenin signalling activation in the vertebrate optic cup. *Development* *138*, 4179-4184.
- French, C.R., Erickson, T., French, D.V., Pilgrim, D.B., and Waskiewicz, A.J. (2009). Gdf6a is required for the initiation of dorsal-ventral retinal patterning and lens development. *Dev Biol* *333*, 37-47.

- Gosse, N.J., and Baier, H. (2009). An essential role for Radar (Gdf6a) in inducing dorsal fate in the zebrafish retina. *Proc Natl Acad Sci U S A* *106*, 2236-2241.
- Hindges, R., McLaughlin, T., Genoud, N., Henkemeyer, M., and O'Leary, D.D. (2002). EphB forward signaling controls directional branch extension and arborization required for dorsal-ventral retinotopic mapping. *Neuron* *35*, 475-487.
- Huillard, E., Laugier, D., and Marx, M. (2005). Defects in chicken neuroretina misexpressing the BMP antagonist *Drm/Gremlin*. *Dev Biol* *283*, 335-344.
- Kelly, G.M., Greenstein, P., Erezyilmaz, D.F., and Moon, R.T. (1995). Zebrafish *wnt8* and *wnt8b* share a common activity but are involved in distinct developmental pathways. *Development* *121*, 1787-1799.
- Kim, H.S., Shin, J., Kim, S.H., Chun, H.S., Kim, J.D., Kim, Y.S., Kim, M.J., Rhee, M., Yeo, S.Y., and Huh, T.L. (2007). Eye field requires the function of *Sfrp1* as a Wnt antagonist. *Neurosci Lett* *414*, 26-29.
- Leyns, L., Bouwmeester, T., Kim, S.H., Piccolo, S., and De Robertis, E.M. (1997). *Frzb-1* is a secreted antagonist of Wnt signaling expressed in the Spemann organizer. *Cell* *88*, 747-756.
- Li, Y., Rankin, S.A., Sinner, D., Kenny, A.P., Krieg, P.A., and Zorn, A.M. (2008). *Sfrp5* coordinates foregut specification and morphogenesis by antagonizing both canonical and noncanonical Wnt11 signaling. *Genes Dev* *22*, 3050-3063.
- Lopez-Rios, J., Esteve, P., Ruiz, J.M., and Bovolenta, P. (2008). The Netrin-related domain of *Sfrp1* interacts with Wnt ligands and antagonizes their activity in the anterior neural plate. *Neural Dev* *3*, 19.
- Lustig, B., Jerchow, B., Sachs, M., Weiler, S., Pietsch, T., Karsten, U., van de Wetering, M., Clevers, H., Schlag, P.M., Birchmeier, W., *et al.* (2002). Negative feedback loop of Wnt signaling through upregulation of *conductin/axin2* in colorectal and liver tumors. *Mol Cell Biol* *22*, 1184-1193.
- Mii, Y., and Taira, M. (2009). Secreted Frizzled-related proteins enhance the diffusion of Wnt ligands and expand their signalling range. *Development* *136*, 4083-4088.
- Mii, Y., and Taira, M. (2011). Secreted Wnt "inhibitors" are not just inhibitors: Regulation of extracellular Wnt by secreted Frizzled-related proteins. *Dev Growth Differ* *53*, 911-923.

- Miller, C.T., and Kimmel, C.B. (2001). Morpholino phenocopies of endothelin 1 (sucker) and other anterior arch class mutations. *Genesis* 30, 186-187.
- Morcillo, J., Martinez-Morales, J.R., Trousse, F., Fermin, Y., Sowden, J.C., and Bovolenta, P. (2006). Proper patterning of the optic fissure requires the sequential activity of BMP7 and SHH. *Development* 133, 3179-3190.
- Morcos, P.A. (2007). Achieving targeted and quantifiable alteration of mRNA splicing with Morpholino oligos. *Biochem Biophys Res Commun* 358, 521-527.
- Morris, A.C. (2011). The genetics of ocular disorders: insights from the zebrafish. *Birth Defects Res C Embryo Today* 93, 215-228.
- Murali, D., Yoshikawa, S., Corrigan, R.R., Plas, D.J., Crair, M.C., Oliver, G., Lyons, K.M., Mishina, Y., and Furuta, Y. (2005). Distinct developmental programs require different levels of Bmp signaling during mouse retinal development. *Development* 132, 913-923.
- Nasevicius, A., and Ekker, S.C. (2000). Effective targeted gene 'knockdown' in zebrafish. *Nat Genet* 26, 216-220.
- Niida, A., Hiroko, T., Kasai, M., Furukawa, Y., Nakamura, Y., Suzuki, Y., Sugano, S., and Akiyama, T. (2004). DKK1, a negative regulator of Wnt signaling, is a target of the beta-catenin/TCF pathway. *Oncogene* 23, 8520-8526.
- Onichtchouk, D., Chen, Y.G., Dosch, R., Gawantka, V., Delius, H., Massague, J., and Niehrs, C. (1999). Silencing of TGF-beta signalling by the pseudoreceptor BAMBI. *Nature* 401, 480-485.
- Peng, G., and Westerfield, M. (2006). Lhx5 promotes forebrain development and activates transcription of secreted Wnt antagonists. *Development* 133, 3191-3200.
- Picker, A., and Brand, M. (2005). Fgf signals from a novel signaling center determine axial patterning of the prospective neural retina. *Development* 132, 4951-4962.
- Robu, M.E., Larson, J.D., Nasevicius, A., Beiraghi, S., Brenner, C., Farber, S.A., and Ekker, S.C. (2007). p53 activation by knockdown technologies. *PLoS Genet* 3, e78.
- Ruiz, J.M., Rodriguez, J., and Bovolenta, P. (2009). Growth and differentiation of the retina and the optic tectum in the medaka fish requires *olSfrp5*. *Dev Neurobiol* 69, 617-632.

- Scheele, S., Nystrom, A., Durbeej, M., Talts, J.F., Ekblom, M., and Ekblom, P. (2007). Laminin isoforms in development and disease. *J Mol Med (Berl)* 85, 825-836.
- Sekiya, T., Oda, T., Matsuura, K., and Akiyama, T. (2004). Transcriptional regulation of the TGF-beta pseudoreceptor BAMBI by TGF-beta signaling. *Biochem Biophys Res Commun* 320, 680-684.
- Sumanas, S., and Larson, J.D. (2002). Morpholino phosphorodiamidate oligonucleotides in zebrafish: a recipe for functional genomics? *Brief Funct Genomic Proteomic* 1, 239-256.
- Summerton, J. (1999). Morpholino antisense oligomers: the case for an RNase H-independent structural type. *Biochim Biophys Acta* 1489, 141-158.
- Summerton, J., and Weller, D. (1997). Morpholino antisense oligomers: design, preparation, and properties. *Antisense Nucleic Acid Drug Dev* 7, 187-195.
- Takahashi, H., Sakuta, H., Shintani, T., and Noda, M. (2009). Functional mode of FoxD1/CBF2 for the establishment of temporal retinal specificity in the developing chick retina. *Dev Biol* 331, 300-310.
- Takahashi, H., Shintani, T., Sakuta, H., and Noda, M. (2003). CBF1 controls the retinotectal topographical map along the anteroposterior axis through multiple mechanisms. *Development* 130, 5203-5215.
- Tendeng, C., and Houart, C. (2006). Cloning and embryonic expression of five distinct *sfrp* genes in the zebrafish *Danio rerio*. *Gene Expr Patterns* 6, 761-771.
- Uren, A., Reichsman, F., Anest, V., Taylor, W.G., Muraiso, K., Bottaro, D.P., Cumberledge, S., and Rubin, J.S. (2000). Secreted frizzled-related protein-1 binds directly to Wingless and is a biphasic modulator of Wnt signaling. *J Biol Chem* 275, 4374-4382.
- Veien, E.S., Rosenthal, J.S., Kruse-Bend, R.C., Chien, C.B., and Dorsky, R.I. (2008). Canonical Wnt signaling is required for the maintenance of dorsal retinal identity. *Development* 135, 4101-4111.
- Yin, A., Korzh, S., Winata, C.L., Korzh, V., and Gong, Z. (2011). Wnt signaling is required for early development of zebrafish swimbladder. *PLoS One* 6, e18431.
- Zhao, X.F., Suh, C.S., Prat, C.R., Ellingsen, S., and Fjose, A. (2009). Distinct expression of two *foxg1* paralogues in zebrafish. *Gene Expr Patterns* 9, 266-272.

Zhou, C.J., Molotkov, A., Song, L., Li, Y., Pleasure, D.E., Pleasure, S.J., and Wang, Y.Z. (2008). Ocular coloboma and dorsoventral neuroretinal patterning defects in Lrp6 mutant eyes. *Dev Dyn* 237, 3681-3689.

Chapter 4

Conclusions and Future Directions

4. Conclusions and Future Directions

Sfrps, once thought of solely as Wnt inhibitors, are now being reexamined as building evidence suggests that these proteins may be interacting with multiple developmental pathways. Sfrps are now accepted as modifiers of BMP and netrin signaling, altering processes such as axis formation during gastrulation and retinal cell differentiation (Esteve et al., 2011a; Lee et al., 2006; Yabe et al., 2003). Attitudes towards Sfrp interaction within certain pathways are also evolving as Sfrps have now been shown to have both permissive and repressive roles, particularly in the Wnt pathway. Sfrps can have opposing effects on Wnt signaling, depending on the biological process and organism. Zebrafish *sfrp1a* overexpression mimics the effects of Wnt antagonists during optic primordium specification but mouse *Sfrp1*, along with *Sfrp2*, act as Wnt facilitators during development of the peripheral optic cup (Esteve et al., 2011b; Kim et al., 2007).

Because of the discrepancy in function between different Sfrps, it argues that Sfrps may have unique functions based on the type of organism and tissue in which it is expressed. For the most part, we have very little understanding of how Sfrps actually function during development. To increase our knowledge of Sfrps, we chose to study the role of zebrafish *sfrp1a* and *sfrp5* and their interactions with intercellular signaling pathways during dorsal-ventral retinal patterning, a process not previously studied. Using morpholino knockdown to inhibit both *sfrp1a* and *sfrp5* function, we were able to show a novel interaction between Sfrps and BMP signaling during dorsal-ventral axis formation of the neural retina.

4.1 Summary of Findings

The zebrafish genes *sfrp1a* and *sfrp5* have only had a few previous studies published investigating their function. In particular, studies have shown that *sfrp1a* can act independently as a Wnt antagonist during eye field specification. Overexpression of *sfrp1a* mRNA causes expansion of the optic primordium and rescues dorsalization phenotypes caused by overexpression of *wnt8b* (Kim et al., 2007). However, previous experiments in *Drosophila*, a model system that does

not endogenously express *sfrp*, suggest that Sfrps act in dose-dependent manner. High doses of Sfrp act as Wnt inhibitors and low doses act as Wnt signaling facilitators (Uren et al., 2000), suggesting that mRNA overexpression experiments could produce different biological effects than those created by the endogenous levels of Sfrp. In addition to optic field patterning, *sfrp1a* works cooperatively with *sfrp5* to pattern the forebrain (Peng and Westerfield, 2006). ISH showed that in addition to being expressed in the developing brain, *sfrp1a* and *sfrp5* have overlapping expression patterns in the eye that extend into later stages of eye morphogenesis and patterning, consistent with previously published results (Tendeng and Houart, 2006). Based on their expression in areas conducive to aid in eye patterning, such as the ventral retina, we predicted that these genes might act cooperatively to impact eye axis formation. Morpholino knockdown of *sfrp1a* and *sfrp5* revealed that these two genes share at least partial functional redundancy during eye development and cause eye defects such as microphthalmia and ocular coloboma.

Choroid fissure can be caused, among other things, by aberrant dorsal-ventral retinal patterning (French et al., 2009; Zhou et al., 2008). Because *sfrp1a* and *sfrp5* are expressed ventrally in the retina, one would predict *sfrp1a/sfrp5* depletion causes dorsalization of the retina. ISH revealed that *sfrp1a/sfrp5* morphant eyes are ventralized, due to the expansion of ventral markers, *aldh1a3* and *vax2*, at 2dpf and the loss of dorsal markers, *aldh1a2*, *bambi*, and *tbx5*, at 28hpf and 2dpf. To determine the cause of ventralization, we chose to look at changes in the common signaling pathways responsible for specifying the dorsal retina.

Wnt signaling impacts dorsal retinal patterning during the maintenance phase of axis formation. Until four years ago, there was limited evidence that Wnt signaling impacts retinal patterning because knockdown experiments of known *wnts* expressed in the eye did not cause any phenotypes; however, over-expression of a widespread Wnt inhibitor (*dkk1*) revealed that Wnt signaling is important for dorsal retina specification (Veien et al., 2008). Our data show

expansion of ventral retina markers (*aldh1a2* and *vax2*) and down-regulation of dorsal markers (*aldh1a3*, *bambi*, and *tbx5*), suggesting ventralization of the retina. Based on the decrease in dorsal retina specification, we predicted that Wnt signaling would be decreased in our *sfrp1a/5* morphants. To investigate changes in Wnt signaling, morpholinos were injected into the transgenic report line, *Tg[*TOP:GFP*]^{w25}*, which drives expression of GFP in tissues where canonical Wnt signaling is active (Dorsky et al., 2002). ISH and qRT-PCR showed a decrease in GFP expression in *sfrp1a/5*-depleted embryos, suggesting that Sfrps facilitate Wnt signaling. Investigation of *wnt* gene expression revealed that *wnt2* and *wnt8b* are actually increased in the dorsal RPE of *sfrp1a/sfrp5* morphants, indicating that the changes we see in Wnt signaling happen downstream of *wnt* expression. This fits with the model where Sfrps act on the Wnt ligand, not regulating *wnt* mRNA transcription, to alter signaling.

Wnts can act through BMP signaling to maintain dorsal retinal patterning. Loss of Wnt signaling does not influence initiation of dorsal retina markers in zebrafish but results in a reduction of a number of dorsal markers including the downstream BMP signaling target, *tbx5*, and various *BMP* genes (*bmp2b*, *bmp4*, and *gdf6a*). Overexpression of *bmp4* mRNA was sufficient to rescue defects in dorsal retina specification, suggesting that Wnt signaling maintains dorsal retina identity through BMP signaling (Veien et al., 2008). To determine alterations in BMP signaling, I used the *Tg[*BRE:eGFP*]* line, which drives the expression of GFP wherever BMP signaling is active (Collery and Link, 2011). Both ISH against GFP and confocal fluorescence imaging showed a decrease in BMP signaling in the dorsal eye. Because both Wnt signaling and BMP signaling is decreased, our data agree with the hypothesis that Sfrps affect the dorsal retina through Wnt-maintained BMP signaling.

The caveat is that changes in *BMP* gene expression do not agree with the simple Wnt-BMP pathway; elimination of canonical Wnt signaling completely abolishes expression of *BMP* genes, *bmp2*, *bmp4*, and *gdf6a* during the maintenance phase of eye patterning. Furthermore, any defects seen in dorsal

retina identity can be rescued by *bmp4* or *gdf6a* overexpression (Veien et al., 2008). In direct contrast, *sfrp1a/sfrp5* morphants have increased *bmp2*, *bmp4*, and *gdf6a* expression and still have reduced dorsal retina specification. The fact that *BMP* gene expression is increased with a corresponding decrease in BMP signaling output suggests that there is inhibition in the pathway downstream of transcription. Interestingly, to date Sfrps have been found to act downstream of BMP transcription only as BMP inhibitors, albeit from a limited number of studies. Our data supports a model in which Sfrp1a and Sfrp5 instead act as BMP facilitators. Additionally, only *crescent*, *sfrp2*, and *sizzled* have been linked, either *in vivo* or *in vitro*, to BMP signaling (Lee et al., 2006; Ploper et al., 2011; Yabe et al., 2003), leading to a novel discovery of *in vivo* interaction between BMPs and Sfrp1a and Sfrp5. Because changes in Wnt signaling cannot account for all of the change we see in BMP signaling, our current model is that Sfrps may act on both Wnt and BMP signaling in multiple parts of the pathway (Figure 4.1).

4.2 Unanswered Questions and Future Directions

4.2.1 Sfrps as BMP Signaling Facilitators

Our discovery of a novel type of positive interaction between BMPs and Sfrp1a/Sfrp5 leads to a series of future experiments that are needed to tease apart how these Sfrps promote BMP signaling. There is the possibility that the Sfrps act at the level of the ligand to facilitate signaling or that they influence other proteins that indirectly impact BMP signaling. Based on previous experiments, Sfrps interact with components further upstream of the BMP ligand, such as Tolloid metalloproteases. For example, *Xenopus* Crescent interferes with Tolloid (*xlr*) cleavage of the BMP inhibitor, Chordin (Ploper et al., 2011). However, immunoprecipitation using a tagged BMP, Tolloid-like protein 1 (Tll1), or metalloprotease-like Bmp1a or Bmp1b construct would allow one to decipher if Sfrp1a/Sfrp5 act on BMPs or upstream metalloproteases in the zebrafish eye. Ideally, the assay would be performed on dissected eyes because of the tissue-specific nature of Sfrp function. A zebrafish Sfrp1a or Sfrp5 antibody has not yet been developed, but there are many Sfrp1 and Sfrp5 antibodies for other model

organisms that have not yet been tested in zebrafish. Additionally, we could look for Tolloid-induced cleavage byproducts of the BMP inhibitor, Chordin using western analysis. If Sfrps inhibit Tolloid metalloprotease activity, *sfrp1a/sfrp5* morphants should have reduced Chordin cleavage.

There are alternative assays that could be performed to determine if Sfrps are acting at the level of the BMP ligand. For example, we could compare the phenotypes of dorsomorphin-treated embryos (a SMAD-specific BMP inhibitor) or noggin-treated embryos (a non-specific BMP sequestering inhibitor) to *sfrp*-depleted embryos to see if interfering with BMP in different parts of the pathway account for the phenotypes seen in *sfrp1a/sfrp5* morphants. Treating *sfrp* morphants with low doses of either inhibitor may also reveal phenotypic synergy, indicating that *sfrp1a/sfrp5* morpholinos act in the same pathway. In addition, we can use overexpression of BMPs to try and rescue morphant phenotypes. Because of the strict requirements of proper BMP levels during early development, overexpression can be accomplished using the *rx3* promoter to drive expression in only the developing eye. Based on the model, overexpression of BMP ligand, such as *gdf6a*, should not rescue the eye phenotypes because Sfrps act downstream of *BMP* transcription and already have increased *BMP* expression. In contrast, over-expression of a constitutively active BMP receptor (eg. caBMPRIa) should act further downstream of Sfrps and be able to rescue *sfrp1a/sfrp5* knockdown phenotypes.

Another remaining question is, if Sfrp1a/Sfrp5 are indeed binding and acting on BMP ligands, how are they altering their function in the embryo. One model of Sfrp/Wnt interaction is that Sfrps allow Wnts to diffuse further in the body. It is possible that Sfrp1a/Sfrp5 are similarly affecting BMP diffusion in the retina. Previous experiments using retinal explants in mice have shown increased GFP-tagged Wnt diffusion when exposed to Sfrps. To determine if this is a general characteristic of Sfrp function, analogous experiments can be performed on zebrafish retina using GFP-tagged BMP and Sfrp1a/Sfrp5. This experiment, along with immunoprecipitation, can be taken even further by altering the

domains (NTR or CRD) of Sfrp1a/Sfrp5 to see which domain is more important for interacting with BMPs.

4.2.2 BMP and Wnt Negative Feedback Loops

Our data present a discrepancy with previously published results in regards to changes in *BMP* gene expression following loss of BMP signaling. *sfrp1a/sfrp5* morphants have decreased BMP signaling but a concurrent increase in a number of *BMP* genes, including *bmp2b*, *bmp4*, and *gdf6a*. These changes could be indicative of a negative feedback loop within the BMP pathway; however, no studies have linked decrease BMP signaling with increased *BMP* gene expression. In direct contrast, other BMP loss-of-function models, such as zebrafish *gdf6a* mutants, have decreased dorsal retina identity including reduction in the expression of other *BMP* genes such as *bmp4* (French et al., 2009; Gosse and Baier, 2009). Because we do not know the exact mechanism behind Sfrp-dependent alteration of BMP signaling, it makes it difficult to predict how *BMP* gene expression should change following loss of Sfrp1a/Sfrp5 function. Instead of influencing the BMP ligand, Sfrps may instead be acting on other components of the pathway that elicit novel changes in *BMP* gene expression. In addition, our *sfrp1a/sfrp5* morphant model is not a complete loss-of-function environment and may produce unexpected changes in gene expression.

Similarly, our *sfrp1a/sfrp5* morphants have reduced Wnt signaling but an increase in *wnt* gene expression (*wnt2* and *wnt8b*). Again, our results could be explained by a negative feedback loop. However, changes in *wnt* gene expression following loss of Wnt signaling have not been previously examined, making it difficult to compare our results to previously published data. To determine how reduced Wnt signaling impacts *wnt* expression, we could perform ISH on *wnt* genes in the *dkk1* overexpression model (*Tg[hsp701:dkk1-GFP]*).

4.2.3 Sfrp Expression in the Ventral Retina

One of the more puzzling aspects of the Sfrp story is that both *sfrp1a* and *sfrp5* are expressed in the ventral retina but facilitate dorsal retina specification. A

logical explanation is that Sfrps may instead act as a repressor of specific ventral retina signals; however, there have not been any studies linking Sfrps with either Shh or RA pathways, except that both Shh and RA have been shown to influence some *sfrp* gene transcription (Chen et al., 2002; Ingram et al., 2002). In fact, the only retinal patterning pathways that Sfrps have been shown to interact with are responsible for dorsal retina identity. One theory is that Sfrps facilitate diffusion of Wnt or BMP ligands by shuttling them further in the embryo. In support of this model, Sfrps are secreted, diffusible proteins, and their expression overlaps with where Wnt and BMP ligands are present. Sfrps may also indirectly influence further diffusion by interfering with metalloproteases such as Tolloid. Metalloproteases are important for processing proproteins into mature, functional proteins, many of which work to remodel the extracellular matrix (Hopkins et al., 2007). As a result of altering the extracellular environment, metalloproteases may change the ability of either Wnts or BMPs to diffuse in the body. To determine a possible relationship with Tolloid, as seen in other Sfrp/BMP models, immunoprecipitation experiments could be extended to investigate binding between Sfrp1a or Sfrp5 and zebrafish Tolloid-like 1 (Tll1) or the metalloprotease-like Bmp1a or Bmp1b.

Alternatively, Sfrp1a/Sfrp5 may instead bind and inhibit an as-yet-undefined BMP or Wnt inhibitor expressed in the ventral retina, analogous to chick Ventropin or Chordin. *BMPs* are strictly regulated and are often expressed in corresponding, opposing patterns with a BMP antagonist. BMP inhibitors have been identified in the ventral retina in chick and mouse, but not in zebrafish.

4.2.4 Discrepancies With Previously Published Data on Sfrp1 and Sfrp5

Morpholino knockdown of *sfrp1* or *sfrp5* in Medaka produces phenotypes consistent with function as Wnt antagonists during eye field specification or dorsal-ventral retinal patterning (Lopez-Rios et al., 2008; Ruiz et al., 2009). Zebrafish Sfrp1a also acts as a Wnt antagonist during eye field development, showing a conservation of function between the two teleost model systems (Kim et al., 2007). There is, however, a discrepancy between zebrafish and Medaka

Sfrp5 function during dorsal retina specification. Sfrp5 knockdown in Medaka produces dorsalization phenotypes in the retina (Ruiz et al., 2009). In contrast, zebrafish *sfrp1a/sfrp5* loss of function produces retina ventralization. Both model systems are teleosts, however, investigation of Sfrp function in other model systems has shown that Sfrps can have varied functions in the same developmental processes between model organisms and even within the same model organism during different biological processes. It is possible that there is a divergence of Sfrp5 function in dorsal-ventral retinal patterning. In addition, our model system is a double knockdown of *sfrp1a* and *sfrp5*, which could produce altered effects during retinal patterning. Changes in dorsal-ventral axis formation caused by *sfrp1* knockdown have also not been investigated in the Medaka and may show altered changes to *osfrp5* knockdown.

4.2.5 Other Future Experiments

In addition to tackling any discrepancies and unanswered questions from the data, there are a number of control experiments that need to be conducted. Although we have evidence that *sfrp1a* and *sfrp5* morpholinos are specifically inhibiting splicing of the *sfrp1a* and *sfrp5* transcripts, exon-exon and exon-intron spanning RT-PCR reactions should be recapitulated for the *sfrp1a* (*S*) morpholino. *sfrp1a* (*S2*) qRT-PCR also needs to be recapitulated for exon-exon and intron-exon spanning reactions to ensure improper splicing. *sfrp1a* (*S*) morpholino specificity could also be further confirmed using qRT-PCR. Additional qRT-PCR trials also need to be run for GFP expression changes in *sfrp1a/sfrp5* morphant *Tg[TOP:GFP]^{w25}*, *Tg[BRE:eGFP]* transgenics. Similarly, ISH of dorsal retina marker changes at 2dpf have only been investigated once and need to be confirmed during at least two other independent experimental trials. We also have evidence that overexpression of *gdf6a* is able to partially rescue defects in the Wnt loss-of-function heat shock *dkk1* model but need more trials to achieve statistical significance. It is also a future direction to overexpress *gdf6a* in *sfrp1a/sfrp5* morphants and look for rescue of dorsal retina specification. Based on our testing

model that Sfrps act downstream of the *BMP* transcription, we predict that misexpression of *gdf6a* would not be sufficient to rescue dorsal retina defects.

4.3 Final Conclusions

Ocular coloboma is a developmental fissure defect that affects a number of ocular tissues and accounts for 5-10% of all congenital blindness cases (Chang et al., 2006). Ocular fissure defects can be caused by alterations in the distinct dorsal and ventral boundaries of gene expression in the retina. By studying how the retina is specified, we can increase our knowledge of important signaling pathways during eye patterning and potentially identify new avenues of prevention or treatment of ocular defects. Interference with the BMP signaling pathway has been shown to cause ocular coloboma in both zebrafish and humans (Asai-Coakwell et al., 2007). Our research has unearthed surprising functions for Sfrp1a and Sfrp5 in retinal patterning, suggesting a novel, positive interaction with the BMP signaling pathway during ocular development.

4.4 Figures

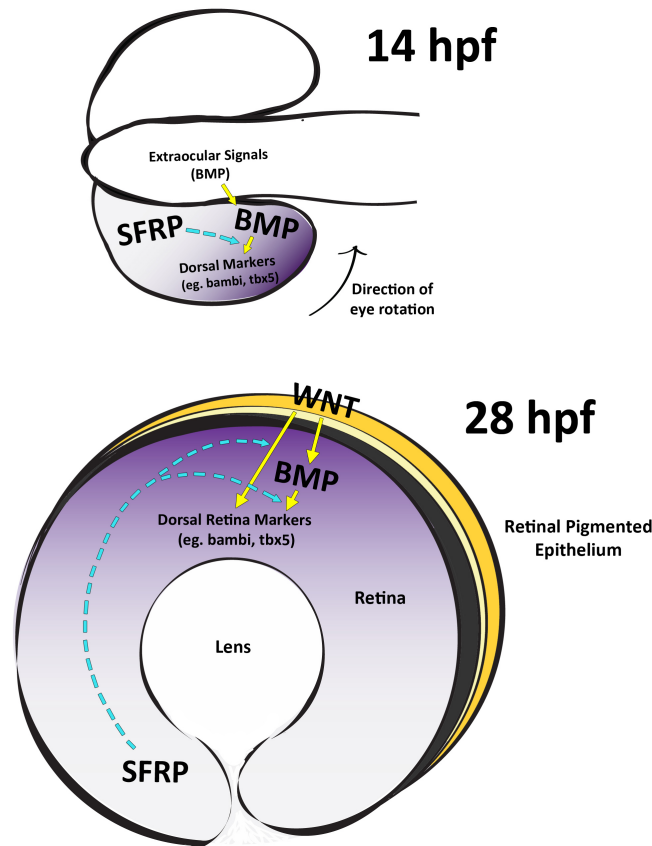


Figure 4.1. Proposed model of Sfrp function during eye patterning. At 14hpf Bone Morphogenic Protein (BMP) expression is turned on the early optic vesicle and initiates expression of dorsal retina genes such as *bambi* and *tbx5*. Secreted frizzled-related protein 1a and 5 (Sfrp) are expressed in the ventral optic vesicle at 14hpf and, based on their role in modulation of BMP signaling at later stages, potentially facilitate BMP signaling during initiation of dorsal retina identity. At 28hpf, Wnts expressed from the retinal pigmented epithelium act upstream of the BMP pathway to maintain dorsal retina gene expression. Sfrps have continued expressed in the ventral retina at this stage and influence both BMP and Wnt signaling in the dorsal eye. However, knockdown phenotypes of *sfrp1a* and *sfrp5* are not entirely explained changes in Wnt signaling, suggesting a model whereby Sfrps act on both Wnt and BMP signaling in multiple parts of the pathway. *bambi* – BMP and activin membrane-bound inhibitor; *tbx5* – T-box 5.

4.5 Literature Cited

- Asai-Coakwell, M., French, C.R., Berry, K.M., Ye, M., Koss, R., Somerville, M., Mueller, R., van Heyningen, V., Waskiewicz, A.J., and Lehmann, O.J. (2007). GDF6, a novel locus for a spectrum of ocular developmental anomalies. *Am J Hum Genet* *80*, 306-315.
- Chang, L., Blain, D., Bertuzzi, S., and Brooks, B.P. (2006). Uveal coloboma: clinical and basic science update. *Curr Opin Ophthalmol* *17*, 447-470.
- Chen, M.H., Antoni, L., Tazi-Ahnini, R., Cork, M., Ward, S.J., and Bavik, C.O. (2002). Identification of known and novel genes whose expression is regulated by endogenous retinoic acid during early embryonic development of the mouse. *Mech Dev* *114*, 205-212.
- Collery, R.F., and Link, B.A. (2011). Dynamic smad-mediated BMP signaling revealed through transgenic zebrafish. *Dev Dyn* *240*, 712-722.
- Dorsky, R.I., Sheldahl, L.C., and Moon, R.T. (2002). A transgenic Lef1/beta-catenin-dependent reporter is expressed in spatially restricted domains throughout zebrafish development. *Dev Biol* *241*, 229-237.
- Esteve, P., Sandonis, A., Cardozo, M., Malapeira, J., Ibanez, C., Crespo, I., Marcos, S., Gonzalez-Garcia, S., Toribio, M.L., Arribas, J., *et al.* (2011a). SFRPs act as negative modulators of ADAM10 to regulate retinal neurogenesis. *Nat Neurosci* *14*, 562-569.
- Esteve, P., Sandonis, A., Ibanez, C., Shimono, A., Guerrero, I., and Bovolenta, P. (2011b). Secreted frizzled-related proteins are required for Wnt/beta-catenin signalling activation in the vertebrate optic cup. *Development* *138*, 4179-4184.
- French, C.R., Erickson, T., French, D.V., Pilgrim, D.B., and Waskiewicz, A.J. (2009). Gdf6a is required for the initiation of dorsal-ventral retinal patterning and lens development. *Dev Biol* *333*, 37-47.
- Gosse, N.J., and Baier, H. (2009). An essential role for Radar (Gdf6a) in inducing dorsal fate in the zebrafish retina. *Proc Natl Acad Sci U S A* *106*, 2236-2241.
- Hopkins, D.R., Keles, S., and Greenspan, D.S. (2007). The bone morphogenetic protein 1/Tolloid-like metalloproteinases. *Matrix Biol* *26*, 508-523.
- Ingram, W.J., Wicking, C.A., Grimmond, S.M., Forrest, A.R., and Wainwright, B.J. (2002). Novel genes regulated by Sonic Hedgehog in pluripotent mesenchymal cells. *Oncogene* *21*, 8196-8205.

- Kim, H.S., Shin, J., Kim, S.H., Chun, H.S., Kim, J.D., Kim, Y.S., Kim, M.J., Rhee, M., Yeo, S.Y., and Huh, T.L. (2007). Eye field requires the function of Sfrp1 as a Wnt antagonist. *Neurosci Lett* 414, 26-29.
- Lee, H.X., Ambrosio, A.L., Reversade, B., and De Robertis, E.M. (2006). Embryonic dorsal-ventral signaling: secreted frizzled-related proteins as inhibitors of tolloid proteinases. *Cell* 124, 147-159.
- Lopez-Rios, J., Esteve, P., Ruiz, J.M., and Bovolenta, P. (2008). The Netrin-related domain of Sfrp1 interacts with Wnt ligands and antagonizes their activity in the anterior neural plate. *Neural Dev* 3, 19.
- Peng, G., and Westerfield, M. (2006). Lhx5 promotes forebrain development and activates transcription of secreted Wnt antagonists. *Development* 133, 3191-3200.
- Ploper, D., Lee, H.X., and De Robertis, E.M. (2011). Dorsal-ventral patterning: Crescent is a dorsally secreted Frizzled-related protein that competitively inhibits Tolloid proteases. *Dev Biol* 352, 317-328.
- Ruiz, J.M., Rodriguez, J., and Bovolenta, P. (2009). Growth and differentiation of the retina and the optic tectum in the medaka fish requires olSfrp5. *Dev Neurobiol* 69, 617-632.
- Tendeng, C., and Houart, C. (2006). Cloning and embryonic expression of five distinct sfrp genes in the zebrafish *Danio rerio*. *Gene Expr Patterns* 6, 761-771.
- Uren, A., Reichsman, F., Anest, V., Taylor, W.G., Muraiso, K., Bottaro, D.P., Cumberledge, S., and Rubin, J.S. (2000). Secreted frizzled-related protein-1 binds directly to Wingless and is a biphasic modulator of Wnt signaling. *J Biol Chem* 275, 4374-4382.
- Veien, E.S., Rosenthal, J.S., Kruse-Bend, R.C., Chien, C.B., and Dorsky, R.I. (2008). Canonical Wnt signaling is required for the maintenance of dorsal retinal identity. *Development* 135, 4101-4111.
- Yabe, T., Shimizu, T., Muraoka, O., Bae, Y.K., Hirata, T., Nojima, H., Kawakami, A., Hirano, T., and Hibi, M. (2003). Ogon/Secreted Frizzled functions as a negative feedback regulator of Bmp signaling. *Development* 130, 2705-2716.
- Zhou, C.J., Molotkov, A., Song, L., Li, Y., Pleasure, D.E., Pleasure, S.J., and Wang, Y.Z. (2008). Ocular coloboma and dorsoventral neuroretinal patterning defects in Lrp6 mutant eyes. *Dev Dyn* 237, 3681-3689.

Appendix A:

Hedgehog acyltransferases and retinal patterning

A.1 Introduction

Shh is a secreted, embryonic signaling molecule that functions during a variety of developmental processes, in both vertebrates and invertebrates (Blagden et al., 1997; Briscoe and Ericson, 1999; Han and Martinage, 1992; Ho and Scott, 2002; Patten and Placzek, 2000). Diffusion of Shh away from its site of creation creates a gradient of expression that is used to differentiate between cell types; high Shh levels induce one identity, lower Shh levels induce another (McGlinn and Tabin, 2006; Zeng et al., 2001). Shh signals by binding to a receptor, Patched (Ptc), located on a target cell's plasma membrane (Marigo et al., 1996a). Binding triggers an intracellular signaling cascade, allowing specific transcription factors to enter the nucleus and alter hedgehog target gene transcription (Lee et al., 1997; Marigo et al., 1996b). Shh is expressed from the notochord, floor plate, and lateral mesenchyme (embryonic mesodermal tissue whose signals help pattern the limb) and plays a vital role in patterning vertebrate muscle and the nervous system (Blagden et al., 1997; Briscoe and Ericson, 1999; Han and Martinage, 1992; Ho and Scott, 2002). Zebrafish *shh* mutants display an array of defects including mispatterning of the neural tube, forebrain, eyes, and somite tissues (Sanek et al., 2009; Stickney et al., 2000; Vanderlaan et al., 2005).

In order to function properly, Shh must undergo specific post-translational modifications. First, Shh is brought into the secretory pathway via an N-terminal localization signal (Buglino and Resh, 2010). Once inside, Shh is autocatalytically cleaved (Chen et al., 2004). Two lipid moieties are then added, one to each end of the newly cleaved protein. Cholesterol is added to the C-terminal end,

and palmitate is added to the N-terminal end of Shh (Chen et al., 2004; Goetz et al., 2006; Zeng et al., 2001) (Figure A1). *In vivo* work in mice has shown that, together, these two lipid groups allow Shh to form stable multimers that are important for long range signaling (Chen et al., 2004) Although much is known about the mechanics of Shh cholesterolization, the details of the palmitoylation reaction remain largely unclear.

A.2 Results

A.2.1 Expression profile of zebrafish *hhatlb*

Recent biochemical work has identified hedgehog acyltransferase (Hhat) as a potential Shh palmitoyl acyltransferase, due to its ability to palmitoylate Shh *in vitro* (Buglino and Resh, 2008). Zebrafish have three *hhat* genes: *hhat*, *hhat-like,a* (*hhatla*), and *hhat-like,b* (*hhatlb*). To date, relatively little work has been done on studying the function of related *hhat* genes in any model system. In zebrafish, these genes are currently uncharacterized. However, previous work has characterized Hhat as a transmembrane protein, likely located on membranes of organelles within the secretory system (Lowe and Marth, 2003). We have also recently investigated gene expression domains for *hhat* and its related genes within the zebrafish embryo. *hhat* is expressed in the anterior, ventral portion of the developing embryo. In contrast, *hhatla* is expressed exclusively in medial somitic tissue, as well pectoral fin and head muscles in later stages of development. Finally, *hhatlb* is expressed maternally, with ubiquitous expression throughout early development and specific expression in the lateral somite and muscle pioneers (a small subpopulation of muscle cells known to require high

levels of Shh signaling (Wolff et al., 2003)) in later stages (Figure A2, Figure A3). Because of its expression in the eye, we chose to focus on *hhatlb* for the remainder of this appendix.

The current theory is that Hhat(like) palmitoylates Shh as it travels through the golgi, before it is secreted from the cell. However, in order for this theory to hold true, both Shh and Hhat isoforms have to be expressed or present in the same tissues, at the same time during development. Interestingly, a comparison of expression profiles between *shh* and the *hhat-like* genes reveals a disconnect between tissues where both Hhat-like proteins are expressed and tissues where Shh is expressed. Shh is secreted from the notochord and floor plate (neural signaling center in anterior, ventral embryo). In contrast, *hhatlb* is expressed in the presumptive floor-plate and notochord tissues only in very early stages of development and *hhatla* is never expressed in either tissue (Figure A3). This incongruity has led to the formation of different theories as to how Shh and Hhat-like interact *in vivo*.

Due to the early ubiquitous expression of *hhatlb* (Figure A3), the first possibility is that protein created from maternally inherited *hhatlb* mRNA is still present in the notochord in later stages to mediate Shh signaling in muscle tissues. However, this still does not address the lack of overlap between *hhatla* and *Shh* expression. The second possibility is that the interaction between *hhatlb* (or *hhatla*) and Shh does not take place cell autonomously within the notochord. The final possibility is that zebrafish hhat-like proteins have alternative palmitoylation substrates. One experiment that could help address these questions is to express

hhat(like) from the notochord versus the muscle and see if it is able to rescue *hhat(like)*-depletion phenotypes. Although we have not created these transgenics, these experiments would be vital to any future work on this group of genes.

A.2.2 *hhatlb* morphant phenotypes

Injection of a translation-blocking *hhatlb* morpholino produced severe phenotypes that included ears abnormalities, misshapen somites, and shortened trunk length, as compared to uninjected controls. *Hhatlb*-depleted embryos also displayed varying degrees of hydrocephaly, heart edema, ocular coloboma and thinning of ventral retinal tissue (Figure A4). When embryos were injected with a non-overlapping translation-blocking *hhatlb* morpholino, only the eye phenotypes were phenocopied, contributing to the conclusion that the trunk phenotypes may be a non-specific defect due to morpholino toxicity. Therefore, the focus will be on ocular defects for the remainder of this appendix. Morpholinos can also cause other defects such as aberrant activation of the p53 apoptosis pathway, leading to non-specific cell death (Robu et al., 2007). To eliminate any defects caused by morpholino-induced p53 pathway activation, our *hhatlb* morphants were co-injected with a p53 morpholino.

In situ hybridization was used as a tool to determine if *hhatlb*-depleted embryos had any changes in gene expression. Shh is important for ventral retina specification, so we predicted that loss of *hhatlb* would cause decreased Shh function and reduced ventral retina specification. In contrast, *hhatlb* morphants showed an expansion of *vax2* (n = 29/34), a Shh-responsive marker, and *aldh1a3* (n = 8/9). Expansion of ventral retina markers persisted to 2dpf, where injection of

hhatlb morpholino causes increased *vax2* (n = 17/17) and *vax1* (n = 10/14) expression. *hhatlb* morphants displayed eye phenotypes that were phenocopied in embryos injected with non-overlapping *hhatlb* morpholino but were unsuccessfully rescued with mRNA overexpression.

A.2.3. Loss of *hhatlb* does not phenocopy loss of Shh signaling

Hhats are proposed to be post-translational modifiers of Shh that allow for increased range of Shh signaling (Chen et al., 2004). Therefore, *hhatlb* knockdown should cause defects in Shh signaling at longer distance signaling targets. Investigation of ventral eye markers unexpectedly revealed retinal ventralization, suggesting that Shh signaling is actually increased with *hhatlb* loss of function. To further examine changes in Shh signaling, we chose to compare phenotypes of *smoothened* mutants (*smo^{b641}*), an integral member of the Shh signal transduction pathway, to *hhatlb* morphants. Again, our data show conflicting results between loss of *hhatlb* and loss of Shh signaling. *Smoothened* mutants have little to no expression of *vax1* (n = 14/15) and *vax2* (n = 15/17) at 2dpf, whereas *hhatlb* morphants still have an expansion in *vax1* (n = 10/14) and *vax2* (n = 17/17) as compared to *p53* morphant controls (Figure A5).

A.3 Conclusions

Multiple discrepancies have surfaced with regards to the model of Sfrps acting cell autonomously to post-translationally modify the Shh precursor for proper function of the mature protein. Investigation of *hhatlb* expression revealed that the gene is expressed in specific types of muscle tissue (lateral somite) but

not in the notochord. Because the notochord is a major source of Shh in the embryo, it argues that *hhatlb* either do not work cell autonomously or has an entirely different function in the developing embryo. In addition, our data suggest that *hhatlb* knockdown produces phenotypes that do not align with decreased Shh signaling, as seen in the expansion of multiple ventral retina markers. Even though these phenotypes could be recapitulated with a non-overlapping morpholino, we could not rescue the ventralization phenotype using mRNA overexpression, leading to uncertainty about the validity of the data. Before drawing any definite conclusions from the results, rigorous specificity controls need to be performed on the morpholinos used in these experiments.

A.4 Figures

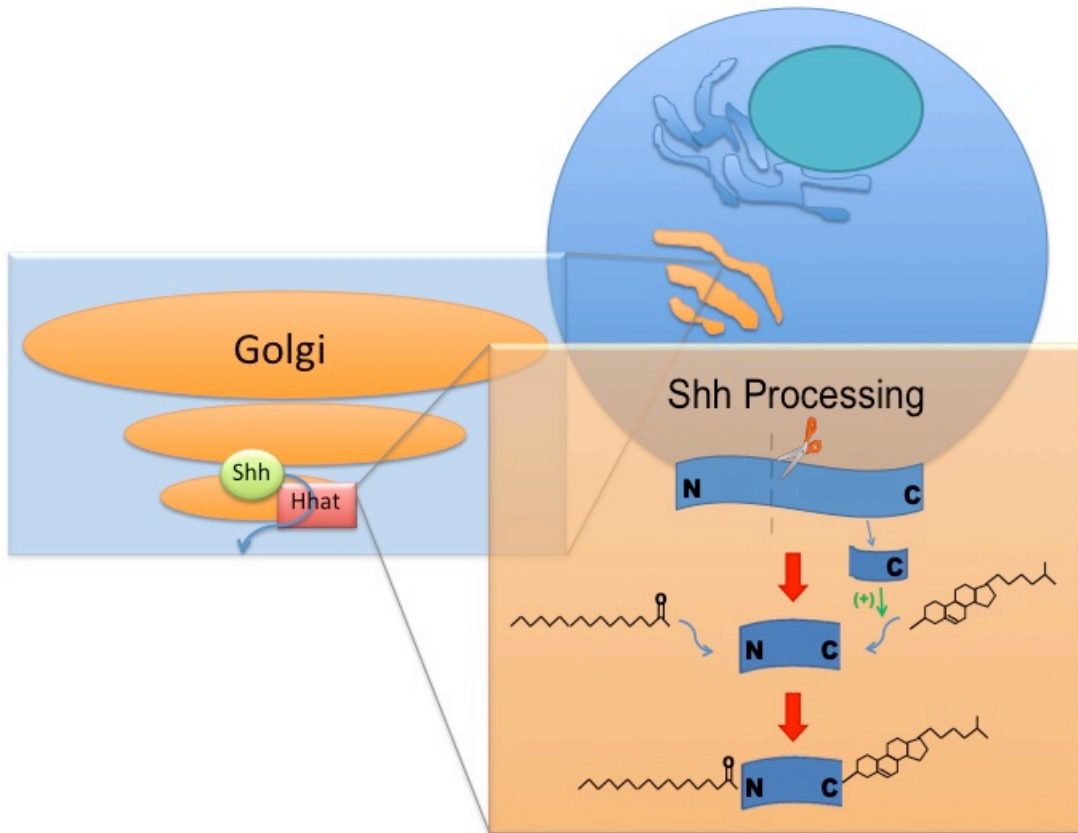


Figure A1. Proposed model of Hhat-mediated Shh palmitoylation. Hhat palmitoyl acyl- transferases are located on the plasma membrane of the golgi and catalyze N-terminal palmitoylation of *Shh* as it passes through the secretory pathway. *Shh* proteins then leave the cell and form multimers that are important for long-range signaling .

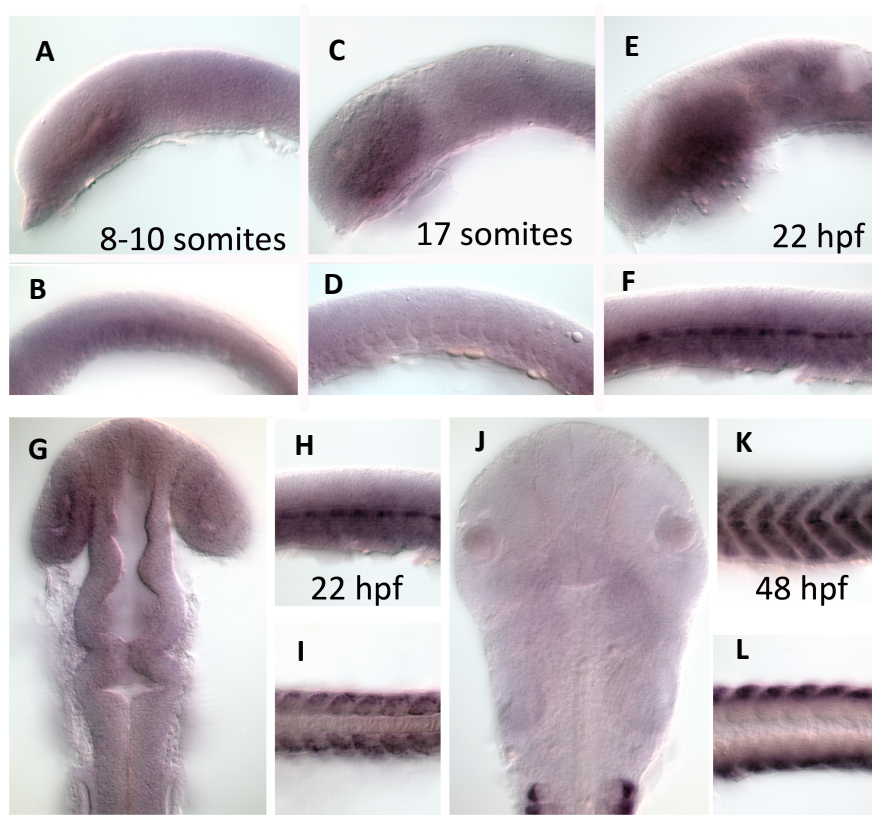


Figure A2. Expression of *hhatlb* during zebrafish development. *hhatlb* is expressed ubiquitously early on (A-D) and develops increased expression in the lateral somite tissue, most notably after 22 hpf (E-L).

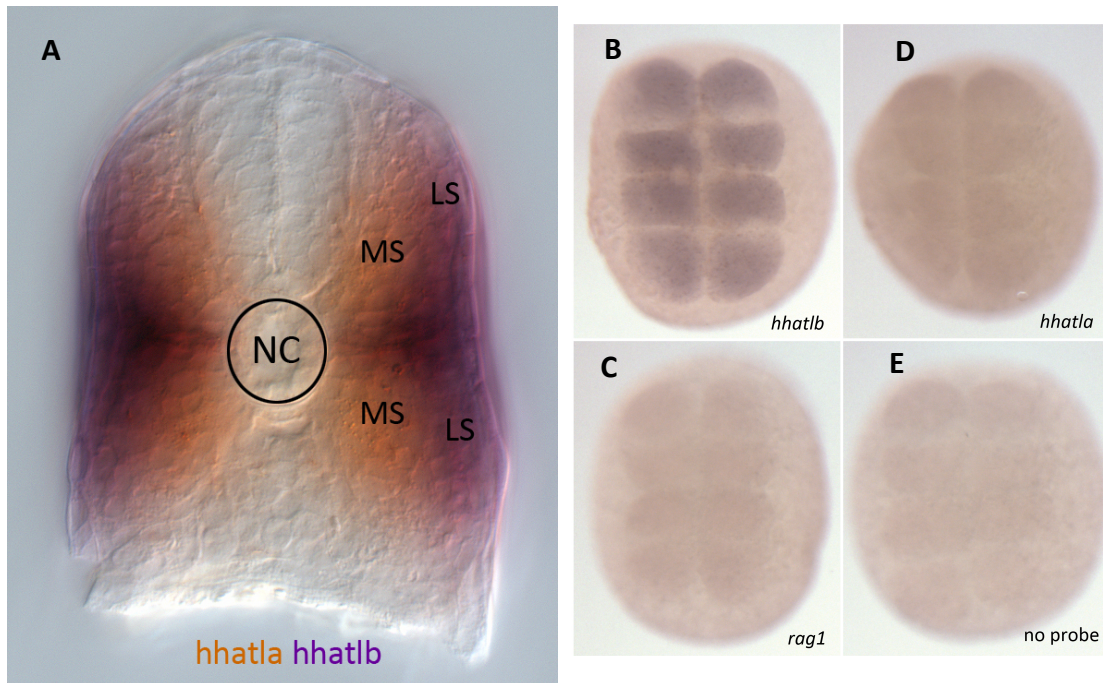


Figure A3. *hhatlb* is not expressed in the notochord but is maternally provided during early embryonic development. Shh is secreted from the notochord, floor plate, and lateral mesenchyme; neither *hhatla* nor *hhatlb* are zygotically expressed in these specific tissues (A). *hhatlb*, however, is expressed maternally and may have leftover maternal proteins acting in the notochord at later stages (B-E). LS – lateral somite, MS – medial somite, NC – notochord.

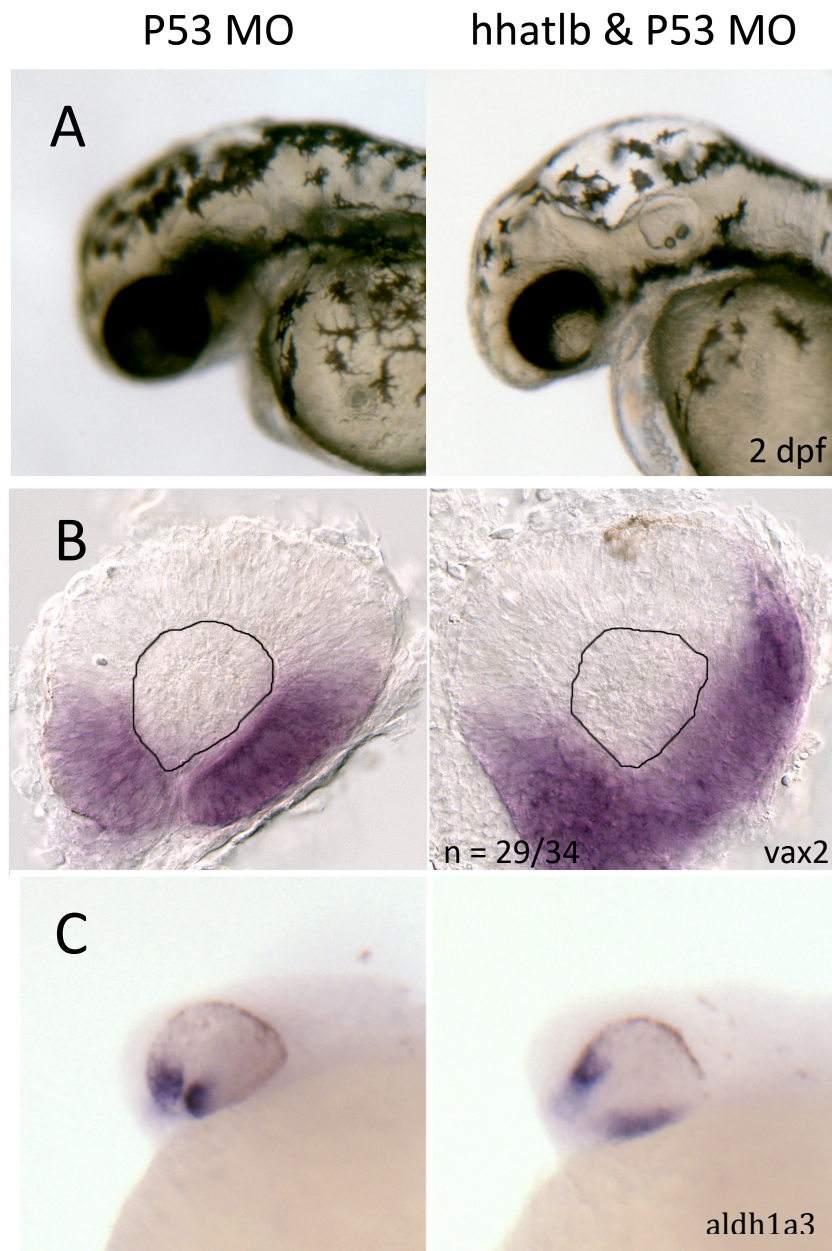


Figure A4. *hhatlb*-depleted embryos have coloboma and changes in ventral eye markers. Lateral views of *hhatlb* morphants show reduction in ventral eye tissue and failure of the choroid fissure to close. *hhatlb* morphants have an expanded temporal domain of *vax2* (B), a *Shh* target in the ventral eye (n = 29/34) and *aldh1a3* (n = 8/9) (C) at 28hpf.

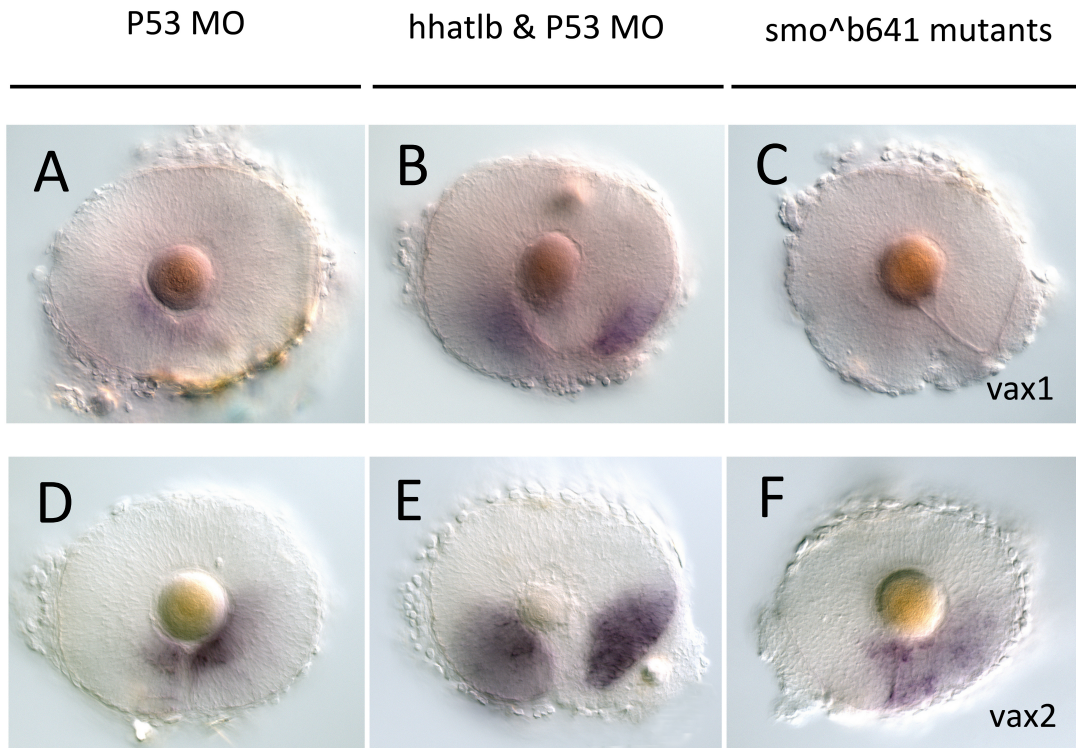


Figure A5. *hhatlb* eye phenotypes do not phenocopy loss of Shh signaling. Morphant eyes (2dpf) were compared with stage-matched *smo^{b641}* mutants, which have mutations in *smoothened*, a member of the Shh signaling pathway. *hhatlb*-depleted embryos had an expansion of *vax1* (n = 10/14) and *vax2* (n = 17/17), whereas *smo^{b641}* mutants have decreased *vax1* (n = 14/15) and *vax2* (n = 15/17) expression.

A.5 Literature Cited

- Blagden, C.S., Currie, P.D., Ingham, P.W., and Hughes, S.M. (1997). Notochord induction of zebrafish slow muscle mediated by Sonic hedgehog. *Genes Dev* 11, 2163-2175.
- Briscoe, J., and Ericson, J. (1999). The specification of neuronal identity by graded Sonic Hedgehog signalling. *Semin Cell Dev Biol* 10, 353-362.
- Buglino, J.A., and Resh, M.D. (2008). Hhat is a palmitoyltransferase with specificity for N-palmitoylation of Sonic Hedgehog. *J Biol Chem* 283, 22076-22088.
- Buglino, J.A., and Resh, M.D. (2010). Identification of conserved regions and residues within Hedgehog acyltransferase critical for palmitoylation of Sonic Hedgehog. *PLoS One* 5, e11195.
- Chen, M.H., Li, Y.J., Kawakami, T., Xu, S.M., and Chuang, P.T. (2004). Palmitoylation is required for the production of a soluble multimeric Hedgehog protein complex and long-range signaling in vertebrates. *Genes Dev* 18, 641-659.
- Goetz, J.A., Singh, S., Suber, L.M., Kull, F.J., and Robbins, D.J. (2006). A highly conserved amino-terminal region of sonic hedgehog is required for the formation of its freely diffusible multimeric form. *J Biol Chem* 281, 4087-4093.
- Han, K.K., and Martinage, A. (1992). Post-translational chemical modification(s) of proteins. *Int J Biochem* 24, 19-28.
- Ho, K.S., and Scott, M.P. (2002). Sonic hedgehog in the nervous system: functions, modifications and mechanisms. *Curr Opin Neurobiol* 12, 57-63.
- Lee, J., Platt, K.A., Censullo, P., and Ruiz i Altaba, A. (1997). Gli1 is a target of Sonic hedgehog that induces ventral neural tube development. *Development* 124, 2537-2552.
- Lowe, J.B., and Marth, J.D. (2003). A genetic approach to Mammalian glycan function. *Annu Rev Biochem* 72, 643-691.
- Marigo, V., Davey, R.A., Zuo, Y., Cunningham, J.M., and Tabin, C.J. (1996a). Biochemical evidence that patched is the Hedgehog receptor. *Nature* 384, 176-179.

- Marigo, V., Johnson, R.L., Vortkamp, A., and Tabin, C.J. (1996b). Sonic hedgehog differentially regulates expression of GLI and GLI3 during limb development. *Dev Biol* *180*, 273-283.
- McGlinn, E., and Tabin, C.J. (2006). Mechanistic insight into how Shh patterns the vertebrate limb. *Curr Opin Genet Dev* *16*, 426-432.
- Patten, I., and Placzek, M. (2000). The role of Sonic hedgehog in neural tube patterning. *Cell Mol Life Sci* *57*, 1695-1708.
- Robu, M.E., Larson, J.D., Nasevicius, A., Beiraghi, S., Brenner, C., Farber, S.A., and Ekker, S.C. (2007). p53 activation by knockdown technologies. *PLoS Genet* *3*, e78.
- Sanek, N.A., Taylor, A.A., Nyholm, M.K., and Grinblat, Y. (2009). Zebrafish *zic2a* patterns the forebrain through modulation of Hedgehog-activated gene expression. *Development* *136*, 3791-3800.
- Stickney, H.L., Barresi, M.J., and Devoto, S.H. (2000). Somite development in zebrafish. *Dev Dyn* *219*, 287-303.
- Vanderlaan, G., Tyurina, O.V., Karlstrom, R.O., and Chandrasekhar, A. (2005). Gli function is essential for motor neuron induction in zebrafish. *Dev Biol* *282*, 550-570.
- Wolff, C., Roy, S., and Ingham, P.W. (2003). Multiple muscle cell identities induced by distinct levels and timing of hedgehog activity in the zebrafish embryo. *Curr Biol* *13*, 1169-1181.
- Zeng, X., Goetz, J.A., Suber, L.M., Scott, W.J., Jr., Schreiner, C.M., and Robbins, D.J. (2001). A freely diffusible form of Sonic hedgehog mediates long-range signalling. *Nature* *411*, 716-720.

Appendix B:

***hmx4* regulates retinoic acid-mediated Shh signaling during forebrain patterning**

Data in this appendix have been previously published

*Gongal, P.A., March, L.D., **Holly, V.L.**, Pillay, L.M., Berry-Wynne, K.M., Kagechika, H., Waskiewicz, A.J. (2011) Hmx4 regulates Sonic hedgehog signaling through control of retinoic acid synthesis during forebrain patterning. *Developmental Biology* 355:55-64.*

B.1 Introduction

Retinoic acid (RA) is a diffusible signaling molecule that functions in patterning various embryonic zebrafish tissues including the ear, heart, fin, neural tube, hindbrain, and forebrain. When RA enters a cell, it binds to retinoic acid receptors (RAR) and retinoid x receptors (RXR), enters the nucleus and initiates transcription of genes (Niederreither and Dolle, 2008). Patterning events involving retinoic acid signaling are dose sensitive; therefore its expression is strictly controlled through opposing gradients of RA synthesis and degradation enzymes (Begemann et al., 2001).

Hmx4 (H6 homeobox 4) is a transcription factor that positively regulates the expression of the RA synthesizing enzyme *aldehyde dehydrogenase 1a3* (*aldh1a2*). Loss of *hmx4* causes decreased *aldh1a2* expression and morphological phenotypes consistent with loss of RA signaling (open neural tube, small ears, loss of pectoral fins) that could be rescued with exogenous RA (Gongal et al., 2011). *Hmx4* morphants also display narrowed eye fields that are more severe than other loss-of-RA models, suggesting that other pathways may be affected (Begemann et al., 2001; Gongal et al., 2011).

B.2 Results

B.2.1 Loss of *hmx4* causes defects in Shh signaling

The Shh pathway plays a well-known role in patterning of the forebrain and separation of the eye field. In addition to having deficient RA signaling, *hmx4* morphants also have reduced Shh signaling, providing a possible explanation for the severely narrowed eye field seen in *hmx4*-depleted embryos. ISH of the Shh signaling targets, *ptc1* and *nkx2.2a* revealed that *hmx4* morphants have reduced domains of expression in the forebrain as compared to control embryos. In addition, expression of the Shh-responsive downstream transcription factor, *gli1* was expanded dorsally and the optic stalk marker, *pax2a*, was ectopically expressed in the forebrain, phenotypes that could be explained by the loss of *gli3* as seen in *hmx4* morphants (Furimsky and Wallace, 2006; Tyurina et al., 2005).

B.2.2 Defects in Shh signaling can be rescued by addition of RA

Addition of exogenous RA to *hmx4* morphants is able to significantly rescue the expression of the Shh signaling targets. *hmx4* morphants had 57% of embryos with reduced *ptc1* (40% moderately reduced, 17% strongly reduced, n = 30) as compared to *hmx4* morphants treated with RA (50% moderately reduced, 0% strongly reduced, n = 46) (Fisher's exact test, p<0.001). Similarly, the expression of *nkx2.2a* is also significantly rescued (Fisher's exact test, p<0.001) in RA-treated *hmx4* morphants (42% moderate reduction, 0% strong reduction, n = 36) as compared to DMSO (dimethyl sulfoxide) treated *hmx4* morphants (43% moderate reduction, 36% strong reduction, n = 44).

B.3 Conclusions

Addition of RA into *hmx4* morphants is able to rescue morphological phenotypes consistent with loss of RA signaling, as well as gene expression changes consistent with alterations in Shh signaling. We believe that the RA-mediated Shh defects seen in *hmx4* morphants are a result of changes in the expression of *gli3*. Gli3 is a Shh-induced transcription activator or repressor (Tyurina et al., 2005). Its expression is significantly reduced in *hmx4* morphants and is highly responsive to changes in RA caused by the addition or exogenous RA or RA degradation cause by diethylaminobenzaldehyde (DEAB) (Gongal et al., 2011). Similar to *ptc1* and *nkx2.2a*, *gli3* expression can be rescued in *hmx4* morphants by RA supplementation (Gongal et al., 2011). In addition, forebrain phenotypes seen in *hmx4*-depleted embryos resemble those seen in Gli3 mouse and zebrafish knockdowns (Furimsky and Wallace, 2006; Tyurina et al., 2005). Therefore, our data suggest that *hmx4* regulates both RA and Shh signaling, with Gli3 as facilitator for interaction between the two pathways.

B.4 Figures

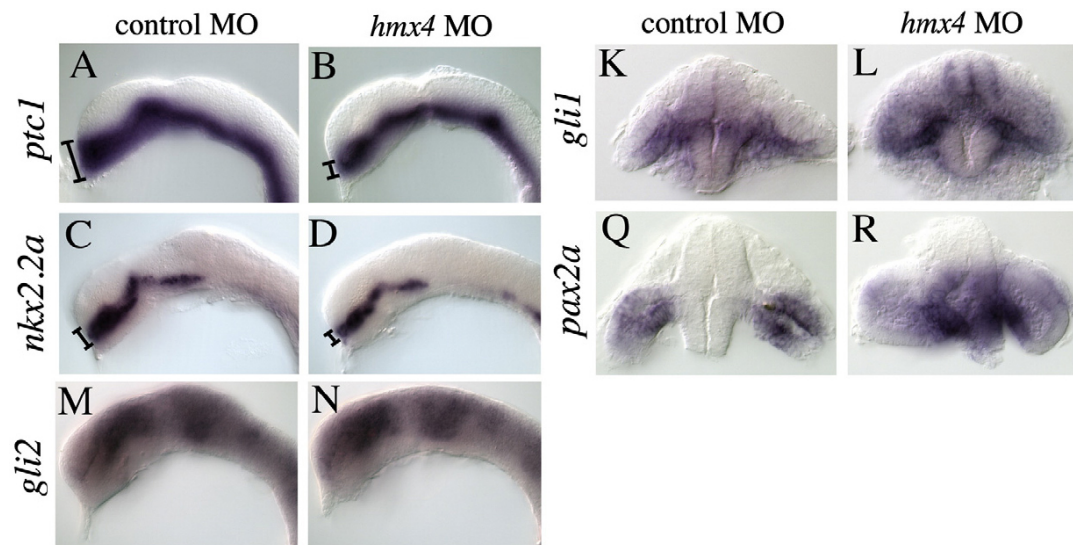


Figure B1. *hmx4* morphants have alterations in Shh signaling. Depletion of *hmx4* causes a reduction in the domains of *ptc1* (A-B) and *nkx2.2a* (C-D), two Shh-responsive genes, in the forebrain at 18-somites. Investigation of a change in *gli2* expression, a downstream Shh-activated transcription factor, in *hmx4* morphants revealed no overt difference as compared to controls (M-N). Loss of *hmx4* causes dorsal expansion of the *gli1* transcription factor (K-L) and ectopic expression of *pax2a* (Q-R) in the forebrain (sections through the forebrain and eyes).

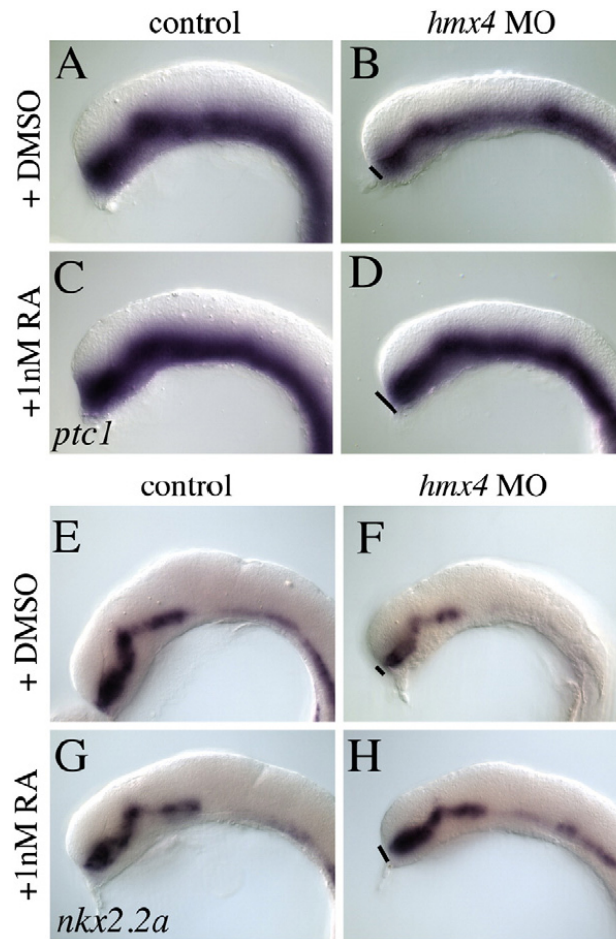


Figure B2. Defects in Shh signaling can be rescued by RA treatment. RA-treated *hmx4* morphants have significant rescue (Fisher's exact test, $p < 0.001$) of *ptc1* expression as compared to dimethyl sulfoxide (DMSO)-treated embryos (*hmx4*: 40% moderately reduced, 17% severely reduced, $n = 30$; *hmx4*, RA: 50% moderately reduced, 0% severely reduced, $n = 46$). Similarly, *hmx4* morphants treated with RA have significantly reduced (Fisher's exact test, $p < 0.001$) numbers of embryos with severe *nkx2.2a* loss as compared to DMSO-treated *hmx4* morphants (*hmx4*: 43% moderately reduced, 36% severely reduced; *hmx4*, RA: 42% moderately reduced, 0% severely reduced, $n = 36$).

A.5 Literature Cited

- Begemann, G., Schilling, T.F., Rauch, G.J., Geisler, R., and Ingham, P.W. (2001). The zebrafish neckless mutation reveals a requirement for raldh2 in mesodermal signals that pattern the hindbrain. *Development* 128, 3081-3094.
- Furimsky, M., and Wallace, V.A. (2006). Complementary Gli activity mediates early patterning of the mouse visual system. *Dev Dyn* 235, 594-605.
- Gongal, P.A., March, L.D., Holly, V.L., Pillay, L.M., Berry-Wynne, K.M., Kagechika, H., and Waskiewicz, A.J. (2011). Hmx4 regulates Sonic hedgehog signaling through control of retinoic acid synthesis during forebrain patterning. *Dev Biol* 355, 55-64.
- Niederreither, K., and Dolle, P. (2008). Retinoic acid in development: towards an integrated view. *Nat Rev Genet* 9, 541-553.
- Tyurina, O.V., Guner, B., Popova, E., Feng, J., Schier, A.F., Kohtz, J.D., and Karlstrom, R.O. (2005). Zebrafish Gli3 functions as both an activator and a repressor in Hedgehog signaling. *Dev Biol* 277, 537-556.